Science
AAAS

Supplementary Materials for

Bronze and Iron Age population movements underlie Xinjiang population history

Vikas Kumar *et al*.

Corresponding authors: Yichen Liu, yichen.liu@ivpp.ac.cn; E. Andrew Bennett, eabennett@gmail.com; Qiaomei Fu, fuqiaomei@ivpp.ac.cn

Science **376**, 62 (2022)
DOI: 10.1126/science.abk1534

The PDF file includes:

Other Supplementary Material for this manuscript includes the following:

Materials and Methods

Ancient DNA extraction, sequencing, and data processing

All ancient DNA procedures were conducted in the clean-room facilities dedicated to ancient DNA work in Key Laboratory of Vertebrate Evolution and Human Origins of Chinese Academy of Sciences, IVPP, CAS. The Institute of Vertebrate Paleontology and Paleoanthropology's review board approved the study of the ancient genomes sampled in this project (review no. 202103180008). Powder was obtained from bone samples by drilling, and DNA was extracted with established protocols (Supplementary Table S1) (*44*). Single-stranded and double-stranded genomic libraries were prepared (Supplementary Table S1) and double-stranded libraries were partially treated with uracil-DNA-glycosylase (UDG) from E. coli and endonuclease (Endo VIII) ("DS_half") to repair deaminated cytosine residues (*23*, *45*). Single-stranded libraries were not treated with UDG ("SS_noUDG"). Libraries were amplified using AccuPrimePfx DNA polymerase with 35 cycles of amplification. Oligonucleotide probes were used to capture mitochondrial genomes (*24*) and enrich for 1.2 million nuclear SNPs (*25*).

Enriched libraries were sequenced on Illumina Miseq or Hiseq4000 platforms using paired end reads (2×76 bp for mitochondria; 2x100 bp or 2x150 bp for nuclear). LeeHom (https://github.com/grenaud/leeHom) (*46*) was used to trim adapters and merge paired ends into a single read (overlap > 11 base pairs). Merged reads with a minimum length of 30 base pairs were then aligned to the published human mitochondrial sequence (*47*) and the *hg19* human reference genome using BWA (-aln -n 0.01 and -l 16500, then -samse). Reads with mapping quality <30 were removed and duplicate reads having the same orientation, start, and end positions as another read were also discarded, keeping only the read with the highest sequence quality.

We tested for mitochondrial contamination of each individual using the ContamMix (*48*) by aligning reads to the mitochondrial genomes including 311 world-wide present-day individuals. To remove the damage pattern caused by cytosine deamination, the first and last two C→T and G→A substitution of the half UDG treated fragments, and the last five C→T and G→A of the no-UDG treated fragments, which were all from single-stranded libraries, were masked with "N". Individuals whose mitochondrial sequence showed >5% modern human contamination were treated as contaminated and removed. For male individuals, we also tested the contamination rate for the X-chromosome using ANGSD (*49*) and removed individuals with a contamination rate above 5%. In addition, we remove the first and last three positions of fragments with at least one C→T substitution using the pmdtools0.60 with the --customterminus parameter (*50*).

Haplogrep 2 (https://haplogrep.i-med.ac.at) was used to assign mtDNA haplogroups (*51*).
Y-chromosome haplogroups for male individuals were determined using all reads mapping to the Y chromosome with a minimum mapping quality of 37. Y-haplogroups were assigned using a custom script that considers the derived allele located furthest upstream and most ancestral allele furthest

downstream in the phylogenetic tree (ISOGG database version 14.164 (http://www.isogg.org/tree). In addition, at least two derived SNPs were required if the upstream-most derived SNP was a C→T or G→A substitution to minimize the impact of ancient DNA damage (*20*). Results for a minimum requirement of one and two derived SNPs are given in Table S1. We additionally made use of the Y haplogroup identification software Yleaf (v2.2) (*52*) installed with a curated version of the ISOGG database v.14. The Yleaf results are also reported in Table S1. Using these two methods with identical inputs, some samples gave slightly different terminal resolutions due to differences in database curation and stringency requirements, with complete agreements representing higher confidence calls. To aid in comparisons with published Y chromosome analyses performed using the earlier 2016 (v11) version of the ISOGG database, roughly equivalent haplogroups are given in a separate column in Table S1. Due to the nature of the changes of some definitions between versions, users are encouraged to consult the raw data for more specific comparisons (*22*).

Kinship, PCA and ADMIXTURE

The program Relationship Estimation from Ancient DNA (READ) was used to detect the degree of kinship relationships between all the Xinjiang individuals (*53*). From each kinship group, we selected the individual with the highest number of SNPs for subsequent genetic analyses (Table S2).

We performed principal component analysis (PCA) using the smartpca program of the EIGENSOFT package (*54*) with default options and the additional options of lsqproject: YES. We used published ancient and present-day genome-wide data for the 1240k panel downloaded from (https://reich.hms.harvard.edu/) and merged with our Xinjiang individuals (Table S16). In total, we used 67 modern populations (Table S16, Fig. S3) and 64 published ancient populations, and 152 Xinjiang individuals (Table S16, Fig. 2, Fig. S1) and projected all the ancient individuals onto the PCA capturing the genetic variation of all the present-day individuals. In addition, we used 37 West-Eurasian present-day populations for projection to generate the additional PCA (Fig. S2).

To determine the population structure, we used the ADMIXTURE (*26*) program after pruning for linkage disequilibrium using PLINK (*66*) with parameters "--maf 0.05 and --indep-pairwise 200 25 0.5" and running five replicates for each value of K with different seeds to estimate the cross validation (CV) error (Fig. S7). We observed that, K=7 showed the lowest CV error which was used for plotting the results (Fig. 2, Fig. S7).

Regrouping of Xinjiang Individuals

The initial results of PCA and ADMIXTURE suggested high variability among the Xinjiang individuals, we first separated the individuals from different time periods within each site. Later we separated the individuals within each site using PCA and ADMIXTURE as they were showing diverse ancestries. We again merged individuals across sites with similar ancestral components and showing similar genetic affinity using PCA, resulted in the 64 sub-groups shown in Table S1.

***f3* and *f4*-statistics**

To perform the *f3*- and *f4*-statistics comparisons we used the program qp3Pop and qpDstat implemented in the AdmixTools (*27*). The Outgroup *f3*-statistics were of the form *f3(Mbuti; X, Y)*, where the outgroup is the central African "Mbuti" and X and Y include diverse ancient population from Eurasia (Table S16. The *f4*-statistics were of the form *f4(X, Y; Z, Mbuti)*, with Mbuti as an outgroup. Significantly positive f4-statistics indicate that Z shares more alleles with X than Y, while significantly negative *f4*-statistics indicate that Z shares more alleles with Y than X (Z-score > 3, Z-score <-3, respectively).

QpAdm analyses

To estimate the admixture proportions for the Xinjiang populations we used qpAdm software implemented in ADMIXTOOLS (*27*, *28*) and modeled in two stages. The details of the strategy are discussed below:

qpAdm modeling strategies

Analyses using PCA, Admixture, and f3 and f4 statistics suggested that the Xinjiang Bronze and Iron Age populations are admixed and show a wide range of diverse ancestries. Thus, we performed qpAdm modeling in two stages, in the first stage we looked for the more distal source populations which include the populations from the Neolithic (pre-Copper Age populations). For proximal sources, we searched for the populations from the Bronze Age to the Iron Age that could be modeled with our Xinjiang populations. We performed qpAdm analysis on pseudo-haploid genotypes using qpAdm in the ADMIXTOOLS package (*27*) with the option "allsnps: YES". We also discarded any model when the *p*-value of nested models (pnest) >0.01.

1. First we performed the distal modeling to assess the main ancestries present in the Xinjiang populations. We used a similar strategy implemented in (*11*), where we selected a set of outgroups, also known as "reference" or "right" populations and rotated the Neolithic samples as possible source populations for one to five sources.

The outgoup populations are shown below. The populations which are shown in "italics" were rotated to get the distal models:

Mbuti, UstIshim, Kostenki14, GoyetQ1161_N, Villabruna, Natufian, Ami, Mixe, *AfontovaGora3, Iron_Gates_HG, Ganj_Dareh_N, Anatolia_N, West_Siberia_N, Onge, YR_MN, Mongolia_N_East, Shamanka_EN*

2. For the second step, we performed the proximal modeling by selecting source populations that are close temporally to the target populations from Xinjiang. To select optimal outgroup populations among the East Asian ancestry sources, we first analyzed the *f4*-statistics between the Xinjiang individual groups and Ami, Papuan, Onge, Han, Mixe, Tianyuan, Shamanka_EN and DevilsCave_N. We observed that Mixe, Ami, and Onge are more informative as outgroups than the other populations in the group, so we included only these samples as outgroups. Similar outgroups have been used in

previous analyses for Xinjiang individuals (*16*). We considered the qpAdm model to be acceptable if it has $p>0.05$ and if the value of the admixture proportion with the standard error was above zero. Smaller *p*-value indicate that a qpAdm model is poorly fit and should be rejected, but the generally used threshold is not fixed and depends on the analyses. Thus, we occasionally also consider models with $0.01<p<0.05$ to be marginally acceptable. For the BA analysis, we additionally, added populations of hunter gatherers (AfontovaGora3 and Karelia) because these ancestries are important in Xinjiang genetic history.

Outgroups (Base): Mbuti, UstIshim, Kostenki14, Villabruna, Natufian, Mixe, Ami, Onge, Ganj_Dareh_N, Anatolia_N

Proximal Model Sources:
Xinjiang Bronze Age: Afanasievo, Gonur1_BA, Xinj_BA1_TMBA1 (Tarim_EMBA1), AfontovaGora3, Shamanka_EBA, Xinj_BA5_oSte (G218_BA3), Xinj_BA7_oEA (SSG_BA3), YR_MN, WLR_MN, DevilsCave_N, Karelia, Botai_CA

Xinjiang Late Bronze Age: Afanasievo, Sintashta_MLBA, Andronovo, Xinj_BA1_TMBA1 (Tarim_EMBA1), Xinj_BA7_oEA (SSG_BA3), Shamanka_EBA, YR_MN, Gonur2_BA, Gonur1_BA

Xinjiang Iron Age and Historical Era: Xinj_BA1_TMBA (Tarim_EMBA1), Xinj_BA6_oEA (SSG_BA3), Xinj_LBA1, Shamanka_EBA, XiongNu, YR_MN, Gonur1_BA, Sintashta_MLBA, Andronovo, Afanasievo, Gonur2_BA, TianShanHun, TianShanSaka, CentralSaka, Tasmola, Han, SPGT include populations Arkotkila_IA, Barikot_IA, Butkara_IA, Gogdara_IA, Katelai_IA, Loebanr_IA, Udegram_IA.

3. Later we also ran the competition models by putting Afanasievo, Andronovo, Shamanka_EBA, and Gonur1_BA in the outgroup set. For the Bronze Age we also tested competition modeling by putting Botai_CA, and Xinj_BA1_TMBA1 as outgroups to test additional competing models during the Bronze Age.

4. We observed that there are many working models when we used proximal sources especially for IA and HE populations, but the populations used as sources were of a similar nature, as all were derived from similar ancestral sources. Initially, for IA and HE populations, we searched for one-, two- and three- source models derived from three basic ancestries of Steppe_MLBA or Xinj_LBA, BMAC (Gonur1_BA) and East Asian source (Shamanka_EBA, YR_MN), as suggested by the ADMIXTURE and *f3* analysis as for the three main prevalent ancestry sources in IA and HE. After this initial search of the basic ancestry population dataset, and if we did not find any working model fitting our criteria, we again searched for feasible models using other proximal sources, and repeated the method as described above.

5. In addition, we also modeled Xinj_LBA, Xinj_IA and Xinj_HE using Xinjiang_BA and Xinjiang_LBA and Xinj_IA.
Source populations used:
Xinj_BA1_TMBA1, Xinj_BA3, Xinj_BA4, Xinj_BA5_aSte, Xinj_BA6_aBMAC, Xinj_BA7_oEA, Xinj_LBA1, Xinj_LBA2, Xinj_IA1, SPGT, Shamanka_EBA, XiongNu, YR_MN, Gonur1_BA, Gonur2_BA, Han

Time of Admixture

DATES (Distribution of Ancestry Tracts of Evolutionary Signals) method (*11*) was used to estimate the time of admixture in the Xinjiang Bronze Age individuals. For this analysis, we tested both BA, LBA and IA individuals showing the admixtures from only two sources. To convert the DATES output to years BP, we took the range of admixture dates (in generation) with one standard of error from the mean, multiplied this by a generation average time of 29 years, and added it to the mean of the calibrated radiocarbon dates of the samples.

HIrisPlex

Probabilities for eye, hair, and skin pigmentation phenotypes were calculated using the predictive forensics analysis tool, HIrisPlex-S (*36*), which uses 41 SNPs whose predictive accuracy of phenotypes has been previously assessed with modern cohorts. The HPS-MPS pipeline (https://hirisplex.erasmusmc.nl/hps/hps.zip) was adapted to accept mapped reads from both our new Xinjiang genomic data as well as the published Bronze Age Tarim and Dzungarian Basin genomic data from (*16*), all of which were filtered for C to T and G to A mismatches as above, and with mapping quality of 37 or better. To increase the probability that both alleles were identified, we required a minimum coverage of 5x for each SNP to be included in the analysis (giving a 93.75% chance of recovering both alleles, assuming no bias). The samples (*16*) were not deeply covered, and did not have enough SNPs at 5x coverage to allow phenotype predictions. By merging identical individuals with those that were also analyzed in the current study, and reducing the coverage requirement to 3x (giving a 75% chance of recovering both alleles, assuming no bias), we were able to obtain results for hair color for two Tarim Basin1 (Xiaohe) and two Dzungarian Basin (Afanasievo) samples, and skin pigmentation results for these plus a later Xiaohe sample. All results for all samples for which a prediction was obtained, including the prediction accuracy expressed as area under the receiver operating characteristics curve (AUC), adjusted for each sample by taking into account missing SNPs, are given in (Table S15).

Supplementary Text

Description of Archaeological Sites

We obtained direct radiocarbon dates for 104 ancient samples out of 201 individuals from 39 archaeological sites dating 5043 to 481 calibrated years before present (cal BP, Table S1). These samples were selected for radiocarbon dating to ensure that important and representative samples were

directly dated. Specifically, at least one sample was directly dated for each of the sites and/or main clusters. When samples from the same site have been suggested to be from different time periods by archeological evidence, we date at least one sample from each of the suggested time periods; all the genetic outliers have also been dated. Samples were directly dated using radiocarbon (^{14}C) dating techniques through accelerator mass spectrometry (AMS), which were then calibrated using the Int Cal 20 calibration curve (*67*) (Table S1). All ages are reported as cal BP, relative to AD 1950. The 201 individuals used in this study across eastern, western, central, southern and northern Xinjiang are classified into three different time periods: Bronze Age (BA, >5000-3000 BP), Iron Age (IA, ~3000-2000 BP) and Historical Era (HE, <2000 BP).

Northern and Eastern Xinjiang Archaeological sites

1. Ayituohan (AYTH)

The **Ayituohan** site (n=2) is located near the Ashele copper mine in Habahe County in northern Xinjiang. Two individuals (M22B andd M22C) are from the same tomb (M22). The central part of the sarcophagus contained Afanasievo-related cultural artifacts with Indo-European features (*68*). The material objects recovered from this site were different from the Chemurchek culture near the Altai Mountains (*68, 69*). We successfully isolated DNA from two tooth samples. The male individual (M22B, C2034) is directly radiocarbon dated to 4574-4422 cal BP in the Bronze Age.

2. Bolati (BLT)

The **Bolati** site (n=2) is located near Bolati village, Buerjin **(**Burqin) County, Aletai **(**Altay) Region in northern Xinjiang. This site contains cemeteries No.1, No. 3 and No.4. The No. 3 cemetery is located in the southwestern Bolati village and contained 46 tombs. The Sarcophagus M18 contained a standing stone with an anthropomorphic figure associated locally with the Chemurchek culture (*70*). We sequenced two individuals, male and female, from graves M18 and M19. The M18 individual (C1707) was radiocarbon dated to 4814-4450 cal BP and was assigned to the Bronze Age, which was consistent with the archaeological information. The M19 individual (C1708) was radiocarbon dated to 2409-2333 cal BP and was assigned to the Iron Age.

3. Chaganguole (Chagangole, CGGL)

The **Chagangole** site (n=11) is located close to the Chaganguole River, Qinghe County, North Xinjiang. This site contained nine cemeteries and 19 tombs, five of which were well-preserved. The eastern side of one of the tombs (called “Chaganguole-Liangzhanshan”) also contained a standing rectangular pillar with an anthropomorphic figure (*71*). All tombs were rectangular in shape and contained sarcophagi covered within low heap stone piles. In Chaganguole-Jiangbutasicun, the tomb structure suggests a “coffin in a coffin”, with a small sarcophagus built using stones from a larger sarcophagus with four layers of stone slabs stacked on top of it. The large sarcophagus matches a burial style of the late Chemurchek culture, while the small sarcophagus is similar to that of nomadic people from the first millennium BCE (*71*). Among the 11 individuals, ten were from the Bronze Age and were radiocarbon dated to 4521-4297 cal BP, 4148-3927 cal BP, 4284-4090 cal BP, 4352-4096 cal BP and 4352-4096 cal BP in BA. One individual from T4MX (C2042) was dated to the IA, 2310-2053 cal BP.

4. Songshugou (SSG)

The **Songshugou** site (n=10) is situated in Jimunai (Jeminay) County in Aletai Region in northern Xinjiang. The feature of potteries in M15 (C3343) was similar to the EBA Afanasievo culture, which was consistent with the radiocarbon date (5043-4861 cal BP). The individual from M20 (C3344) was radiocarbon dated to 4242-4019 cal BP in BA, which was inconsistent with the sample age suggested by circumstantial archaeological information (*72*). We used the direct radiocarbon date for further this study. The individual from M25 (C3348) was from the Late BA (LBA) and dated to 3336-3077 cal BP. The rest of the remains are from the IA and are grouped together. One of them was dated to 2722-2426 cal BP.

5. Tuoganbai (TGB)

The **Tuoganbai** site (n=6) lies close to the village of Kabuhatale, Saertamu township, Habahe County, northern Xinjiang. The cemetery, No.2 contained tombs: M1, M2, M2A, M2B, M2C, M3, and M4. Tomb M4 contained a rectangular stone stela with an anthropomorphic carving similar to the Chemurchek culture burials and radiocarbon dated to be 4200 BP in the BA (*73, 74*).

6. Dongtalede (DTLD)

The **Dongtalede** site (n=4) is located in the Habahe County region of Aletai, northern Xinjiang. An early assessment of this site suggested it to be from the Spring and Autumn Period of the Western Han Dynasty (*9*, *75*). Unearthed materials from Tomb M2, Area1 included pottery similar to the Okunevo culture of the Minusinsk Basin in the Altai region (*75, 76*). Other Tombs (M5 from Area I, Tomb No. 17) contained bronze and copper arrowheads of a type found extensively in the Eurasian Steppe, similar with those found in Keermuqi site dating from the 6th century BCE, along with agate beads and turquoise processing technologies (*9*, *77, 78*). Other tombs (M27, Area I) in this area include stone and wooden coffins with horse saddles indicating archaeological dates from ~3rd-8th century BCE (*75, 79*). Many ornaments made up of animal bones and gold were also discovered from this site, suggesting a relationship with the Pazyryk culture. In addition, gold pieces were similar to those found at the Aluchaideng site of the Xiongnu culture of Inner Mongolia (*80*). The individual from M5 (C1711) was directly radiocarbon dated to 2705-2370 cal BP in the IA, which was consistent with the archaeological date. The individual from M47 (C1712) was radiocarbon dated to 1058-957 cal BP in the HE.

7. Tuwaxingcun (TWXC)

The **Tuwaxingcun** site (n=1) is located in Buerjin County, northern Xinjiang and close to the Altai Mountains**.** This site includes 55 tombs containing many important burial items including ornaments made from gold, bronze and sheep bones. Horse burials were also observed in this site, suggesting a nomadic way of life. The pottery excavated from tombs M5 and M8 show similarities with the DTLD site, mostly dated to the Early Iron Age (EIA), while more recent tombs date to the Sui and Tang Dynasties (*81*). The single individual (C1709) used in this study was radiocarbon dated to 2308-2120 cal BP in the IA.

8.Kalatasi (KLTS)

The **Kalatasi** site (n=2) is located in Buerjin County, northern Xinjiang. The site contains a pair of anthropomorphic stelae, and was considered to be a remnant of the Chemurchek culture (*82*). Two individuals were sequenced from this site and one (C1706) was directly radiocarbon dated to the IA with the dates ranging from 2318 to 2123 cal BP.

9. Sandaohaizi (SDHZ)

The **Sandaohaizi** (n =1) site is located at Chaganguole village, on the southern slope of the Aletai Region, close to the Chinese and Mongolian border. This site is at the confluence of three mountain lakes known as the "Three Seas". The archaeological site information suggests the single individual (C2057) to be from the Iron Age.

Eastern Xinjiang Archaeological sites

1. Baiyanghe (BYH)

The **Baiyanghe** site **(**n=3) lies in Qitai county, Changji Region, eastern Xinjiang. We successfully sequenced two individuals from tomb M25 (C3617 and C3616) who were directly radiocarbon dated to 2337-2150 cal BP and 2107-1943 cal BP, and one individual from tomb M34 (C3619) who was directly radiocarbon dated to 1178-1000 cal BP in the HE.

Southern Xinjiang Archaeological sites

1. Hetian (Hotan/Khotan, HET) and 2. Shanpula (Sampula, SPL)

The **Hetian** (n=9) and **Shanpula (**n=6) sites are located at Shanpula village, Luopu County, in the Hetian Region of southern Xinjiang. The excavated items displayed both European and East Asian characteristics with most of the objects (70%) excavated from these cemeteries consisting of woolen textiles or items made from wood, porcelain, metal, or glass. The presence of glass objects may link the sites to Central Asia (*83, 84*). These sites share cultural affinities with another Iron Age site from southern Xinjiang (Zhagunluke, ZGLK) (*84*). One individual from tomb M16 (C390) in the HET site was directly radiocarbon dated to 1727-1575 cal BP in the HE. We sequenced six individuals from the SPL site, one of which (C3622) was radiocarbon dated to 1866-1711 cal BP in the HE.

3. Jierzankale (Jirzankal, JEZK)

The **Jierzankale** site (n=13) lies in Tashikuergan (Tazkorgan) County, Kashi (Kashgar) Region, southwestern Xinjiang. Archaeological findings include C3 crops such as barley and wheat which were dated to ~2400 BP (*85*). Wooden burial objects showed similarities with other burial sites in Xinjiang, while bronze vessels unearthed may indicate an East-Asian connection. In addition, fire altars suggest a relationship with Zoroastrianism and the celestial burial types may be linked to those present in the Pamir Plateau region (*85, 86*). Skeletons had both Western and Eastern Eurasian features and $^{87}Sr/^{86}Sr$ isotopic ratios suggests that these individuals were not local, but rather originated outside Xinjiang (*87*). One of the samples from M25 (C1220) was radiocarbon dated to 2683-2347 cal BP in the IA.

4. Liushui (LSH)

The **Liushui** site (n=4) is located at Liushui village, Yutian (Keriya) County, Hetian Region of the southern Tarim Basin, close to the Kunlun Mountains. Animal sacrifices were found in some tombs. Sheep remains were found in tomb M3, M13, M54, M55, and horse remains in M10, M12, M37, M45, M49, M55. The excavated relics consisted of bronze, iron, stone, gold, and some pottery, similar to that associated with the Karasuk culture (3250-2750 BP), which originated from Minusinsk Basin in the Altai region. Other pottery was similar to that associated with the Yanbulake culture in eastern Xinjiang. Bronze axes excavated from tomb M55 resembled those from the Andronovo culture (*88*). All the individuals from M01, M31, M50, and M52 were directly radiocarbon dated to 2775-2728 cal BP, 2843-2745 cal BP, 2992-2798 cal BP and 2715-2439 cal BP, and were assigned to the IA in this study.

5. Zhagunluke (Zaghunluq, ZGLK)

The **Zhagunluke** site **(**n=16) is in Qiemo (Qarqan/Cherchen) County, southern Xinjiang. The tombs contained black pottery, wooden barrels and combs. These items suggest a link to cultures such as Pazyryk in the Altai region near Kazakhstan (*77, 89*). We successfully sequenced 16 individuals from this site, six of which were radiocarbon dated to 2302-2059 cal BP, 2292-2004 cal BP, 2465-2342 cal BP, 2000-1889 cal BP, 2111-1942 cal BP and 2491-2339 cal BP in the IA.

Central Xinjiang Archaeological sites

1. Xianshuiquangucheng (XSQG)

The Xianshuiquangucheng site (n =2) is located in Xinashuiquan Ancient City of Yuli County, Bayinguoleng (Bayingolin) Region in the Central part of Xinjiang. Teeth were recovered from two individuals in the same tomb M3 and were successfully sequenced. One, a male individual (C2032), was dated from 1880-1742 cal BP in the HE.

2. Xikakandasayi (XKKD)

The Xikakandasayi site (n=1) is located at Aoyiyayilake village, Qiemo County, Bayinguoleng Region, close to Tibet in Xinjiang. The archaeological context suggests the individual is from the Iron Age. The single individual from M4 (C795) was directly radiocarbon dated to 1696-1544 cal BP.

Western Xinjiang Archaeological sites

1. Abusanteer (ABST)

Abusanteer site (n= 7) is located at Aixinsheli village, Chabuchaer (Qapqal) County, Yili (Ili) Region in western Xinjiang, close to the Kazakhstan border. The cultural affinity suggest that the individuals were from the Iron Age. A distinct feature is found in tomb M27, which is surrounded by two stone rings with stones shaped like toads, possibly linking it to the Yangshao culture in the Central plain, Majiayao culture in Gansu-Qinghai Province, and Taosi site in Shanxi Province. Toad worship found in the Yili

Region may indicate the connection between the Yili region and the Central Plain. Two individuals from M6 (C4127) and M24 (C4131) were directly radiocarbon dated to 2340-2152 cal BP and 2739-2494 cal BP in the IA, and one individual from M14 (C4140) was directly radiocarbon dated to 1865-1709 cal BP in the HE.

2. Eminhuojierte (EMHJ)

Eminhuojierte site (n=1) is located in Huojierte Mongol township, Emin County, Tacheng Region. The single individual from M29 (C4255) was directly radiocarbon dated to 2678-2356 cal BP, and was assigned to the IA in this study.

3. Kafulang (KFL)

Kafulang site (n=1) is in Tekesi County, Yili Region, western Xinjiang. The single individual from M1 (C4149) was directly radiocarbon dated to 1058-958 cal BP, and was assigned to the HE in this study.

4. Keqikesubutai (KQKS)

The Keqikesubutai cemetery (n=1) is in Subutai township, Nileke (Nilka) County, Yili Region. The single individual from M4A (C4150) was directly radiocarbon dated to 1686-1419 cal BP, and was assigned to the HE in this study.

5. Wulanbuluke (WLBL)

The **Wulanbuluke** site (n=3) is found at Wulanbuluke village, Nileke County, Yili Region. Among the three individuals, one from southern M3 (C4278) was directly radiocarbon dated to 2335-2147 cal BP and was assigned to IA in this study.

6. Qiafuqihaishuiku (QFQH)

Qiafuqihaishuiku site (n=1) is at Kalatuohai village, Tekesi County, Yili Region. Funerary objects were found in 39 of the 73 tombs, and contained pottery, bronze, iron, stone, and animal bones (mainly sheep bones). The 73 tombs were divided into three regions by their geographical location: eastern, western, and middle, with tombs M01-M35, M54, M55, and M57-M59 in middle region; 13 tombs (M60-M72) in the eastern region, and 20 tombs (M36-M53, M56 and M73) in the western. The features of tombs and human bones observed from the eastern and middle regions show some similarity. Moreover, some pottery in the Han style was excavated from some eastern and western region tombs of this site. Bronze coins found at some tombs in the western region may have come from the eastern Han. QFQH is considered to be associated with Scythian-Wusun remains (700-300 BCE), with some tombs containing artifacts linked to the late eastern Han Dynasty (*90*). The single individual from M25 in A_XV region (C4276) was directly radiocarbon dated to 2492-2347 cal BP and was assigned to the IA in this study.

7. Axile (AXL) and 8. Sahaxibei (SHXB)

The **Axile** (n=2) and **Sahaxibei** sites (SHXB, n=1) are located in Zeketai, Xinyuan County, Yili Region. The two samples from M4 (C3362) and M6 (C3363) in AXL were directly radiocarbon dated

to 2340-2156 cal BP and 2347-2159 cal BP, the single individual from M5 (C3365) in SHXB site was dated to 2704-2362 cal BP. All of these individuals were assigned to the IA in this study.

9.Dongmaili (DML) and 10. Wuzan (WZ)

Both **Dongmaili** (n=3) and **Wuzan** (n=5) sites are located in Jilintai Power Station in Nileke County, Yili Region in western Xinjiang. The two individuals from M24 (C847), and M31A (C799) in WZ were directly radiocarbon dated to 2693-2349 cal BP and 2490-2336 cal BP and were assigned to the IA in this study.

11. Jirentaigoukou (JRTG)

The **Jirentaigoukou** site (n=11) is located in the Qialegeer village, Nileke County, Yili Region in western Xinjiang (*91, 92*). The material objects and remains were dated from the Bronze Age to the historical times of the Song and Yun Dyanaty (*93*). Also, coal was excavated from this site, which predates the history of coal use by more than 1000 years in China (*93*). The pottery, copper, and the Bronze Age artefacts are associated with the Andronovo culture. We successfully radiocarbon dated all 11 individuals and eight dated to the Iron Age, ranging from 2351 to 2056 cal BP, two individuals from M49 (C1367) and M75 (C1365) were directly radiocarbon dated to the LBA (3166-3002 cal BP and 3341-3150 cal BP), and one from M4 (C1370) was dated to the HE to 1346-1290 cal BP.

12. Junmachanyilian (JMCY)

The **Junmachanyilian** cemetery (n=6) is located in Tekesi County, Yili Region. Excavated Pig Iron materials suggest the presence of iron smelting technologies in Xinjiang (*94*). All the sequenced individuals were directly radiocarbon dated, two of them from M14 (C1650) and M8 (C1655) were directly radiocarbon dated to the IA (2490-2350 cal BP and 2402-2332 cal BP). The other four individuals were dated to the HE with dates of between 1688-1413 to 642-515 cal BP.

13. Kuokesuxi (KKSX)

The **Kuokesuxi** No.2 tomb group (n=8) is located in the Southeast of Tsoutheast of Tekesi County, Yili Region in western Xinjiang. The first excavation of 30 tombs in the eastern part was carried out in 1978 by the Institute of Archaeology of the Xinjiang Academy of Social Sciences, and 93 more graves were excavated in 2010 (*95*). The archaeological excavation reports showed the individuals in KKSX site were divided into two time periods: BA and EIA according to the artifacts: Pottery from M53 showed Andronovo cultural features in the LBA, and iron objects found in M2S, M16, M17, M18, M20, M66, and M89_C1 were assigned to the IA. (*95*). We successfully sequenced eight individuals, among them seven were directly radiocarbon dated from 2488-2349 to 2094-1974 cal BP, and were assigned to the IA. One from M53 (C1662) was dated to the LBA (3448-3271 cal BP). All the radiocarbon dates were consistent with the archaeological dates.

14. Tielieketesai (TLKT)

Tielieketesai site (n=3) is located at Kalaaoyi village, Xinyuan County, Yili Region. Two individuals from M3 (C3354) and M6A (C3356) were directly radiocarbon dated to 2341-2158 cal BP and 2099-2009 cal BP, assigned to the IA.

15. Caishichang (CSC)

The **Caishichang** (n=8) site is located in Nileke County, Yili Region in western Xinjiang. We successfully radiocarbon dated three individuals from M6 (C3320), M3 (C3318), M1 (C3315), and with a range of 2345-2159 cal BP, 2286-2003 cal BP and 2102-1973 cal BP, which were all assigned to the IA.

16. G218 (G218)

The **G218** site (n=10) is located close to the Gongnaisi River, Nileke County, Yili Region, western Xinjiang. A total of 112 tombs were excavated (*96, 97*). Importantly, the M5 tomb had two Afanasievo culture-type pots, with human bones dating to ~4800-4600 BP (*96, 97*). Three samples were from the tomb M5 in this study, two of them (C3339, C3341) were directly radiocarbon dated to 4963-4839 cal BP and 4815-4526 cal BP in the BA, consistent with the archaeological dates. Six individuals were from the IA and three of them M61 (C3324), M20 (C3325), and M64 (C3333) were radiocarbon dated to 2336-2153 cal BP, 2111-1942 cal BP and 2311-2124 cal BP in the IA. One individual from M15 (C3326) was dated to 669-555 cal BP in the HE.

17. Guanjingtai (GJT)

The **Guanjingtai** (n=1) is located in Nileke County, Yili Region. The single individual from M7 (C3316) in this site was dated to 2111-1942 cal BP, which was assigned to the IA in this study.

18. Tangbalesayi (TBLS)

The **Tangbalesayi** site (n=11) is located in Karwoyi village, Nileke County, Yili region, West Xinjiang. In total, 26 tombs were discovered which included 15 earth tombs, and 11 stone tombs from the Bronze Age (M12-17, M23, M24, M26), Iron Age (M2, M3, M5-8, M11, M18, M20, M21, M25), and the rest from a later time period (M1, M4, M9, M10, M19, M22 (*98*). The Bronze Age tombs show cultural affinity with the Andronovo culture, while the Iron Age burials appear to be associated with the Saka and Wusun (dated to the 5th and 3rd centuries BCE) (*98*). Five individuals were directly radiocarbon dated, the individual from M3 (C1714) was dated to 3571-3460 cal BP in the LBA, three of them from M8 (C787), M19A (C4260), and M1 (C628) were dated to 2318-2123 cal BP, 2301-2002 cal BP, and 2305-2064 cal BP in the IA, one sample from M22 (C789) was dated to 959-919 cal BP in the HE. Among them, the radiocarbon dates of M3 (C1714) in LBA, and M19 (C4260) and M1 (C628) in the IA were inconsistent with the archaeological dates, we used the radiocarbon dates for further analysis.

19. Wutulan (WTL)

The **Wutulan** (n=13) site is located north of Wulanbuluk village, Nileke County, Yili Region. Seventeen tombs along with three sacrificial sites were excavated in 2001, 2006, 2013, and 2014. The Tomb structures were dated archaeologically to the Bronze Age (tombs M1-4, and M15-17 excavated

in 2013), early IA (M7-M12, M14 excavated in 2013, and M6, M7A/B, M8 excavated in 2014, and some individuals excavated in 2001 and 2006), and West Han Dynasty (M5-M6 excavated in 2013, M1A/B/C, M2, M3A/B/C/D, M4A/B/C, M5 excavated in 2014, and some individuals excavated in 2001 and 2006) (*99*). Two individuals from M4 (C1639) and M17 (C4282) were directly radiocarbon dated to 3570-3412 cal BP and 3451-3374 cal BP in the LBA, the remaining samples gave dates ranging from 2353-2183 cal BP to 2299-2007 cal BP in the IA. All the radiocarbon dates were consistent with the archaeological dates.

20 Ayousaigoukou (AYSG)

The **Ayousaigoukou** site (n=4) is located in Zeketai, Xinyuan County in western Xinjiang. From this site a total of 315 tombs were discovered, seven of which have been excavated so far. The objects found in these tombs suggest an affinity with an Andronovo-related culture and belong to high status individuals (*100, 101*). All the individuals sequenced were directly radiocarbon dated, three of them from western M2 (C1660), M6 (C1658), and M7 (C1659) gave dates ranging from 2704-2362 cal BP, 2342-2154 cal BP, and 2342-2154 cal BP in the IA, and the sample from M2M (C1661) was dated to 515-481 cal BP in the HE.

21. Simutasi (SMTS)

The **Simutasi** site (n=3) is located in Zhaosu County, Yili Region, western Xinjiang. Almost 200 tombs were discovered, widely distributed west of the Akeyazi River. The individual from M88 (C1678) was directly radiocarbon dated to 2343-2156 cal BP in IA, and that from M70 (C1677) was dated to 957-793 cal BP in the HE.

22. Zeketai (ZKT)

The **Zeketai** site (n=2) is present in Zeketai, Xinyuan County, Yili Region. Unearthed objects include many Bronze artifacts dating from the Spring and Autumn period to the Han Dynasty. The two individuals in this study were from the same tomb M01B, and the individual C3359 was directly radiocarbon dated to 2116-1939 cal BP in the IA.

Unknown Archaeological site information

Archaeological site information is unavailable for ‘Xinj_Unknown’ (n=1), however the PCA and ADMIXTURE analyses suggest this sample is similar to IA samples.

Sample curation using kinship results and archeological records

Among these 201 individuals, six pairs of individuals were classified as twin/same individual in the kinship analysis:

C2034 (teeth) from site ‘AYTH’ in Habahe County and C794 (teeth) from a site listed as “Habahe”: the two samples were collected in two separate periods of sampling. Archaeological information about the site Habahe, from which C794 was collected, was unavailable. Although the site information of these two individuals is different, the burial numbers of the two samples are the same - both M22B.

Considering the kinship result suggested the two individuals were “Identical twins/Same individual”, these two samples are likely collected from the same individual. Therefore, we selected the sample (C2034, AYHT site) with a higher number of SNPs for further analysis (Table S1).

C1713 (bones) and C1711 (teeth) from site ‘DTLD’: both of them were excavated from the tomb ‘M5’, and the archaeological reports showed only one individual was buried in this tomb (*76*). As the kinship result also suggested these two individuals were “Identical twins/Same individual”, C1713 and C1711 are likely obtained from the same individual. Therefore, we selected the sample (C1711) with a higher number of SNPs for further analysis (Table S1).

C4257 (teeth) and C627 (teeth) from site ‘TBLS’: the archaeological records showed both of them were excavated from the same tomb (M7), and only one individual was identified in this tomb (*100*). The kinship results suggest these two individuals were “Identical twins/Same individual”, confirming C1713 and C1711 were sampled from the same individual. Therefore, we selected the sample (C627) with a higher number of SNPs for further analysis (Table S1).

C629 (teeth) and C789 (teeth) from site ‘TBLS’: the archaeological records suggest they were excavated from the same tomb (M22), in which only one individual was found (*100*) The kinship results found these two individuals were “Identical twins/Same individual” and confirmed they were sampled from the same individual. Therefore, we selected the sample (C789) with the highest number of SNPs for further analysis (Table S1).

C4263 (teeth) and C785 (teeth) from site ‘TBLS’: the two samples were collected in two separate periods of sampling, and the tomb number of both is M5. The kinship result suggests these two individuals were “Identical twins/Same individual”, thus they are likely the same individual. We selected the sample (C785) with a higher number of SNPs for further analysis (Table S1).

C1659 (teeth, tomb number M7) and C1658 (teeth, tomb number M6) from ‘AYSG’: these two individuals were excavated from different tombs, and the kinship results suggest they were “Identical twins/Same individual”. We selected the sample (C1658) with a higher number of SNP for further analysis (Table S1).

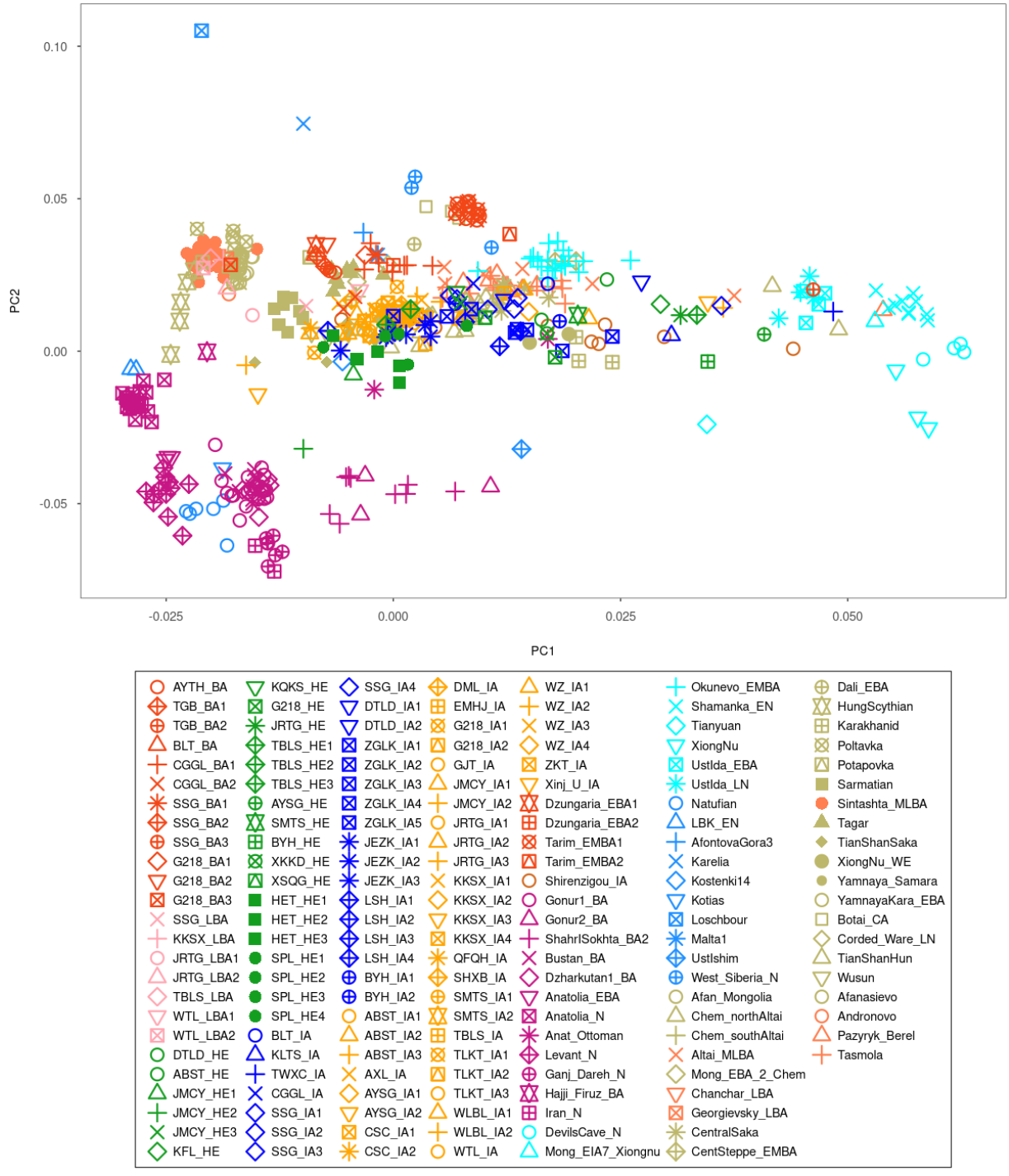

Fig. S1. Principal component analysis (PCA) of all ancient Xinjiang individuals along with ancient-Eurasian populations. The Bronze Age populations show greater affinity with Siberian/North-East Asian populations compared to the Iron Age and Historical Era (HE) Xinjiang populations, which lie along a cline of Eurasian populations extending from east to west Eurasia.

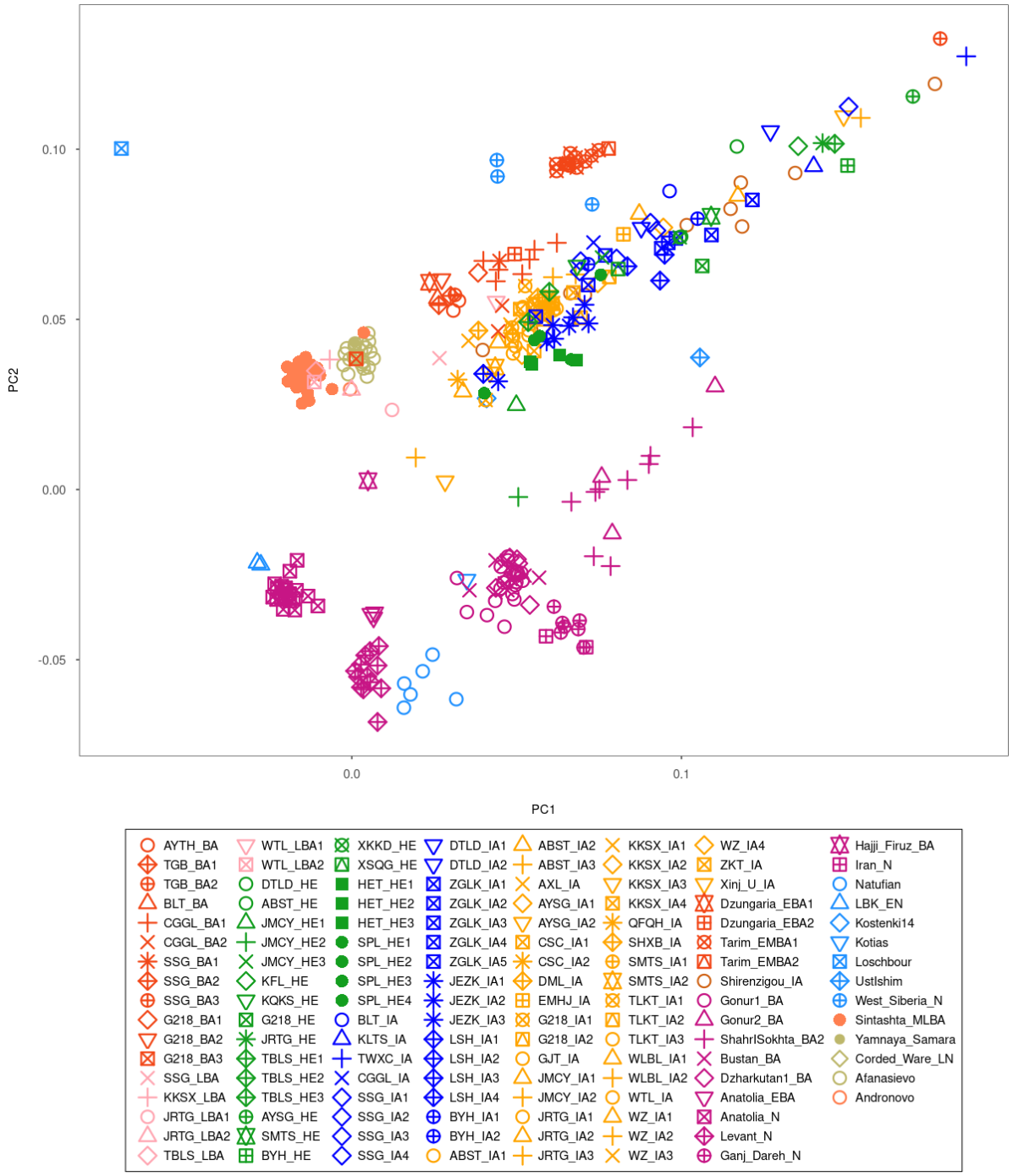

Fig. S2. Principal component analysis (PCA) of all ancient Xinjiang individuals along with ancient West- Eurasian populations. After removing the East-Eurasians, all the other West-Eurasian populations are used for projection. We observe similar orientation and cline of Xinjiang individuals as observed in Fig S1. The Xinjiang individuals with East Asian affinity are separated from the larger group of Xinjiang individuals that clusters close to the ancient populations with Steppe ancestry.

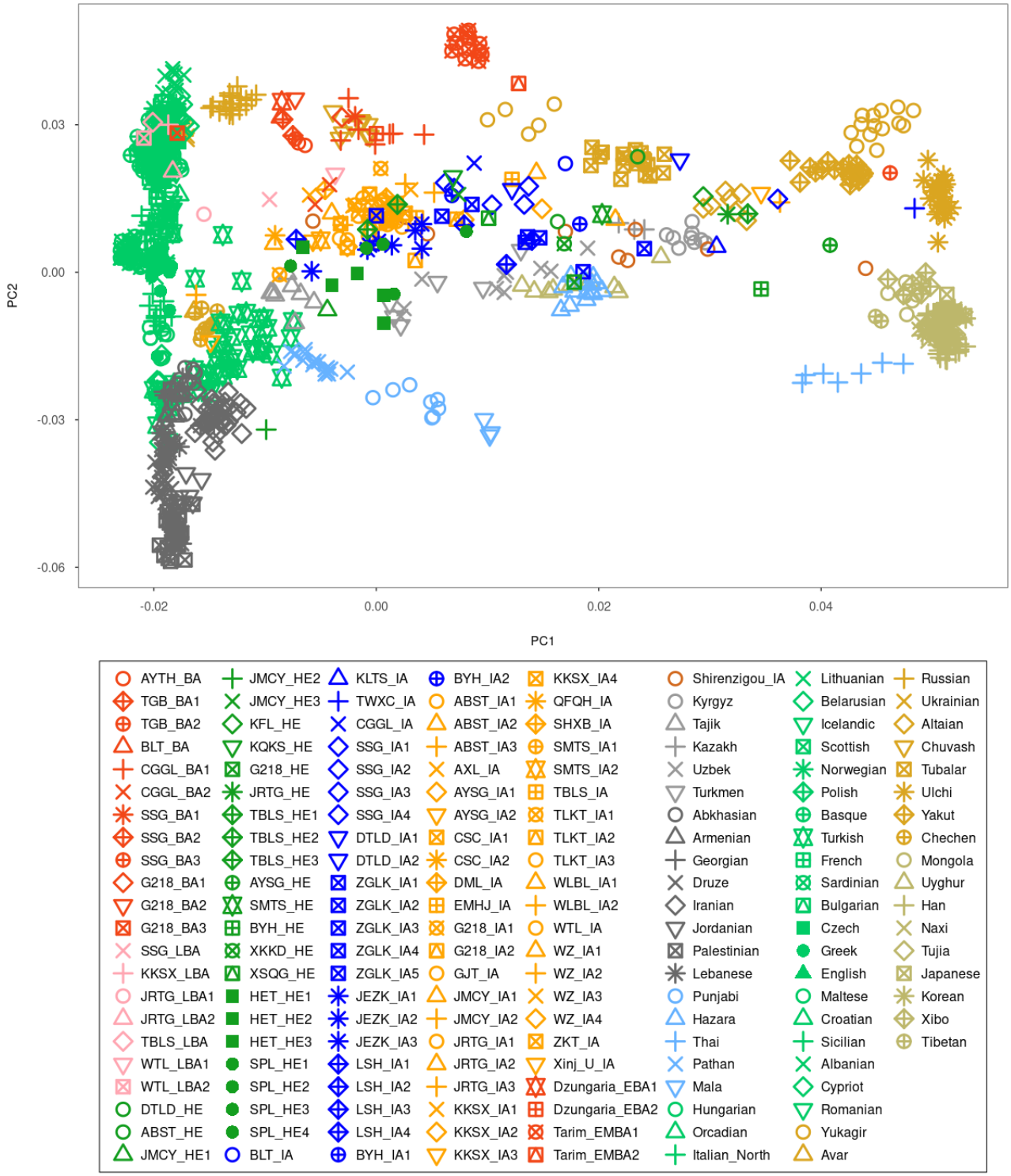

Fig. S3. Principal component analysis (PCA) of all ancient Xinjiang individuals along with present-day populations. The Bronze Age populations show greater affinity with present-day Siberian populations compared to the Iron Age and Historical Era (HE) Xinjiang populations which lie along a cline of Eurasian populations extending from west to east. Outlier present-day populations Surui, Australian, Papuan, Mixe, Egyptian, Atayal, and Onge were removed.

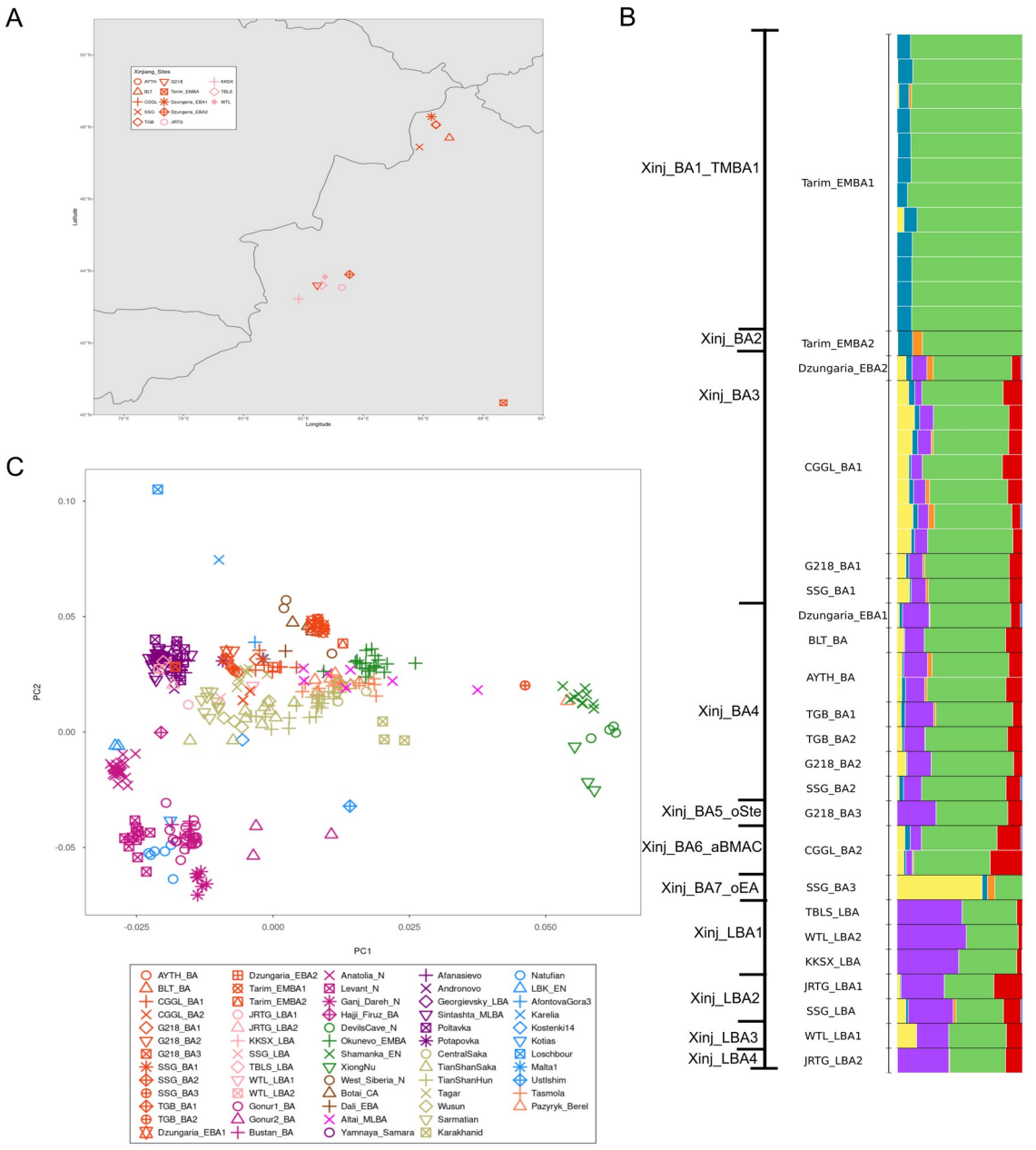

Fig. S4. Archaeological sites, ADMIXTURE and PCA plots of Xinjiang Bronze and Late Bronze Age populations A. Geographic locations of all Xinjiang BA and LBA populations. B. Admixture plot with K=7. The four major ancestry components are maximized in populations: ANE (green), Iranian farmer (red), Anatolian farmer (violet), East Asian Hunter Gatherer (yellow). The other three are maximized in Han (orange), Mixe (cyan), and Papuan (dark blue). C. PCA of BA and LBA Xinjiang individuals projected onto present-day populations. Only a limited number of ancient populations are shown. We have combined our dataset with the published populations of Tarim_EMBA and Dzungaria_EBA from Xinjiang *(16)*.

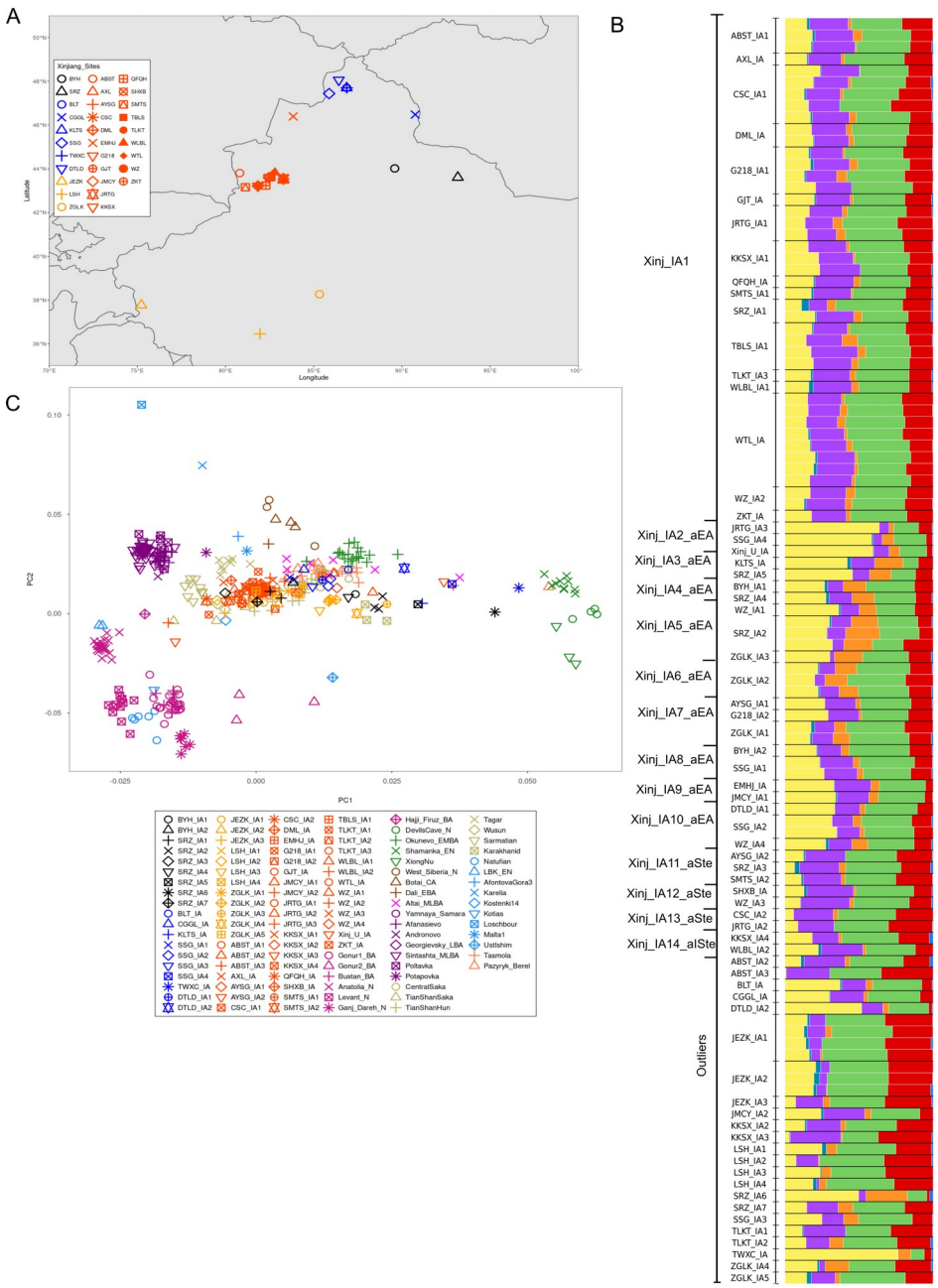

Fig. S5. Archaeological sites, ADMIXTURE and PCA plots of Xinjiang Iron Age populations A. Geographic locations of all the Xinjiang IA populations. B. Admixture plot with K=7. The four major components are maximized in populations: ANE (green), Iranian farmer (red), Anatolian farmer (violet), East Asian Hunter Gatherer (yellow). The other three are maximized in Han (orange), Mixe (cyan), and Papuan (dark blue).C. PCA of IA Xinjiang individuals projected onto present-day populations. Only a limited number of ancient populations are shown. The published Xinjiang IA population from Shirenzigou site is represented with SRZ _IA in the PCA and ADMIXTURE.

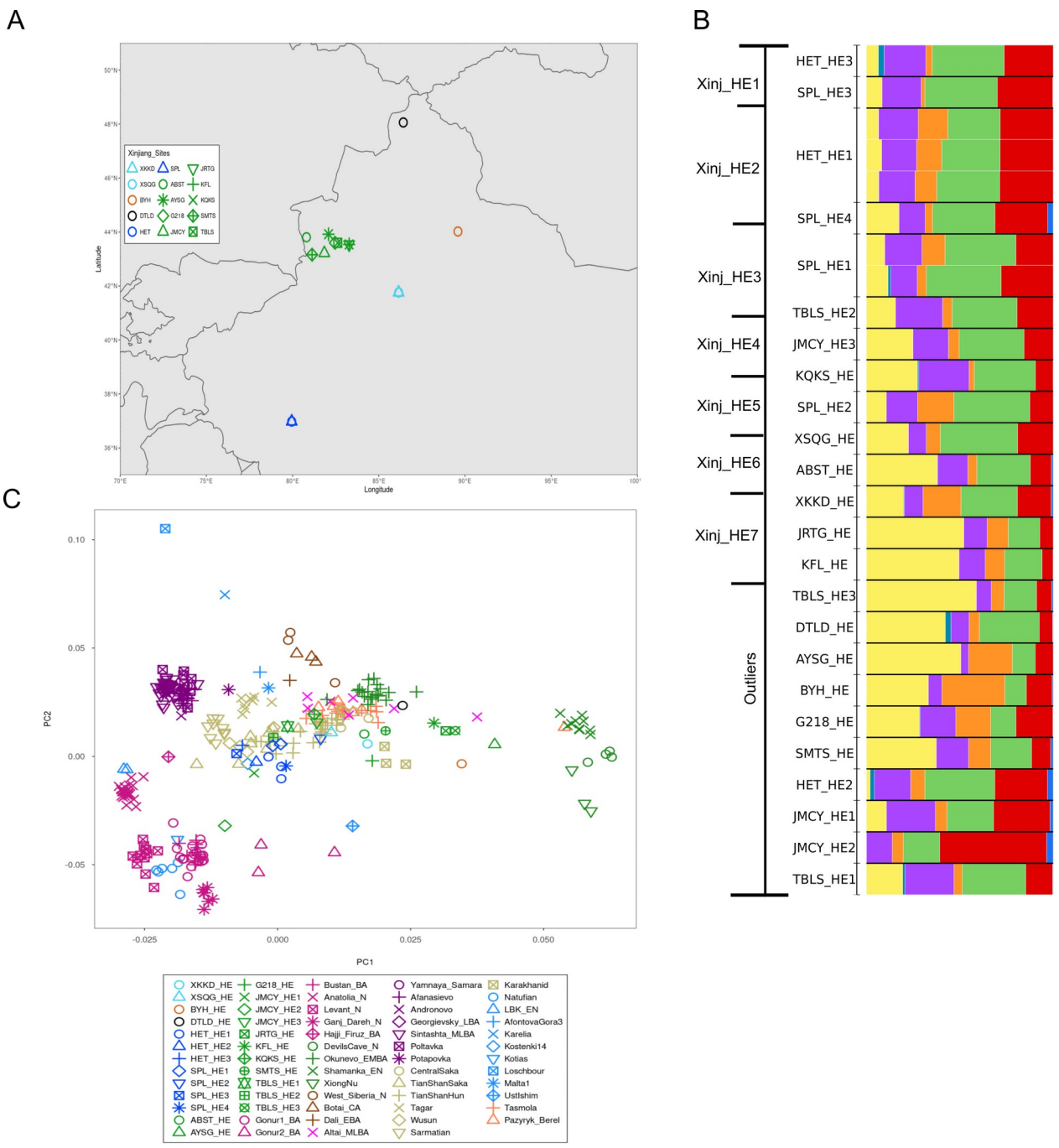

Fig. S6. Archaeological sites, ADMIXTURE and PCA plots of Xinjiang Historical Era (HE) populations. A. Geographic locations of all the Xinjiang_HE populations B. The four major components are maximized in populations: ANE (green), Iranian farmer (red), Anatolian farmer (violet), East Asian Hunter Gatherer (yellow). The other three are maximized in Han (orange), Mixe (cyan), and Papuan (dark blue). C. PCA of Xinj_HE individuals projected onto present-day Eurasian populations. For clarity, only a limited number of ancient populations are shown.

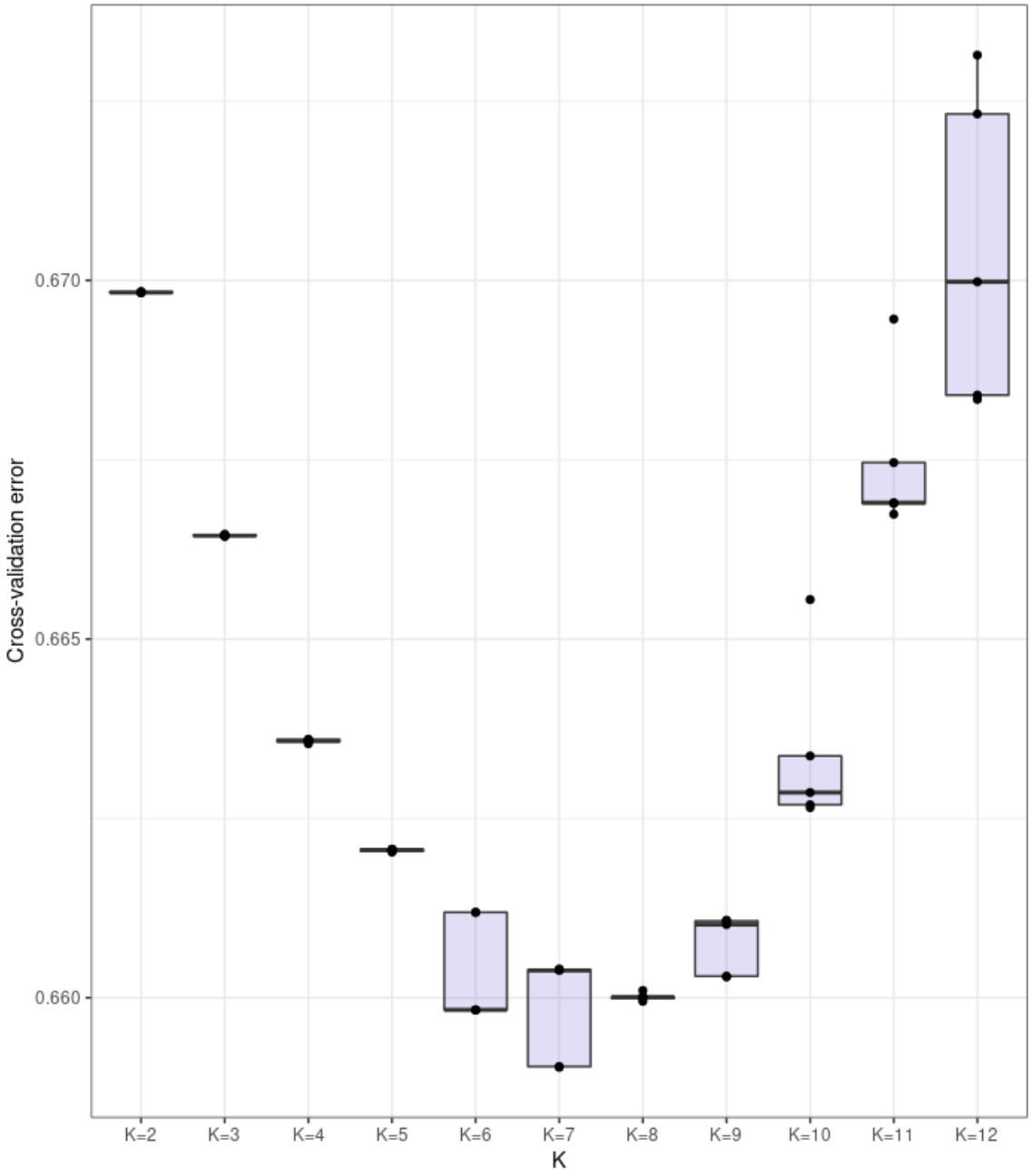

Fig. S7. Admixture cross-validation error analysis for K (K=2-12) with five replicates. Admixture with K=7 showed the lowest Cross Validation (CV) error.

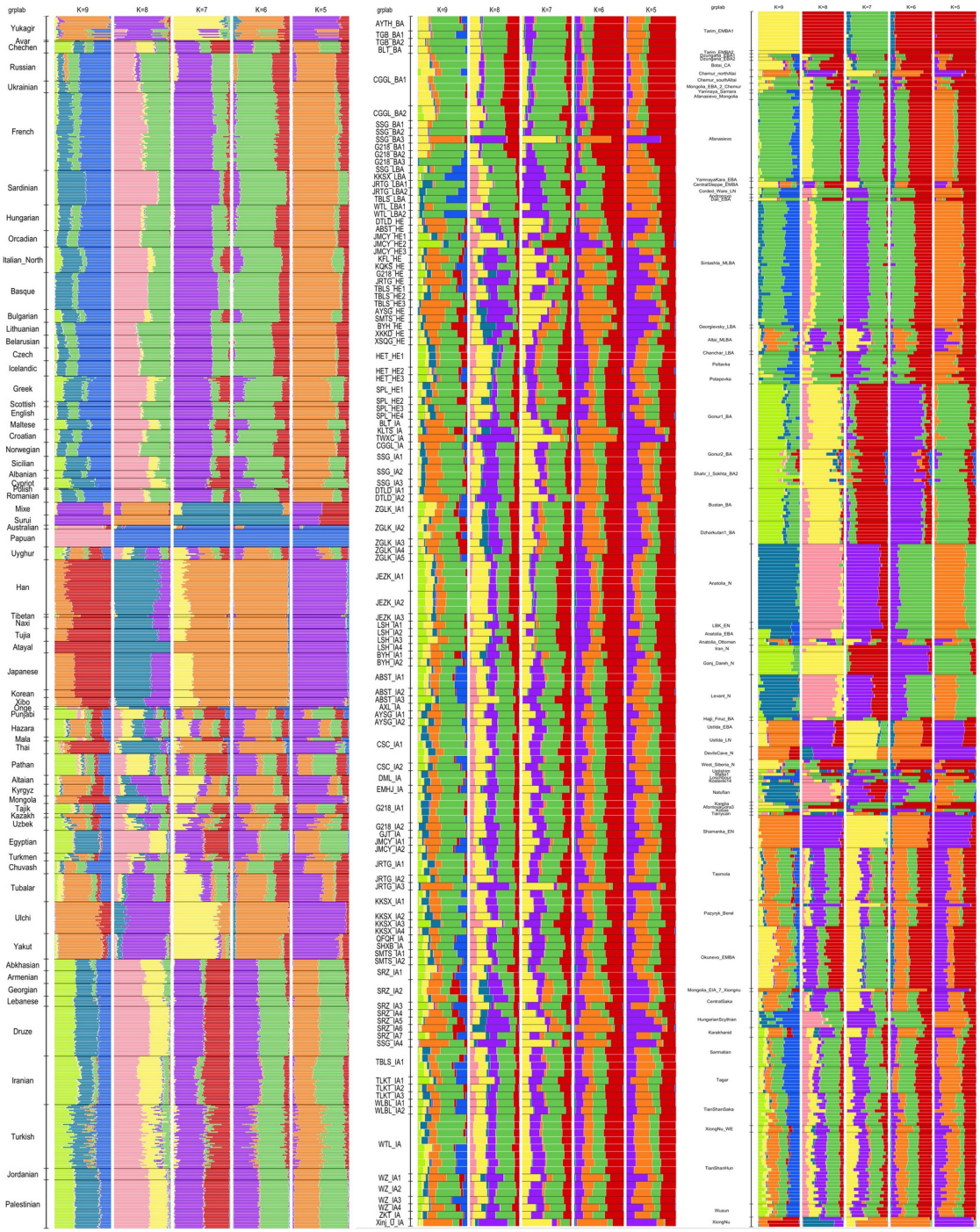

Fig. S8. Results of ADMIXTURE run from K=5-9 with 5 replicates. ADMIXTURE run with K=7 gave the lowest Cross Validation (CV) error. The four major components are maximized in populations: ANE (green), Iranian farmer (red), Anatolian farmer (violet), East Asian Hunter Gatherer (yellow). The other three are maximized in Han (orange), Mixe (cyan), and Papuan (dark blue).

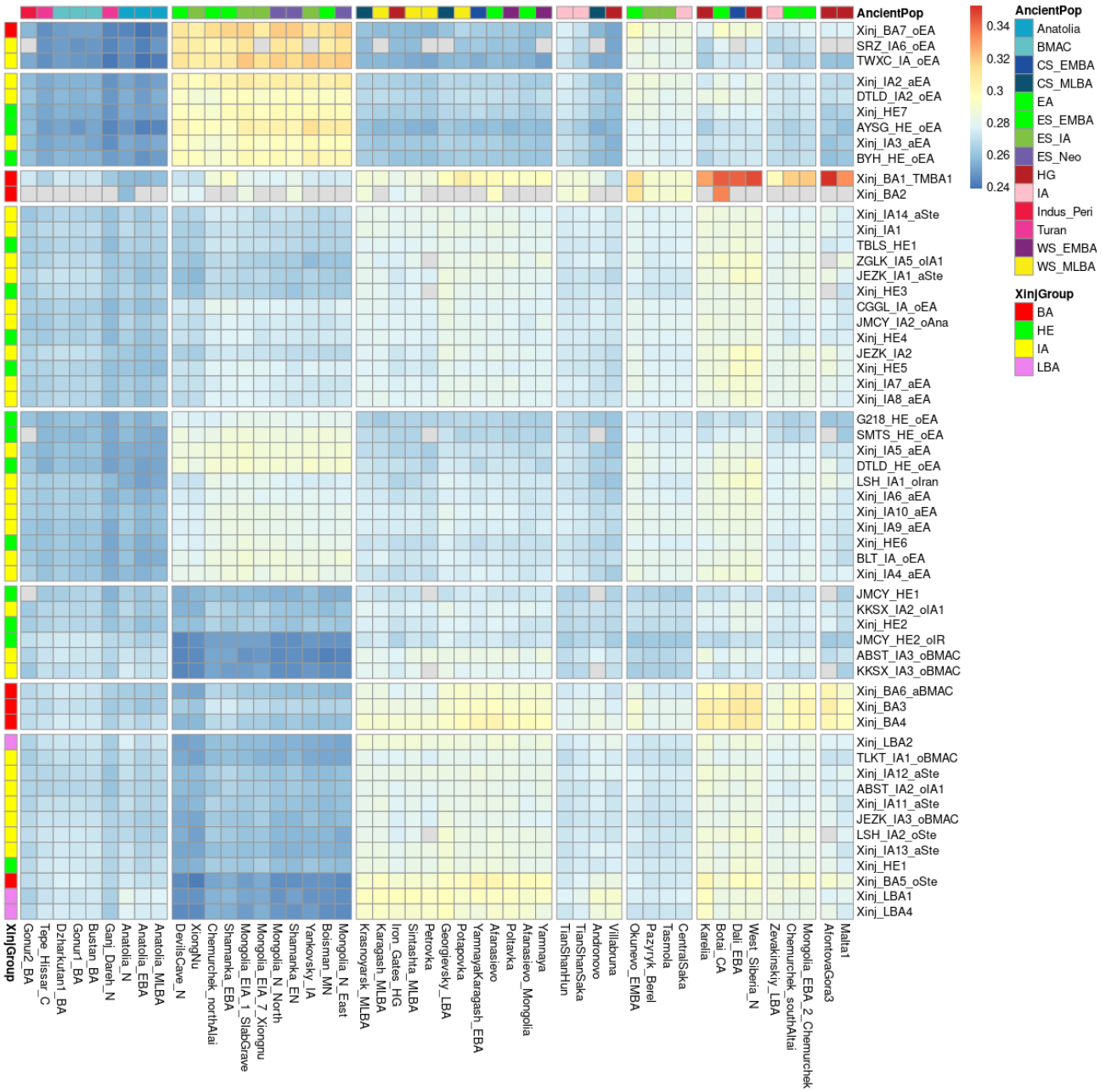

Fig. S9. Outgroup f_3-statistics of all Xinjiang populations with selected ancient Eurasian populations. Ancient populations are grouped as Anatolia, Bactria Margiana Archaeological Complex (BMAC), Central Steppe EMBA (CS_EMBA), Central Steppe MLBA (CS_MLBA), East Asian (EA), Eastern Steppe IA (ES_IA), Eastern Steppe Neolithic (ES_Neo), Hunter Gatherer (HG), Iron Age (IA), Indus Periphery (Indus_Peri), Turan region, Western Steppe EMBA (WS_EMBA) and Western Steppe MLBA (WS_MLBA). Xinjiang populations were divided into Bronze Age (BA), Late Bronze Age (LBA), Iron Age (IA) and Historical Era (HE). Only populations with a minimum of 100,000 SNPs in f_3-statistics comparisons are plotted. All the f_3 values have Z-score >3.0.

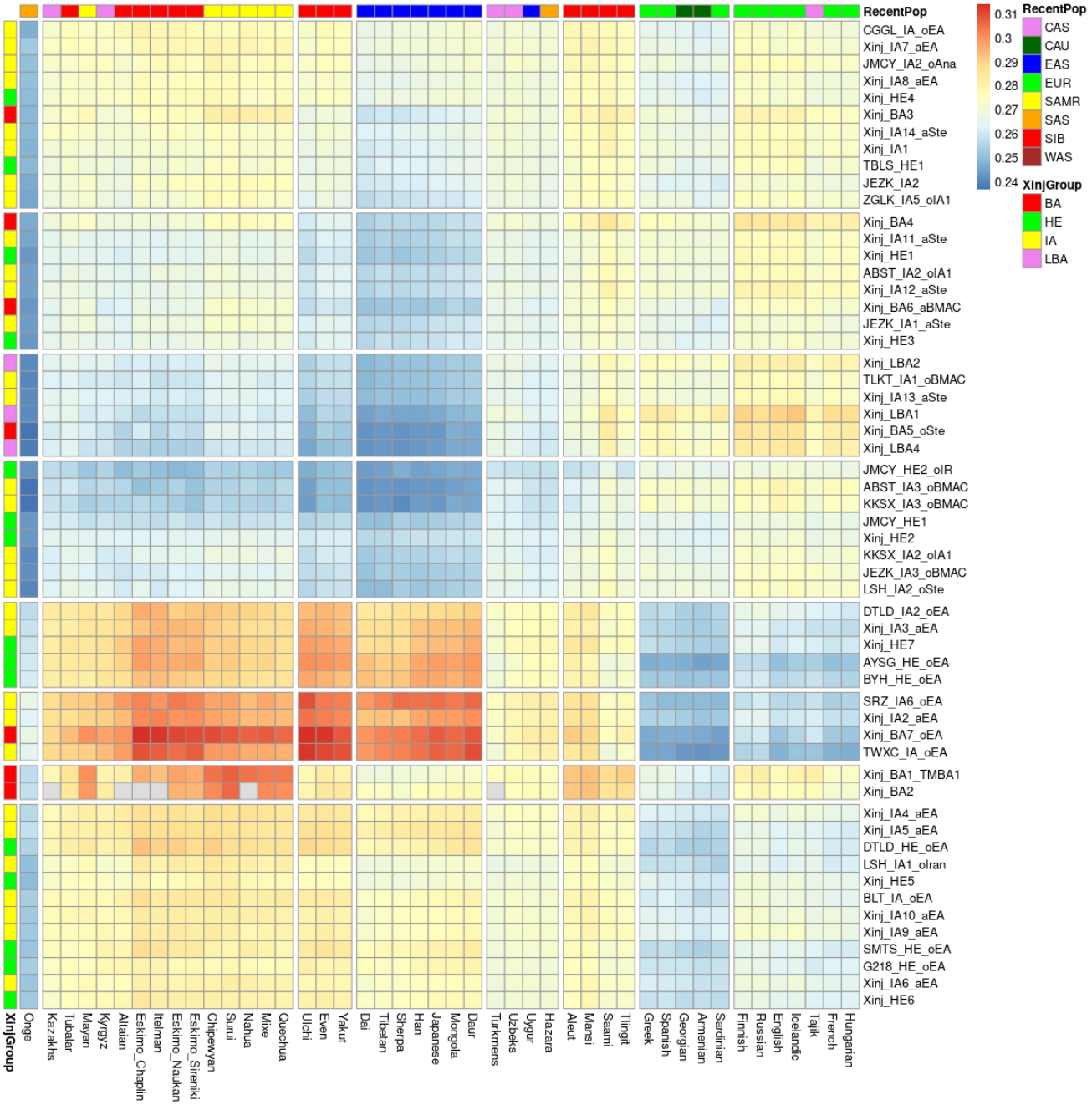

Fig. S10. Outgroup f_3-statistics of all Xinjiang populations with selected present-day east and west Eurasian and South American populations. Present-day populations are grouped as Central Asia (CAS), Caucasus (CAU), East Asia (EAS), Europe (EUR), South America (SAMR), South Asia (SAS), Siberia (SIB) and West Asia (WAS). Xinjiang populations were divided into Bronze Age (BA), Late Bronze Age (LBA), Iron Age (IA) and Historical Era (HE). Only populations with a minimum of 100,000 SNPs in f_3-statistics comparison are plotted. All the f_3 values have Z-scores >3.0.

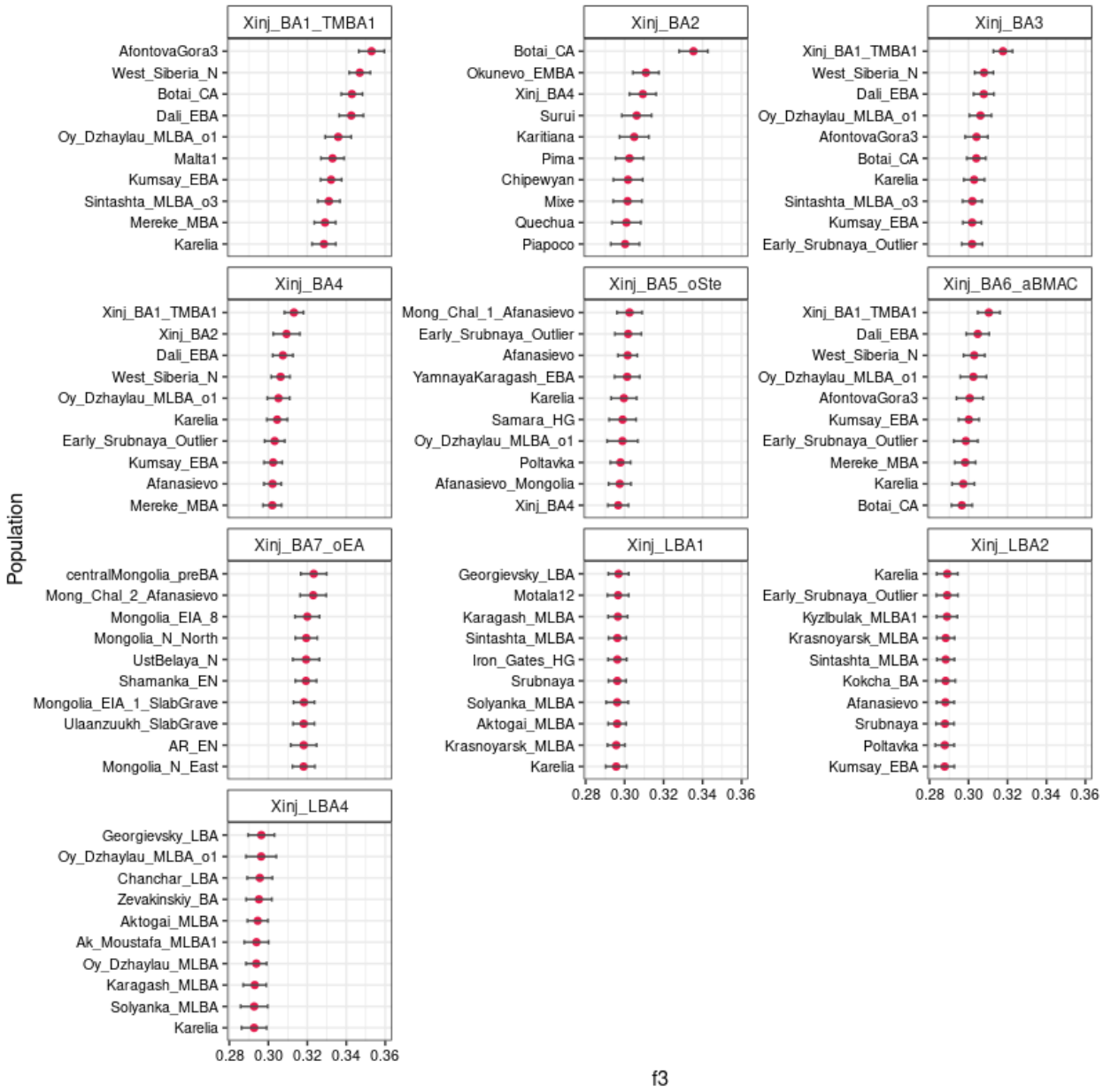

Fig. S11. Top ten Outgroup f_3-statistics results of Xinj_BA and Xinj_LBA with ancient Eurasian populations. The f_3-statistics are of the form f_3*(Ancient population, Xinjiang Population; Mbuti)*. Only populations with a minimum of 100,000 SNPs in the f_3-statistics comparisons are plotted. All the f_3 values have Z-scores >3.0.

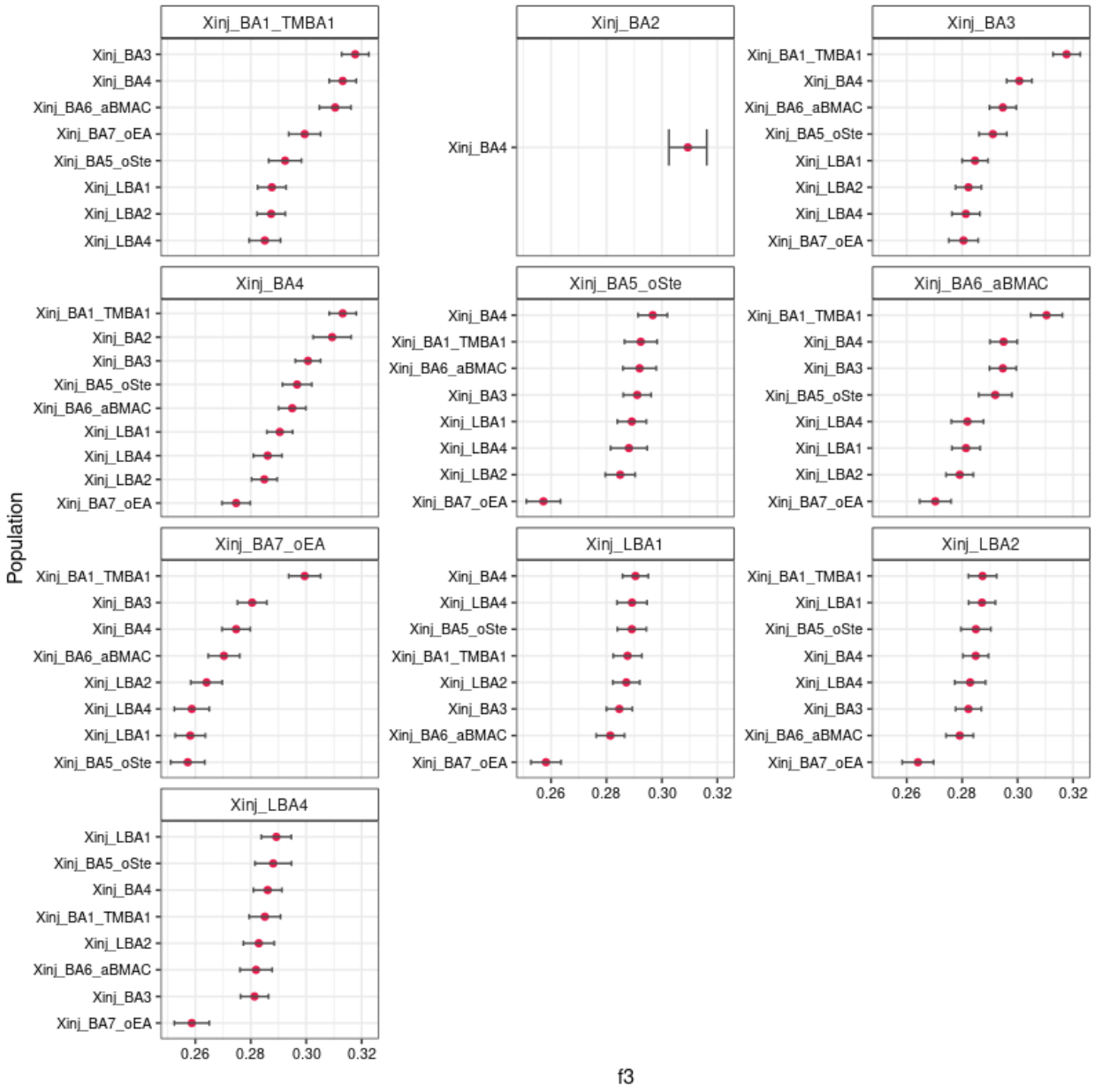

Fig. S12. Outgroup f_3-statistics results for ancient Bronze and Late Bronze Age Xinjiang populations. The f_3-statistics are of the form f_3*(Xinj_BA/LBA, Xinj_BA/LBA; Mbuti)* were tested. Only populations with a minimum of 100,000 SNPs in the f_3-statistics comparison are plotted. All the f_3 values have Z-scores >3.0.

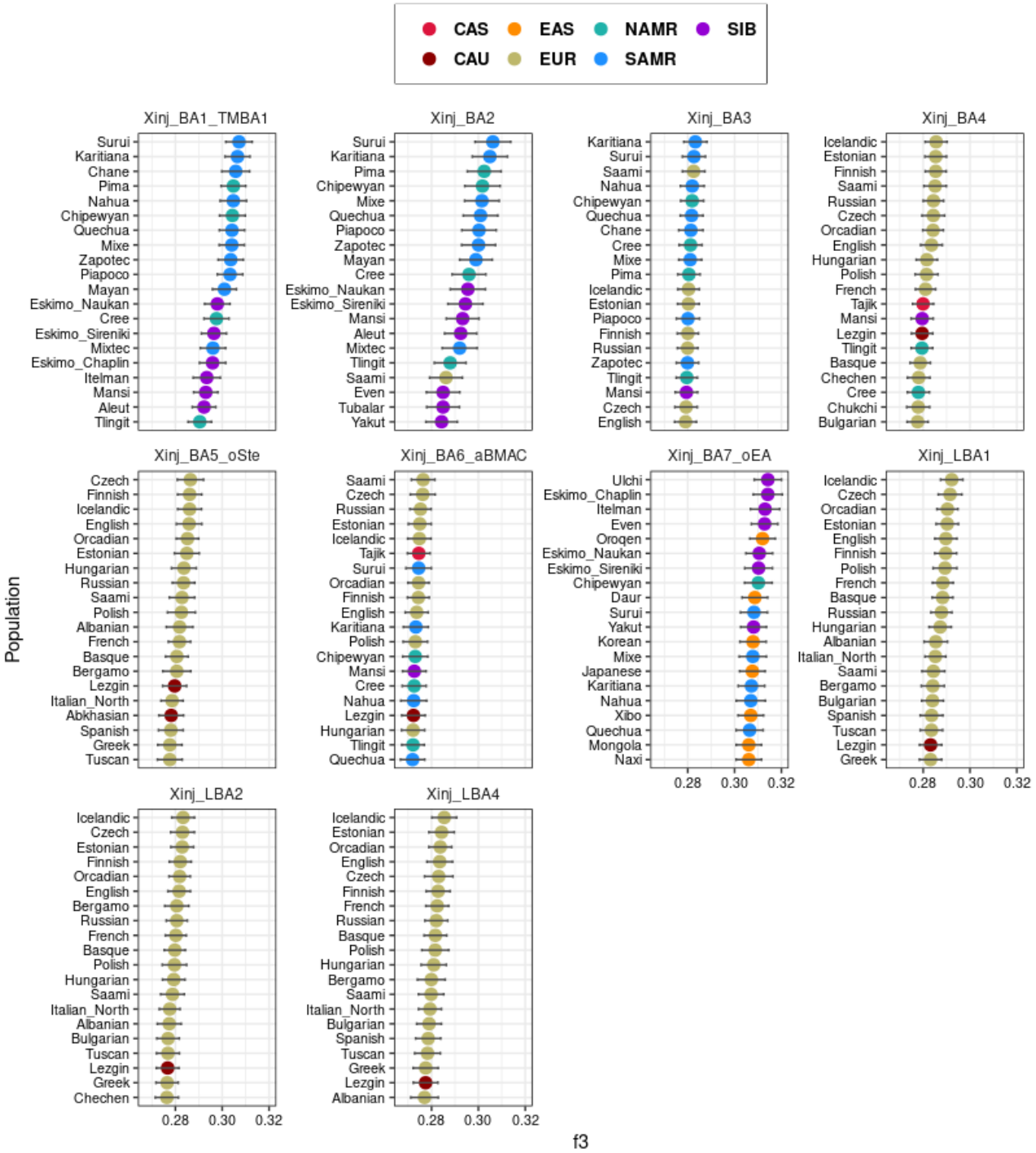

Fig. S13. Top 20 Outgroup f_3-statistics results of ancient BA Xinjiang and present-day populations. The *f*3-statistics are of the form f_3*(Xinj_BA/LBA, Present-day Population; Mbuti),* where Xinj_BA shows the highest genetic affinity for European, Siberian and South American present-day populations. The Xinjiang LBA populations show greatest affinity with European populations. Present-day populations are grouped as Central Asia (CAS), East Asia (EAS), North America (NAMR), Siberia (SIB), Caucasus (CAU), Europe (EUR), South America (SAMR). Only populations with a minimum of 100,000 SNPs in the f_3-statistics comparison are plotted. All the f_3 values have Z-score >3.0.

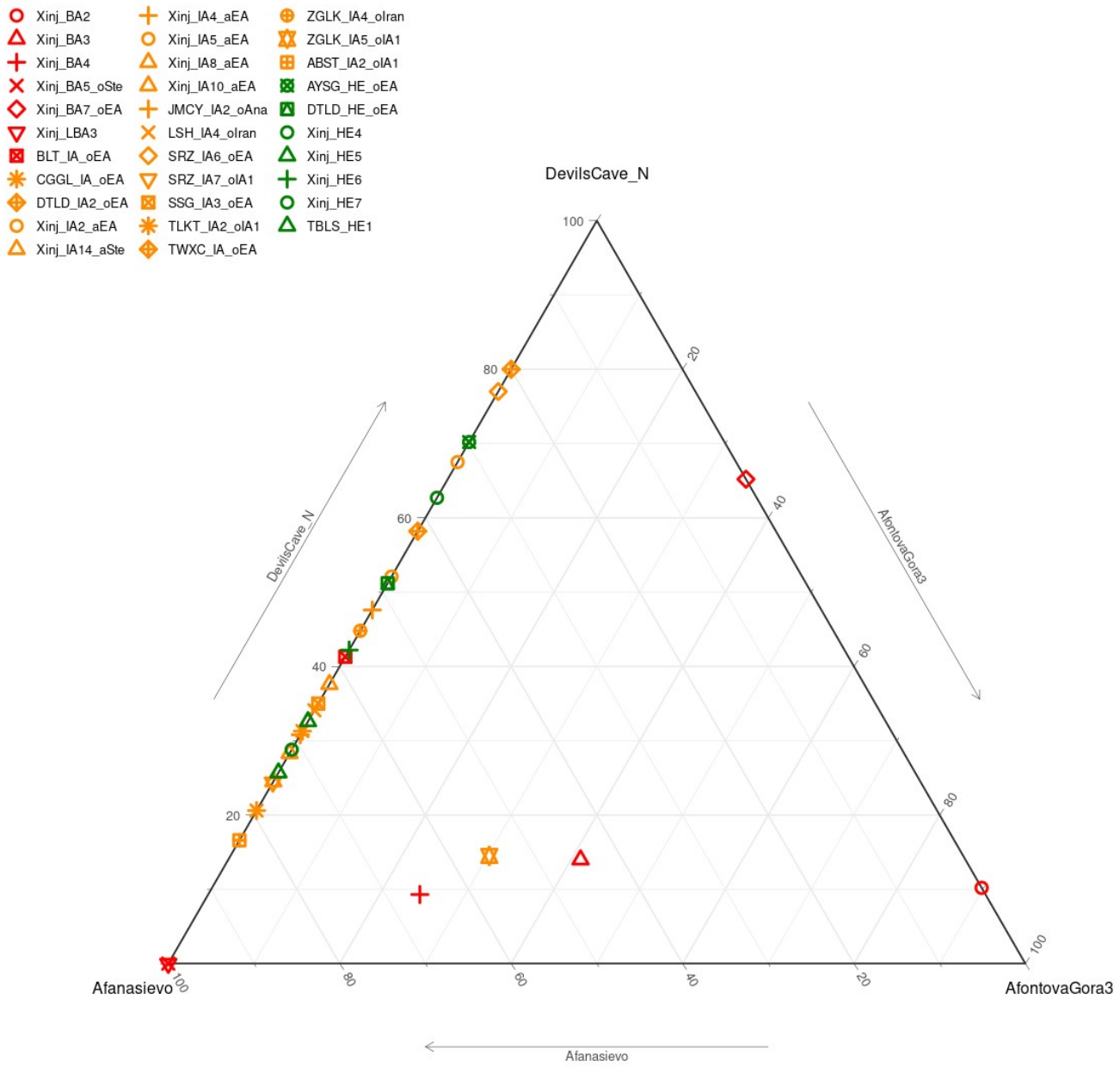

Fig. S14. qpAdm estimation of genetic coefficients of the Xinjiang populations from three ancestry sources of AfontovaGora3 (AG3), Afanasievo and DevilsCave_N. Bronze Age and Late Bronze Age individuals (red) show greater affinity for AG3 compared to the Iron Age (orange) and Historical Era (green) Xinjiang populations, which show more affinity with the Afanasievo.

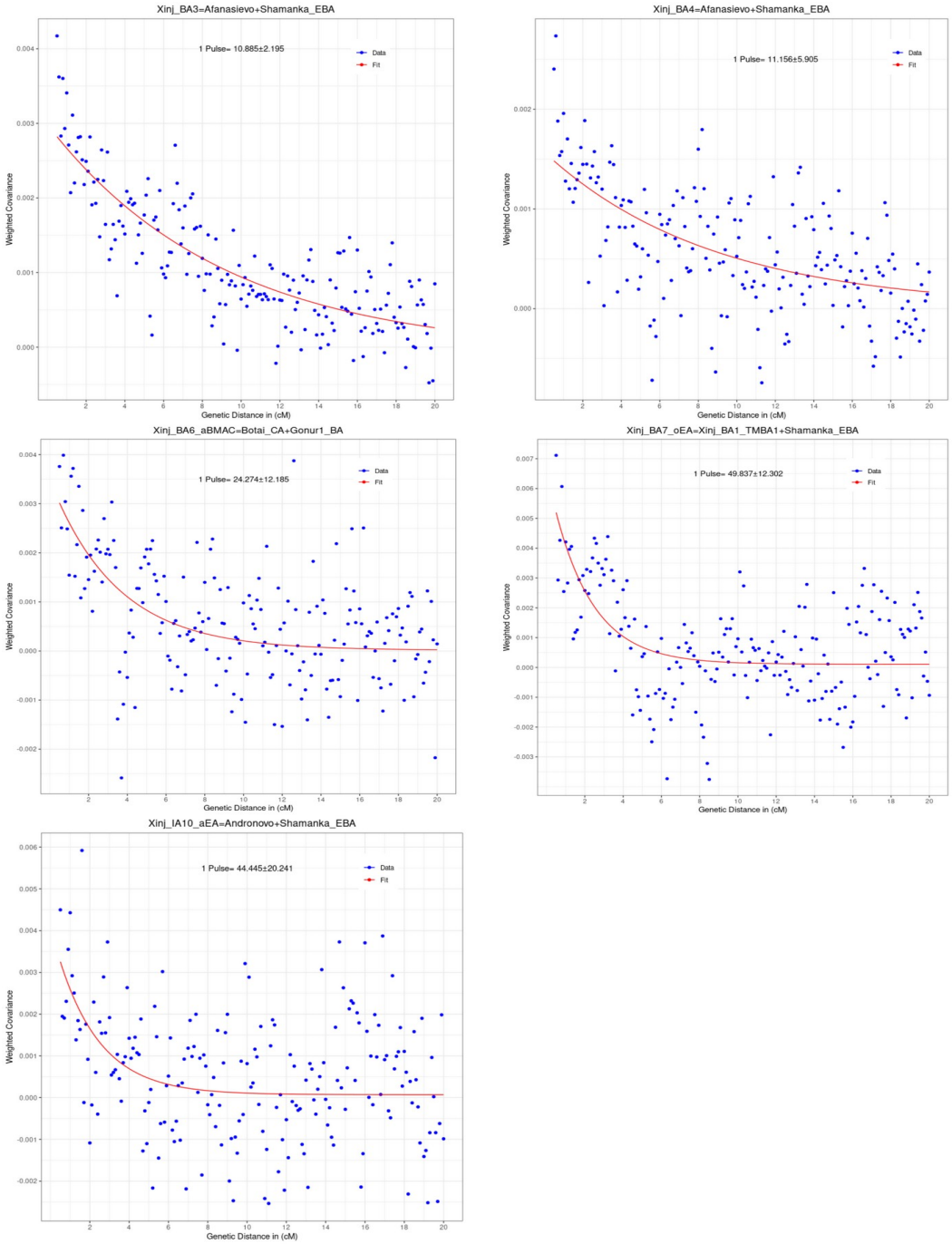

Fig. S15. Decay of admixture linkage disequilibrium datings for Xinjiang Bronze Age and Iron Age individuals with working 2-source qpAdm models containing Steppe ancestry, implemented with the program *DATES*. We set the parameter for Genetic distance to be 0.45cM and estimated a standard error by performing a weighted block jackknife. We additionally present the Xinj_IA10_aEA plot with other BA individuals as this individual could be modeled with both Afanasievo and Andronovo using qpAdm, and the graph is not noisier compared to the other IA individuals that could be modeled using Afanasievo and Andronovo, although we note these results present a broad range of admixture dates for Andronovo ancestry.

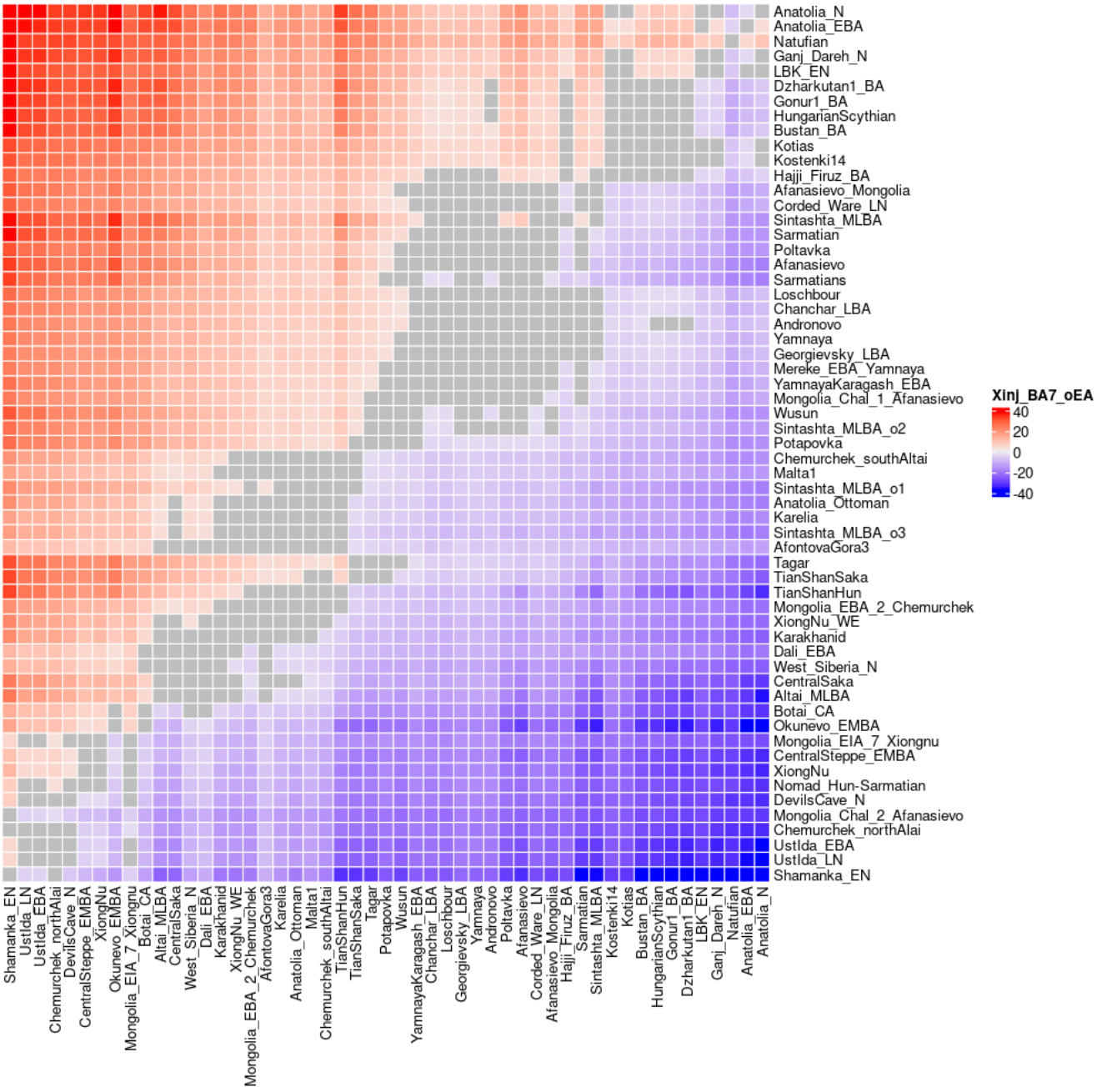

Fig. S16. Heat plot of Z-scores of f4-statistics of the form *(f_4(Ancient PopulationX, Ancient PopulationY; Xinj_BA7_oEA, Mbuti)*. The X-axis shows Ancient_Pop1 and Y-axis shows Ancient_pop2. A positive Z-score shows a higher affinity of X than Y to Xinj_BA7_oEA while a negative value shows a higher affinity for Y than X to Xinj_BA7_oEA. The heat plot shows that the majority of the ancient populations with East Asian ancestry show greater affinity to Xinj_BA7_oEA (e.g. Shamanka_EN) compared to other Steppe populations. Ancient populations from Central Asia, Anatolia and Steppe regions have been included in this comparison.

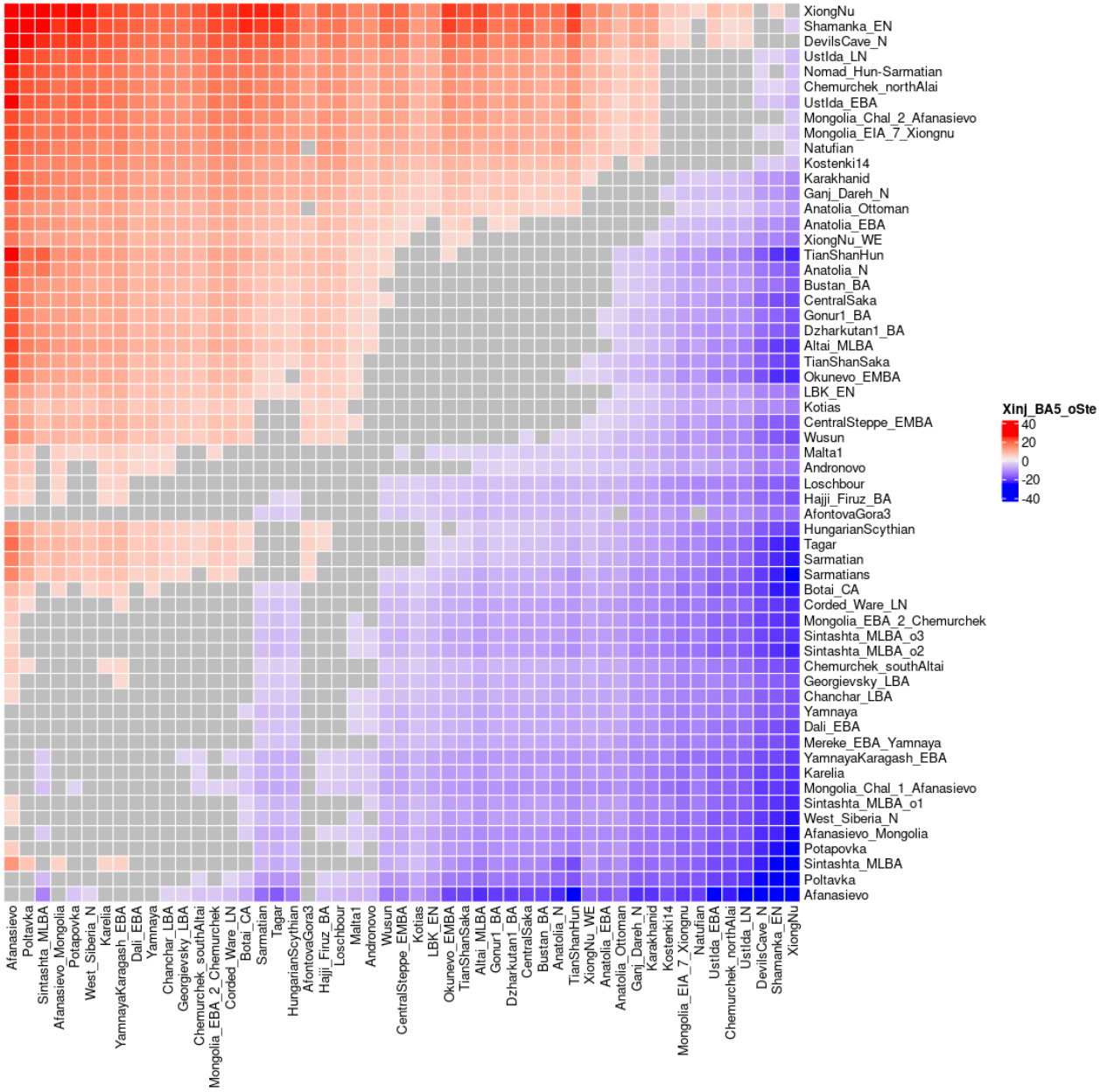

Fig. S17. Heat plot of Z-scores of f_4-statistics of the form *(f_4(Ancient PopulationX, Ancient PopulationY; Xinj_BA5_oSte, Mbuti))*. The X-axis shows Ancient_Pop1 and Y-axis shows Ancient_pop2. A positive Z-score shows a higher affinity of X than Y to Xinj_BA5_oSte while a negative value shows a higher affinity of Y than X to Xinj_BA5_oSte. The Xinj_BA5_oSte shows greater overall affinity to populations with Steppe ancestry (e.g. Afanasievo). Ancient populations from Central Asia, Anatolia and Steppe regions have been included in this comparison.

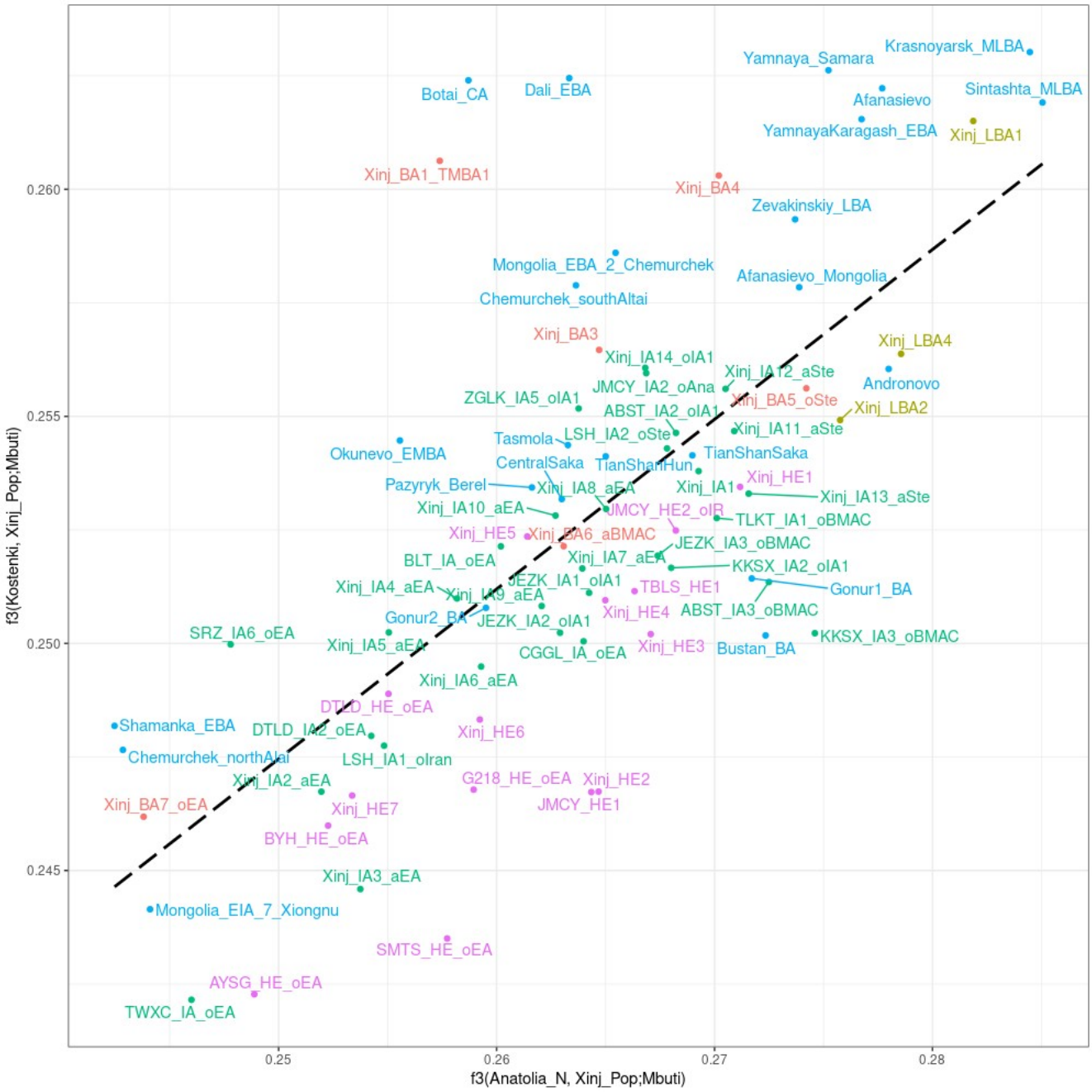

Fig. S18. Biplot of f_3-outgroup tests illustrating Kostenki14- and Anatolia_N- like ancestries in Xinjiang populations. Compared to the Bronze Age populations, IA and HE populations shows greater affinity with Anatolian farmer type ancestry. Previously published individuals are shown in blue. The regression line is shown as black dashed line. Only populations with a minimum of 100,000 SNPs in f_3-statistics comparisons are plotted. All the f_3 values have Z-score >3.0.

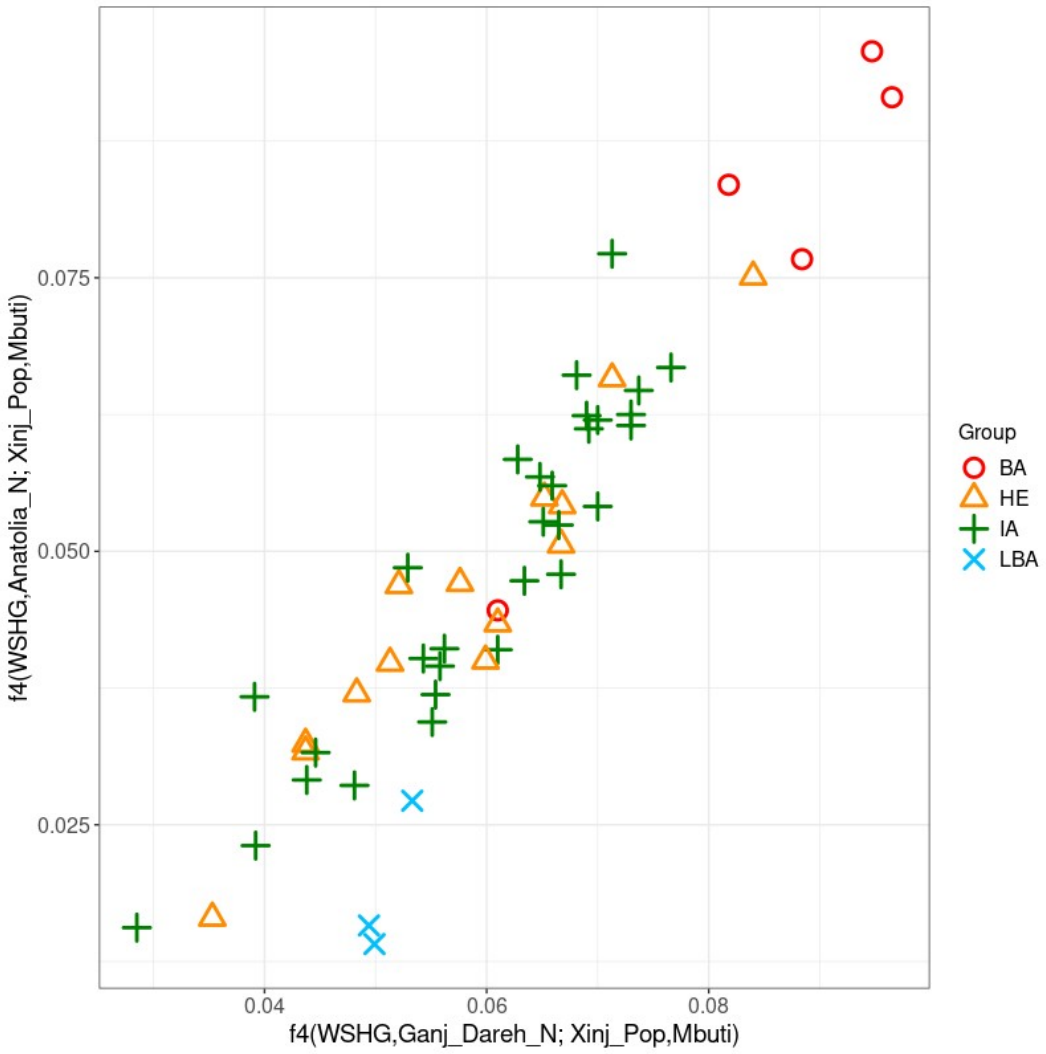

Fig. S19. Biplot of f_4-statistics comparisons of Xinjiang populations to show affinities for Anatolian/Iranian farmers. *f_4(WSHG, GanjDareh_N; Xinj_Pop, Mbuti)* against *f_4(WSHG, Anatolia_N; Xinj_Pop, Mbuti)*. Xinj_BA populations make a separated cluster suggesting strong ANE ancestry while the Xinj_LBA populations show greater drift with Anatolian farmers compared to Xinj_IA/HE/BA populations. Anatolia_N (Anatolian farmer) and Iranian_N (Iranian farmer) have more genetic affinity for Xinjiang_IA populations than to Xinjiang_BA populations. All the f_4 values have significant Z-scores >3.0.

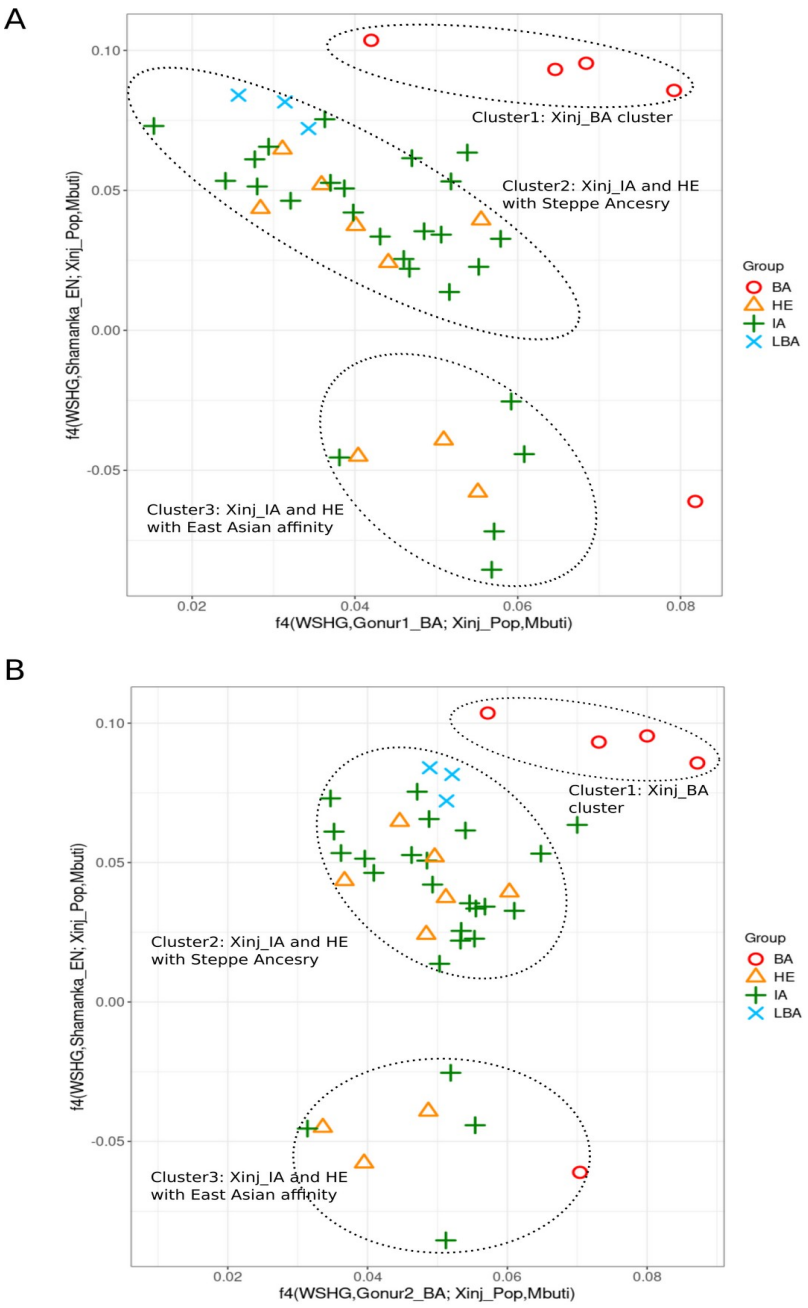

Fig. S20. Biplot of f_4-statistics comparisons of Xinjiang populations to show affinities for Shamanka_EN/BMAC (Gonur1_BA) and Shamanka_EN/Indus Periphery populations (Gonur2_BA). A. *f_4(WSHG, Shamanka_EN; Xinj_Pop, Mbuti)* and *f_4(WSHG, Gonur1_BA; Xinj_Pop, Mbuti)*. B. *f_4(WSHG, Shamanka_EN; Xinj_Pop, Mbuti)* and *f_4(WSHG, Gonur2_BA; Xinj_Pop, Mbuti)*. We observe three separate clusters: Cluster 1 includes Xinj_BA populations, Cluster 2 contains majority of LBA/IA/HE populations and Cluster 3 includes populations with more East Asian (Shamanka_EN) affinity compared to the WSHG (West_Siberia_N) ancestry. All the f_4 values have significant Z-scores >3.0.

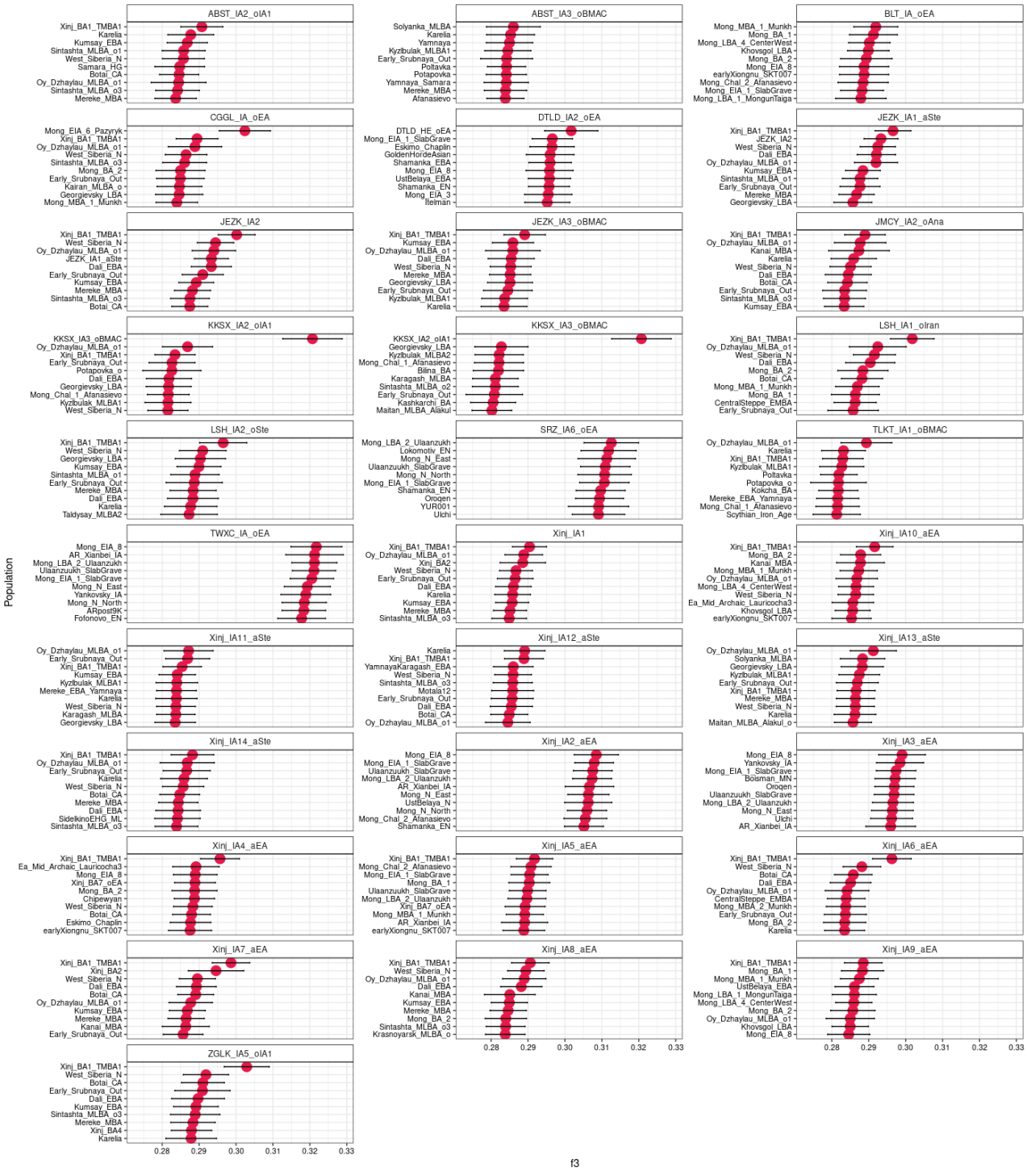

Fig. S21. Top ten f_3-statistics results of the Iron Age Xinjiang populations and ancient Eurasian populations. The f_3-statistics are of the form f_3*(Ancient Population, Xinj_IA; Mbuti)*. Only populations with a minimum of 100,000 SNPs in f_3-statistics comparisons are plotted. All the f_3 values have Z-score >3.0.

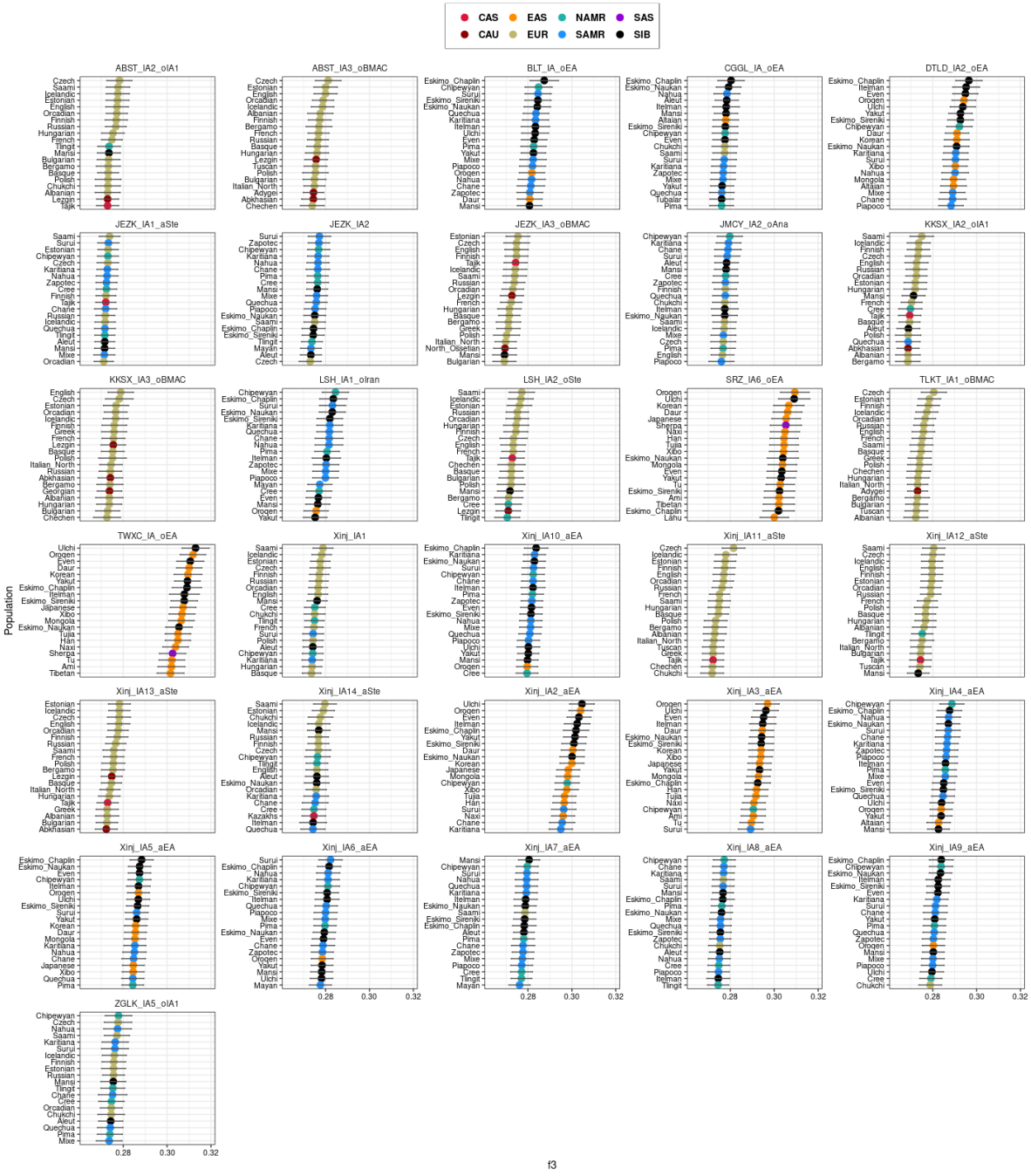

Fig. S22. Top-20 outgroup f_3-statistics for Xinj_IA populations and present-day populations. The f_3-statistics are of the form f_3*(Present-day Population, Xinj_IA; Mbuti)* and show Xinj_IA to have the highest genetic affinity for European, Siberian, South American and North-East Asian populations. Present-day populations are grouped as Central Asia (CAS), East Asia (EAS), North America (NAMR), South Asia (SAS), Caucasus (CAU), Europe (EUR), South America (SAMR) and Siberia (SIB). Only populations with a minimum of 100,000 SNPs in f_3-statistics comparisons are plotted. All the f_3 values have Z-score >3.0.

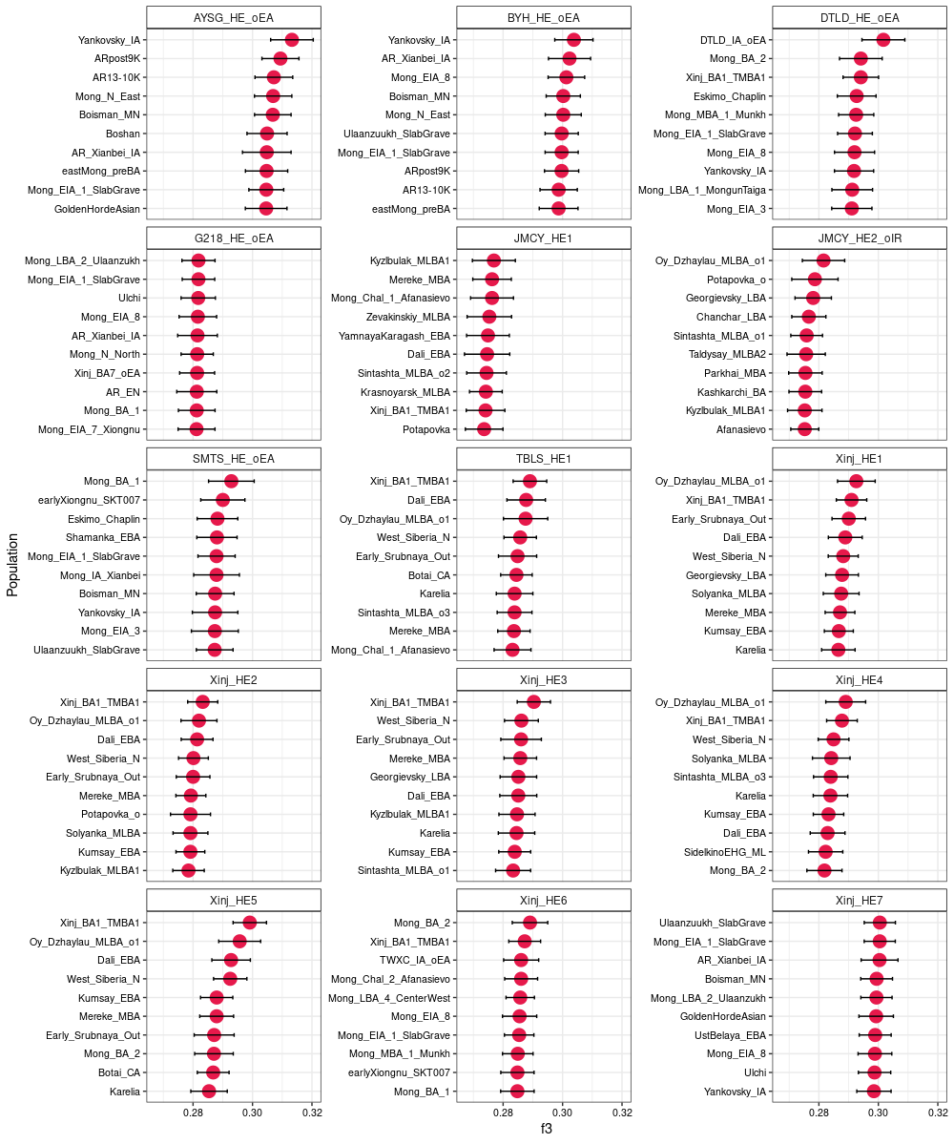

Fig. S23. Top ten f_3-statistics results of the Historical Era Xinjiang populations and ancient Eurasian populations. The outgroup f_3-statistics are of the form *f_3(Ancient Population, Xinjiang_HE; Mbuti)*. All the f_3 values have significant Z-scores >3.0.

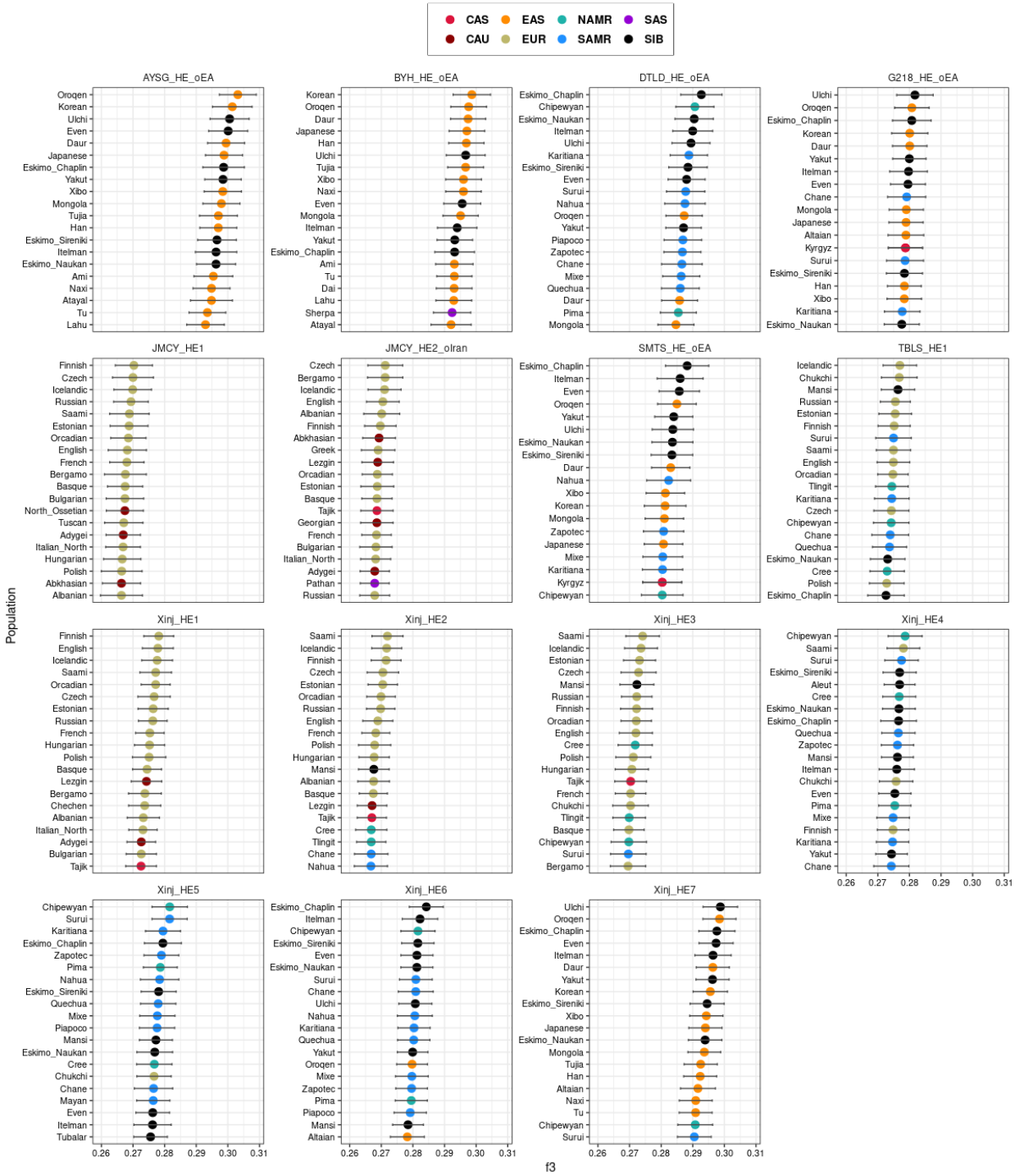

Fig. S24. Top-20 outgroup f_3-statistics for Historical Era Xinjiang and present-day populations from Eurasian and America. The f_3-statistics are of the form *f_3(Xinj_HE, Present-day Population; Mbuti)* and show Xinj_HE to have the highest genetic affinity for European, Siberian and East Asian populations. Present-day populations are grouped as Central Asia (CAS), East Asia (EAS), North America (NAMR), South Asia (SAS), Caucasus (CAU), Europe (EUR), South America (SAMR), and Siberia (SIB). Only populations with a minimum of 100,000 SNPs in f_3-statistics comparisons are plotted. All the f_3 values have Z-score >3.0.

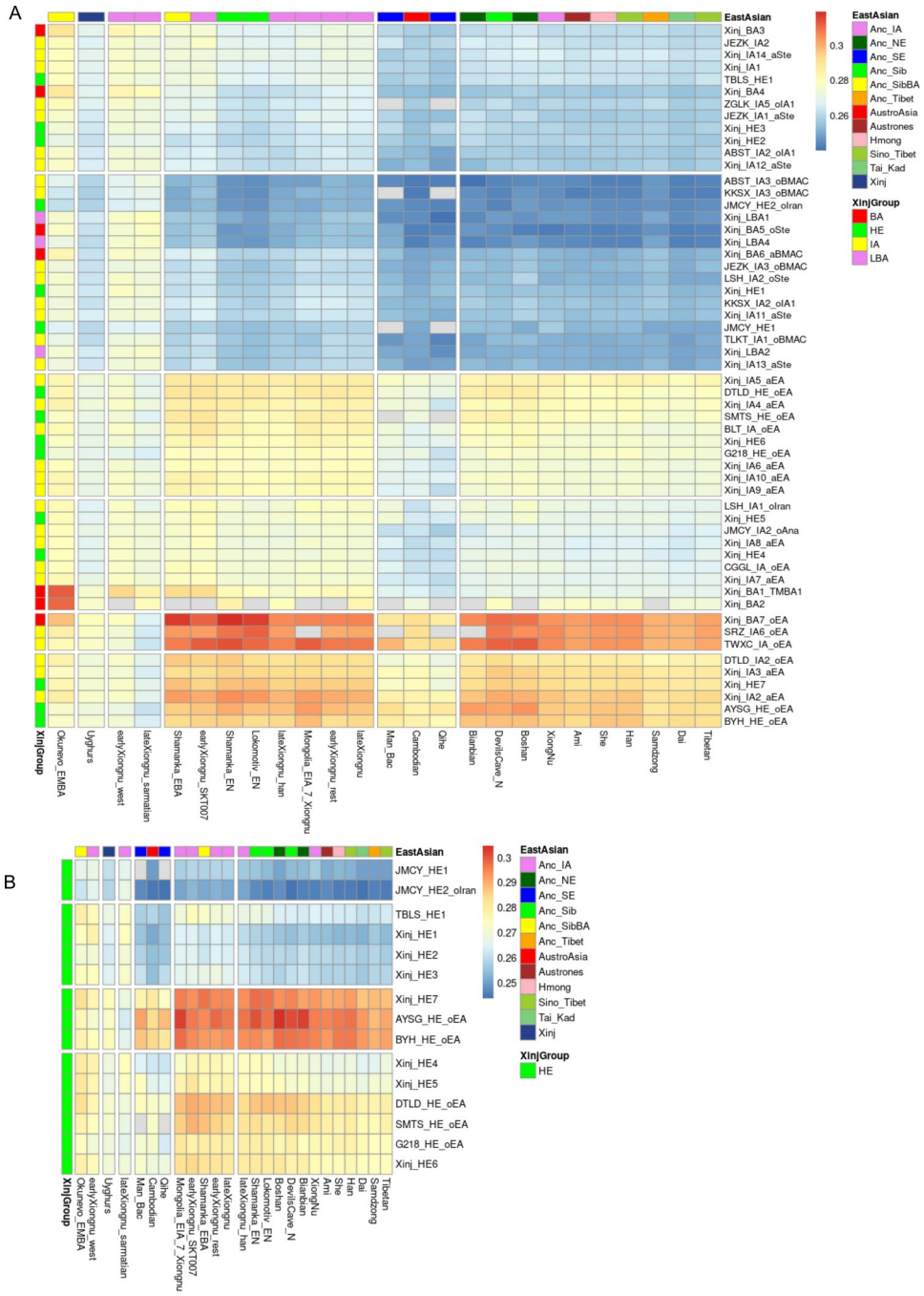

Fig. S25. Outgroup f_3-statistics of the form *f_3(Xinj_Pop, East-Asian; Mbuti)* to measure the shared genetic drift with diverse East Asian populations. A. The f_3 statistics with all the Xinjiang populations B. Only the Historical Era populations are plotted with East Asian populations. Among the HE populations, Xinj_HE7, AYSG_HE_oEA and BYH_HE_oEA show comparatively higher East Asian affinity compared to the other HE populations. The East Asian populations are grouped as Ancient Iron Age (Anc_IA), North East (Anc_NE), South East (Anc_SE), Siberia (Anc_Sib), Tibet (Anc_Tibet), Austroasiatic (AustorAsia), Austronesian (Austrones), Hmong, Sino-Tibet, Tai Kadai, Xinjiang (Xinj).

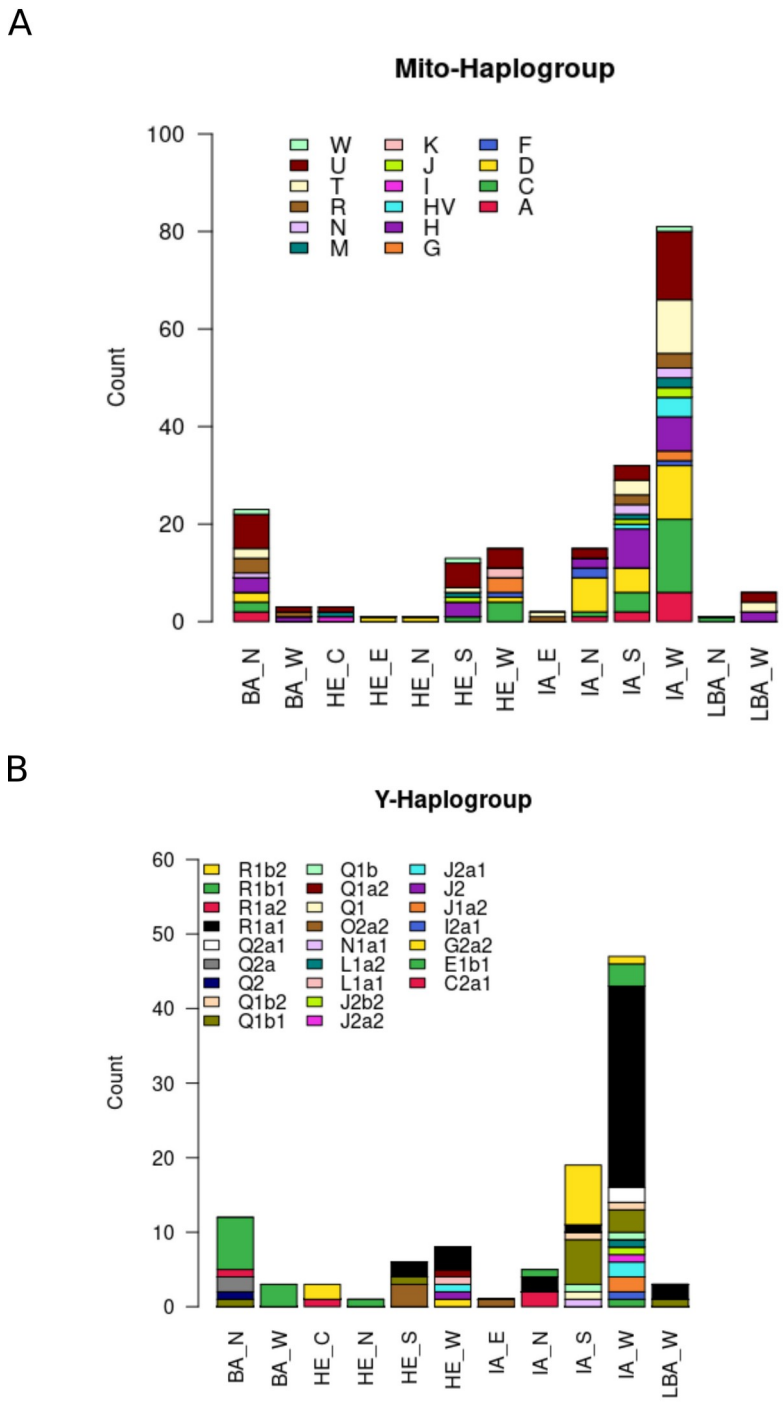

Fig. S26. Mitochondrial and Y-Chromosomal haplogroups of ancient Xinjiang individuals. Xinjiang individuals are divided into groups of Bronze Age (BA), Historical Era (HE), and Iron Age North (IA). Geographical orientation is depicted as North (_N), South (_S), West (_W), East (_E), and Central (_C). For the BA individuals, we observe more of the R1b1/R1b2 Y-haplogroup typical of Steppe EMBA populations, whereas the IA more typically have the R1a1 Y-haplogroup associated with Steppe_MLBA populations.

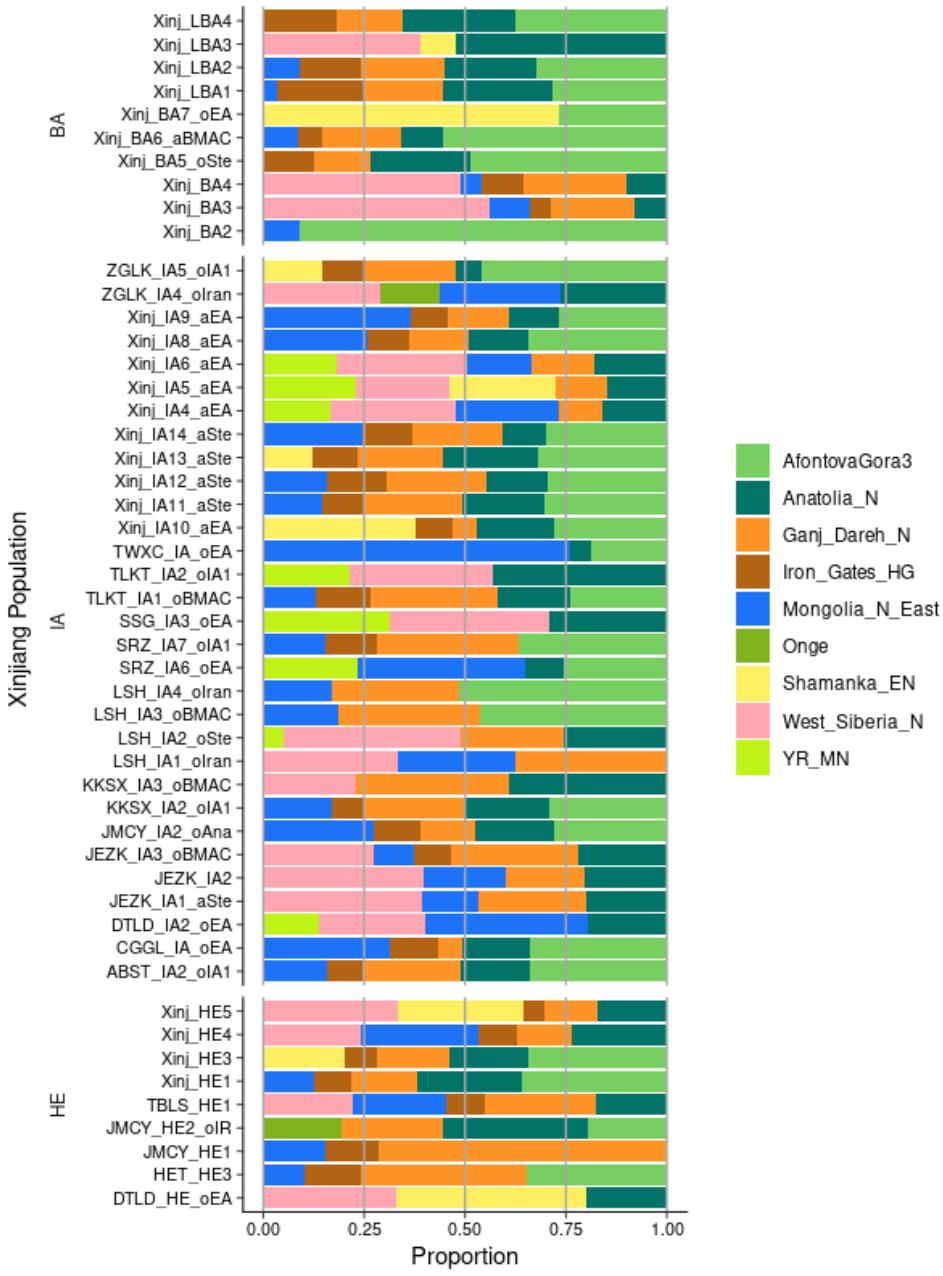

Fig. S27. Working distal qpAdm models with different ancestral sources. Bronze Age populations show high levels of ANE ancestry. In general, we observed that the LBA populations showed greater Anatolian farmer related ancestry compared to BA populations, a trend which further continued into the IA and HE. We also see outlier populations containing elevated East Asian ancestry. Bronze Age (BA), Historical Era (HE) and IA (Iron Age).

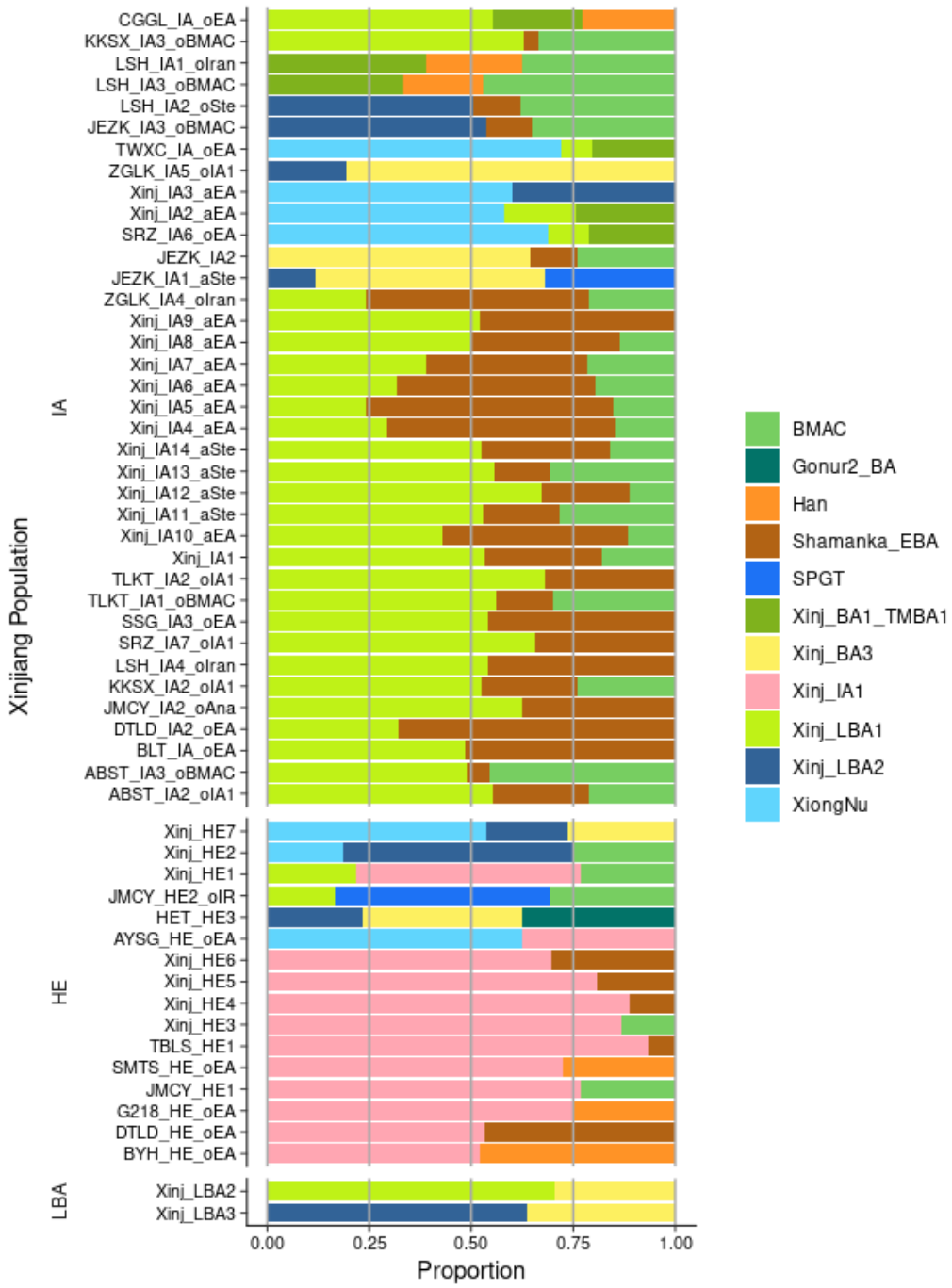

Fig. S28. Working proximal qpAdm models for Xinjiang Late BA, Iron Age and Historical Era populations using ancient Xinjiang populations as possible sources. Most of the Xinjiang IA and HE populations could be modeled using the Xinjiang_LBA with additional ancestries being derived from East Asian or BMAC populations. While most of the HE populations could be modeled using the Iron Age populations.

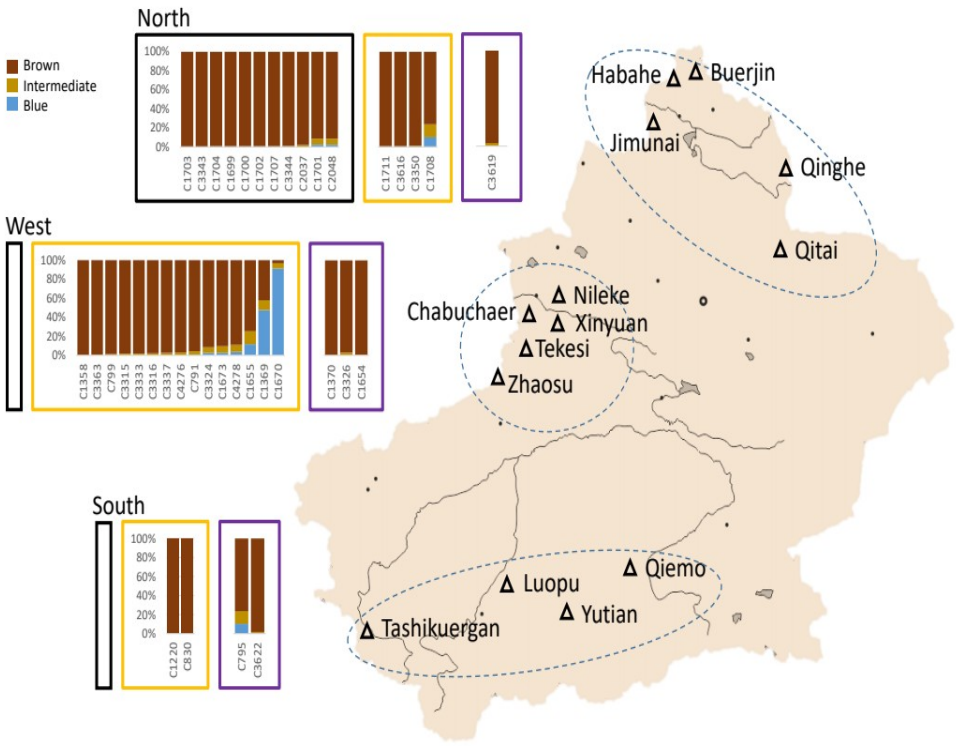

Fig. S29. Phenotypic analysis of eye color for Xinjiang samples using HIrisPlex-S. Predicted eye color given as a probability of either brown, blue, or intermediate for samples having a minimum depth of 5x for each covered SNP. Samples grouped in boxes according to time period: black, BA (5000-3000 BP); orange, IA (3000-2000 BP); purple, HE (<2000 BP). Blank boxes denote a lack of available samples or lack of samples passing depth threshold for that time period. Prediction accuracies as expressed by the area under the curve of a receiver operating characteristic curve (AUC) are given in Table S15.

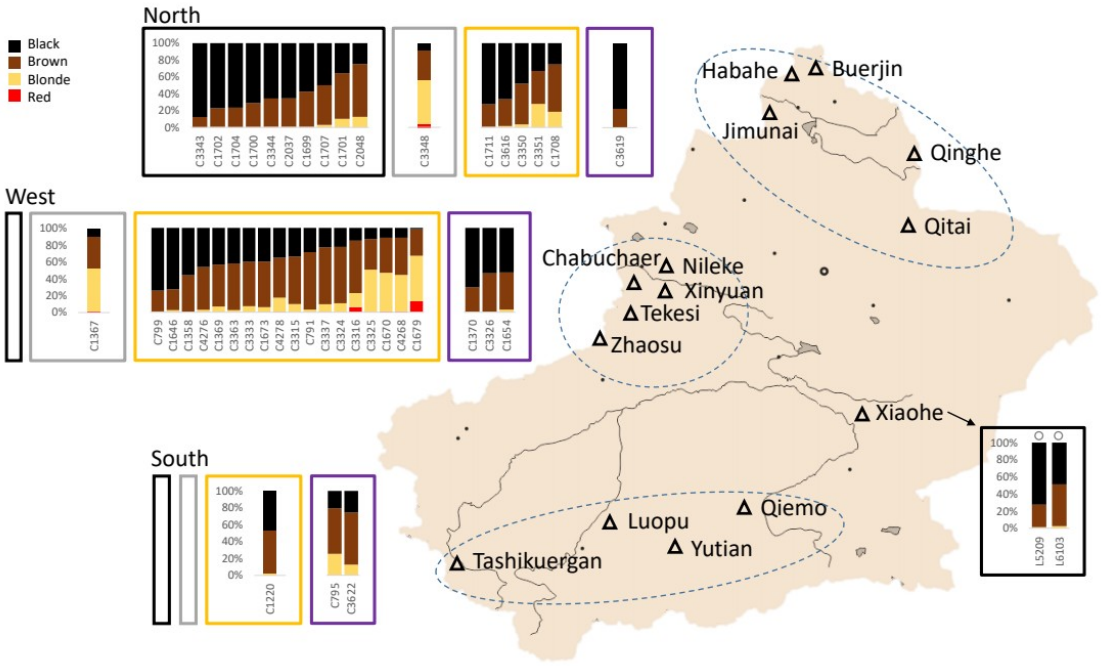

Fig. S30. Phenotypic analysis of hair color for Xinjiang samples using HIrisPlex-S. Predicted hair color given as a probability of either black, brown, blonde, or red for samples having a minimum depth of 5x for each covered SNP. Samples grouped in boxes according to time period: black, BA (5000-3500 BP); gray, LBA (3500-3000 BP); orange, IA (3000-2000 BP); purple, HE (<2000 BP). Blank boxes denote a lack of available samples or lack of samples passing depth threshold for that time period. Samples for the Xiaohe site from Zhang et al. 2021 *(16)* are indicated with a gray circle above them and are predicted at a lower minimal depth of 3x for each covered SNP. Prediction accuracies as expressed by the area under the curve of a receiver operating characteristic curve (AUC) are given in Table S15.

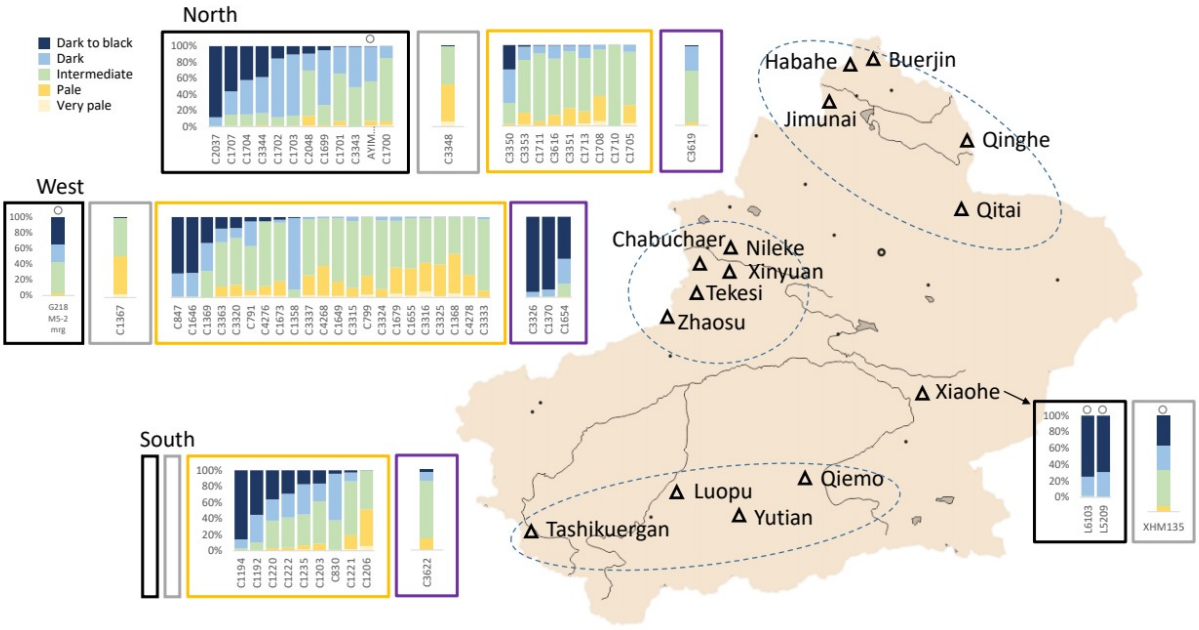

Fig. S31. Phenotypic analysis of skin tone for Xinjiang samples using HIrisPlex-S. Predicted skin tone given as a probability of either dark to black, dark, intermediate, pale, or very pale for samples having a minimum depth of 5x for each covered SNP. Samples grouped in boxes according to time period: black, BA (5000-3500 BP); gray, LBA (3500-3000 BP); orange, IA (3000-2000 BP); purple, HE (<2000 BP). Blank boxes denote a lack of available samples or lack of samples passing depth threshold for that time period. Samples marked with a gray circle are from Zhang et al. 2021 *(16)* and are predicted at a lower minimal depth of 3x for each covered SNP. Prediction accuracies as expressed by the area under the curve of a receiver operating characteristic curve (AUC) are given in Table S14. Images of skin color categories can be found in Chaitanya et al. *(36)*.

References and Notes

1. P. B. Damgaard, N. Marchi, S. Rasmussen, M. Peyrot, G. Renaud, T. Korneliussen, J. V. Moreno-Mayar, M. W. Pedersen, A. Goldberg, E. Usmanova, N. Baimukhanov, V. Loman, L. Hedeager, A. G. Pedersen, K. Nielsen, G. Afanasiev, K. Akmatov, A. Aldashev, A. Alpaslan, G. Baimbetov, V. I. Bazaliiskii, A. Beisenov, B. Boldbaatar, B. Boldgiv, C. Dorzhu, S. Ellingvag, D. Erdenebaatar, R. Dajani, E. Dmitriev, V. Evdokimov, K. M. Frei, A. Gromov, A. Goryachev, H. Hakonarson, T. Hegay, Z. Khachatryan, R. Khaskhanov, E. Kitov, A. Kolbina, T. Kubatbek, A. Kukushkin, I. Kukushkin, N. Lau, A. Margaryan, I. Merkyte, I. V. Mertz, V. K. Mertz, E. Mijiddorj, V. Moiyesev, G. Mukhtarova, B. Nurmukhanbetov, Z. Orozbekova, I. Panyushkina, K. Pieta, V. Smrčka, I. Shevnina, A. Logvin, K.-G. Sjögren, T. Štolcová, A. M. Taravella, K. Tashbaeva, A. Tkachev, T. Tulegenov, D. Voyakin, L. Yepiskoposyan, S. Undrakhbold, V. Varfolomeev, A. Weber, M. A. Wilson Sayres, N. Kradin, M. E. Allentoft, L. Orlando, R. Nielsen, M. Sikora, E. Heyer, K. Kristiansen, E. Willerslev, 137 ancient human genomes from across the Eurasian steppes. *Nature* **557**, 369–374 (2018). doi:10.1038/s41586-018-0094-2 Medline

2. A. Betts, P. Jia, I. Abuduresule, A new hypothesis for early Bronze Age cultural diversity in Xinjiang, China. *Archaeol. Res. Asia* **17**, 204–213 (2019). doi:10.1016/j.ara.2018.04.001

3. A. V. G. Betts, M. Vicziany, P. Jia, A. A. Di Castro, *The Cultures of Ancient Xinjiang, Western China: Crossroads of the Silk Roads* (Archaeopress, 2020).

4. Y. Li, Agriculture and palaeoeconomy in prehistoric Xinjiang, China (3000–200 BC). *Veget. Hist. Archaeobot.* **30**, 287–303 (2021). doi:10.1007/s00334-020-00774-2

5. J. A. Millward, *Eurasian Crossroads: A History of Xinjiang* (Columbia Univ. Press, 2007).

6. K. Li, S. Qin, X. Yang, B. Xu, L. Zhang, G. Mu, D. Wei, C. Wang, Y. Wu, X. Tian, Y. Lin, W. Li, J. Liu, Y. Jiao, Human activity during the late Pleistocene in the Lop Nur region, northwest China: Evidence from a buried stone artifact. *Sci. China Earth Sci.* **61**, 1659–1668 (2018). doi:10.1007/s11430-017-9257-3

7. M. Peyrot, The deviant typological profile of the Tocharian branch of Indo-European may be due to Uralic substrate influence. *Indo-Euro. Linguist.* **7**, 72–121 (2019). doi:10.1163/22125892-00701007

8. Y. Zhang, A brief introduction to Xinjiang archaeology [in Chinese]. *Archaeology* **6**, 3–13 (2002).

9. J. Yu, J. Ma, A preliminary study on the Dongtalede cemetery of Habahe County, Xinjiang [in Chinese]. *Cult. Relics* **3**, 53–57 (2013).

10. P. de Barros Damgaard, R. Martiniano, J. Kamm, J. V. Moreno-Mayar, G. Kroonen, M. Peyrot, G. Barjamovic, S. Rasmussen, C. Zacho, N. Baimukhanov, V. Zaibert, V. Merz, A. Biddanda, I. Merz, V. Loman, V. Evdokimov, E. Usmanova, B. Hemphill, A. Seguin-Orlando, F. E. Yediay, I. Ullah, K.-G. Sjögren, K. H. Iversen, J. Choin, C. de la Fuente, M. Ilardo, H. Schroeder, V. Moiseyev, A. Gromov, A. Polyakov, S. Omura, S. Y. Senyurt, H. Ahmad, C. McKenzie, A. Margaryan, A. Hameed, A. Samad, N. Gul, M. H. Khokhar, O. I. Goriunova, V. I. Bazaliiskii, J. Novembre, A. W. Weber, L. Orlando, M. E. Allentoft, R. Nielsen, K. Kristiansen, M. Sikora, A. K. Outram, R. Durbin, E. Willerslev, The first horse herders and the impact of early Bronze Age steppe expansions into Asia. *Science* **360**, eaar7711 (2018). doi:10.1126/science.aar7711 Medline

11. V. M. Narasimhan, N. Patterson, P. Moorjani, N. Rohland, R. Bernardos, S. Mallick, I. Lazaridis, N. Nakatsuka, I. Olalde, M. Lipson, A. M. Kim, L. M. Olivieri, A. Coppa, M. Vidale, J. Mallory, V. Moiseyev, E. Kitov, J. Monge, N. Adamski, N. Alex, N. Broomandkhoshbacht, F. Candilio, K. Callan, O. Cheronet, B. J. Culleton, M. Ferry, D. Fernandes, S. Freilich, B. Gamarra, D. Gaudio, M. Hajdinjak, É. Harney, T. K. Harper, D. Keating, A. M. Lawson, M. Mah, K. Mandl, M. Michel, M. Novak, J. Oppenheimer, N. Rai, K. Sirak, V. Slon, K. Stewardson, F. Zalzala, Z. Zhang, G. Akhatov, A. N. Bagashev, A. Bagnera, B. Baitanayev, J. Bendezu-Sarmiento, A. A. Bissembaev, G. L. Bonora, T. T. Chargynov, T. Chikisheva, P. K. Dashkovskiy, A. Derevianko, M. Dobeš, K. Douka, N. Dubova, M. N. Duisengali, D. Enshin, A. Epimakhov, A. V. Fribus, D. Fuller, A. Goryachev, A. Gromov, S. P. Grushin, B. Hanks, M. Judd, E. Kazizov, A. Khokhlov, A. P. Krygin, E. Kupriyanova, P. Kuznetsov, D. Luiselli, F. Maksudov, A. M. Mamedov, T. B. Mamirov, C. Meiklejohn, D. C. Merrett, R. Micheli, O. Mochalov, S. Mustafokulov, A. Nayak, D. Pettener, R. Potts, D. Razhev, M. Rykun, S. Sarno, T. M. Savenkova, K. Sikhymbaeva, S. M. Slepchenko, O. A. Soltobaev, N. Stepanova, S. Svyatko, K. Tabaldiev, M. Teschler-Nicola, A. A. Tishkin, V. V. Tkachev, S. Vasilyev, P. Velemínský, D. Voyakin, A. Yermolayeva, M. Zahir, V. S. Zubkov, A. Zubova, V. S. Shinde, C. Lalueza-Fox, M. Meyer, D. Anthony, N. Boivin, K. Thangaraj, D. J. Kennett, M. Frachetti, R. Pinhasi, D. Reich, The formation of human populations in South and Central Asia. *Science* **365**, eaat7487 (2019). doi:10.1126/science.aat7487 Medline

12. X. Zhou, J. Yu, R. N. Spengler, H. Shen, K. Zhao, J. Ge, Y. Bao, J. Liu, Q. Yang, G. Chen, P. Weiming Jia, X. Li, 5,200-year-old cereal grains from the eastern Altai Mountains redate the trans-Eurasian crop exchange. *Nat. Plants* **6**, 78–87 (2020). doi:10.1038/s41477-019-0581-y Medline

13. C. Li, C. Ning, E. Hagelberg, H. Li, Y. Zhao, W. Li, I. Abuduresule, H. Zhu, H. Zhou, Analysis of ancient human mitochondrial DNA from the Xiaohe cemetery: Insights into prehistoric population movements in the Tarim Basin, China. *BMC Genet.* **16**, 78 (2015). doi:10.1186/s12863-015-0237-5 Medline

14. W. Wang, M. Ding, J. D. Gardner, Y. Wang, B. Miao, W. Guo, X. Wu, Q. Ruan, J. Yu, X. Hu, B. Wang, X. Wu, Z. Tang, A. Niyazi, J. Zhang, X. Chang, Y. Tang, M. Ren, P. Cao, F. Liu, Q. Dai, X. Feng, R. Yang, M. Zhang, T. Wang, W. Ping, W. Hou, W. Li, J. Ma, V. Kumar, Q. Fu, Ancient Xinjiang mitogenomes reveal intense admixture with high genetic diversity. *Sci. Adv.* **7**, eabd6690 (2021). doi:10.1126/sciadv.abd6690 Medline

15. B. E. Hemphill, J. P. Mallory, Horse-mounted invaders from the Russo-Kazakh steppe or agricultural colonists from western Central Asia? A craniometric investigation of the Bronze Age settlement of Xinjiang. *Am. J. Phys. Anthropol.* **124**, 199–222 (2004). doi:10.1002/ajpa.10354 Medline

16. F. Zhang, C. Ning, A. Scott, Q. Fu, R. Bjørn, W. Li, D. Wei, W. Wang, L. Fan, I. Abuduresule, X. Hu, Q. Ruan, A. Niyazi, G. Dong, P. Cao, F. Liu, Q. Dai, X. Feng, R. Yang, Z. Tang, P. Ma, C. Li, S. Gao, Y. Xu, S. Wu, S. Wen, H. Zhu, H. Zhou, M. Robbeets, V. Kumar, J. Krause, C. Warinner, C. Jeong, Y. Cui, The genomic origins of the Bronze Age Tarim Basin mummies. *Nature* **599**, 256–261 (2021). doi:10.1038/s41586-021-04052-7 Medline

17. C. Jeong, K. Wang, S. Wilkin, W. T. T. Taylor, B. K. Miller, J. H. Bemmann, R. Stahl, C. Chiovelli, F. Knolle, S. Ulziibayar, D. Khatanbaatar, D. Erdenebaatar, U. Erdenebat, A. Ochir, G. Ankhsanaa, C. Vanchigdash, B. Ochir, C. Munkhbayar, D. Tumen, A. Kovalev, N. Kradin,

B. A. Bazarov, D. A. Miyagashev, P. B. Konovalov, E. Zhambaltarova, A. V. Miller, W. Haak, S. Schiffels, J. Krause, N. Boivin, M. Erdene, J. Hendy, C. Warinner, A Dynamic 6,000-Year Genetic History of Eurasia's Eastern Steppe. *Cell* **183**, 890–904.e29 (2020). doi:10.1016/j.cell.2020.10.015 Medline

18. C. Jeong, A. T. Ozga, D. B. Witonsky, H. Malmström, H. Edlund, C. A. Hofman, R. W. Hagan, M. Jakobsson, C. M. Lewis, M. S. Aldenderfer, A. Di Rienzo, C. Warinner, Long-term genetic stability and a high-altitude East Asian origin for the peoples of the high valleys of the Himalayan arc. *Proc. Natl. Acad. Sci. U.S.A.* **113**, 7485–7490 (2016). doi:10.1073/pnas.1520844113 Medline

19. H. W. Bailey, Saka Studies: The Ancient Kingdom of Khotan. *Iran* **8**, 65–72 (1970). doi:10.1080/05786967.1970.11834790

20. C. Ning, C. C. Wang, S. Gao, Y. Yang, X. Zhang, X. Wu, F. Zhang, Z. Nie, Y. Tang, M. Robbeets, J. Ma, J. Krause, Y. Cui, Ancient Genomes Reveal Yamnaya-Related Ancestry and a Potential Source of Indo-European Speakers in Iron Age Tianshan. *Curr. Biol.* **29**, 2526–2532.e4 (2019). doi:10.1016/j.cub.2019.06.044 Medline

21. See the supplementary materials.

22. A. W. Briggs, P. Heyn, Preparation of next-generation sequencing libraries from damaged DNA. *Methods Mol. Biol.* **840**, 143–154 (2012). doi:10.1007/978-1-61779-516-9_18 Medline

23. M.-T. Gansauge, M. Meyer, Single-stranded DNA library preparation for the sequencing of ancient or damaged DNA. *Nat. Protoc.* **8**, 737–748 (2013). doi:10.1038/nprot.2013.038 Medline

24. Q. Fu, M. Meyer, X. Gao, U. Stenzel, H. A. Burbano, J. Kelso, S. Pääbo, DNA analysis of an early modern human from Tianyuan Cave, China. *Proc. Natl. Acad. Sci. U.S.A.* **110**, 2223–2227 (2013). doi:10.1073/pnas.1221359110 Medline

25. Q. Fu, M. Hajdinjak, O. T. Moldovan, S. Constantin, S. Mallick, P. Skoglund, N. Patterson, N. Rohland, I. Lazaridis, B. Nickel, B. Viola, K. Prüfer, M. Meyer, J. Kelso, D. Reich, S. Pääbo, An early modern human from Romania with a recent Neanderthal ancestor. *Nature* **524**, 216–219 (2015). doi:10.1038/nature14558 Medline

26. D. H. Alexander, J. Novembre, K. Lange, Fast model-based estimation of ancestry in unrelated individuals. *Genome Res.* **19**, 1655–1664 (2009). doi:10.1101/gr.094052.109 Medline

27. N. Patterson, P. Moorjani, Y. Luo, S. Mallick, N. Rohland, Y. Zhan, T. Genschoreck, T. Webster, D. Reich, Ancient admixture in human history. *Genetics* **192**, 1065–1093 (2012). doi:10.1534/genetics.112.145037 Medline

28. W. Haak, I. Lazaridis, N. Patterson, N. Rohland, S. Mallick, B. Llamas, G. Brandt, S. Nordenfelt, E. Harney, K. Stewardson, Q. Fu, A. Mittnik, E. Bánffy, C. Economou, M. Francken, S. Friederich, R. G. Pena, F. Hallgren, V. Khartanovich, A. Khokhlov, M. Kunst, P. Kuznetsov, H. Meller, O. Mochalov, V. Moiseyev, N. Nicklisch, S. L. Pichler, R. Risch, M. A. Rojo Guerra, C. Roth, A. Szécsényi-Nagy, J. Wahl, M. Meyer, J. Krause, D. Brown, D. Anthony, A. Cooper, K. W. Alt, D. Reich, Massive migration from the steppe was a source for Indo-European languages in Europe. *Nature* **522**, 207–211 (2015). doi:10.1038/nature14317 Medline

29. A. S. Kassian, M. Zhivlov, G. Starostin, A. A. Trofimov, P. A. Kocharov, A. Kuritsyna, M. N. Saenko, Rapid radiation of the inner Indo-European languages: An advanced approach to Indo-European lexicostatistics. *Linguistics* **59**, 949–979 (2021). doi:10.1515/ling-2020-0060

30. D. Cong, P. Jia, B. Ailisen, X. Jia, D. Baola, Adunqiaolu: A new type of Bronze Age remains in the western Tianshan Mountains [in Chinese]. *West. Reg. Stud.* **4**, 15–27 (2017).

31. J. Han, *Cultures in Xinjiang from the Bronze Age to the early Iron Age* [in Chinese] (Wenwu Press, 2007).

32. C. Posth, K. Nägele, H. Colleran, F. Valentin, S. Bedford, K. W. Kami, R. Shing, H. Buckley, R. Kinaston, M. Walworth, G. R. Clark, C. Reepmeyer, J. Flexner, T. Maric, J. Moser, J. Gresky, L. Kiko, K. J. Robson, K. Auckland, S. J. Oppenheimer, A. V. S. Hill, A. J. Mentzer, J. Zech, F. Petchey, P. Roberts, C. Jeong, R. D. Gray, J. Krause, A. Powell, Language continuity despite population replacement in Remote Oceania. *Nat. Ecol. Evol.* **2**, 731–740 (2018). doi:10.1038/s41559-018-0498-2 Medline

33. J. Mei, *A Metallurgical Study of Early Copper and Bronze Artefacts from Xinjiang, China* (Archaeopress, 2000).

34. L. Wang, F. Chen, Y. Wang, W. Qian, J. Mei, M. Martinón-Torres, K. Chen, Copper metallurgy in prehistoric upper Ili Valley, Xinjiang, China. *Archaeol. Anthropol. Sci.* **11**, 2407–2417 (2019). doi:10.1007/s12520-018-0679-6

35. J. Li, W. Zeng, Y. Zhang, A. M.-S. Ko, C. Li, H. Zhu, Q. Fu, H. Zhou, Ancient DNA reveals genetic connections between early Di-Qiang and Han Chinese. *BMC Evol. Biol.* **17**, 239 (2017). doi:10.1186/s12862-017-1082-0 Medline

36. L. Chaitanya, K. Breslin, S. Zuñiga, L. Wirken, E. Pośpiech, M. Kukla-Bartoszek, T. Sijen, P. de Knijff, F. Liu, W. Branicki, M. Kayser, S. Walsh, The HIrisPlex-S system for eye, hair and skin colour prediction from DNA: Introduction and forensic developmental validation. *Forensic Sci. Int. Genet.* **35**, 123–135 (2018). doi:10.1016/j.fsigen.2018.04.004 Medline

37. C. Keyser, C. Bouakaze, E. Crubézy, V. G. Nikolaev, D. Montagnon, T. Reis, B. Ludes, Ancient DNA provides new insights into the history of south Siberian Kurgan people. *Hum. Genet.* **126**, 395–410 (2009). doi:10.1007/s00439-009-0683-0 Medline

38. Q. Feng, Y. Lu, X. Ni, K. Yuan, Y. Yang, X. Yang, C. Liu, H. Lou, Z. Ning, Y. Wang, D. Lu, C. Zhang, Y. Zhou, M. Shi, L. Tian, X. Wang, X. Zhang, J. Li, A. Khan, Y. Guan, K. Tang, S. Wang, S. Xu, Genetic History of Xinjiang's Uyghurs Suggests Bronze Age Multiple-Way Contacts in Eurasia. *Mol. Biol. Evol.* **34**, 2572–2582 (2017). doi:10.1093/molbev/msx177 Medline

39. P. Jia, A. Betts, D. Cong, X. Jia, P. Dupuy, Adunqiaolu: New evidence for the Andronovo in Xinjiang, China. *Antiquity* **91**, 621–639 (2017). doi:10.15184/aqy.2017.67

40. X. Mao, H. Zhang, S. Qiao, Y. Liu, F. Chang, P. Xie, M. Zhang, T. Wang, M. Li, P. Cao, R. Yang, F. Liu, Q. Dai, X. Feng, W. Ping, C. Lei, J. W. Olsen, E. A. Bennett, Q. Fu, The deep population history of northern East Asia from the Late Pleistocene to the Holocene. *Cell* **184**, 3256–3266.e13 (2021). doi:10.1016/j.cell.2021.04.040 Medline

41. M. Lipson, P. Skoglund, M. Spriggs, F. Valentin, S. Bedford, R. Shing, H. Buckley, I. Phillip, G. K. Ward, S. Mallick, N. Rohland, N. Broomandkhoshbacht, O. Cheronet, M. Ferry, T. K.

Harper, M. Michel, J. Oppenheimer, K. Sirak, K. Stewardson, K. Auckland, A. V. S. Hill, K. Maitland, S. J. Oppenheimer, T. Parks, K. Robson, T. N. Williams, D. J. Kennett, A. J. Mentzer, R. Pinhasi, D. Reich, Population Turnover in Remote Oceania Shortly after Initial Settlement. *Curr. Biol.* **28**, 1157–1165.e7 (2018). doi:10.1016/j.cub.2018.02.051 Medline

42. Y. Wang, F. Song, J. Zhu, S. Zhang, Y. Yang, T. Chen, B. Tang, L. Dong, N. Ding, Q. Zhang, Z. Bai, X. Dong, H. Chen, M. Sun, S. Zhai, Y. Sun, L. Yu, L. Lan, J. Xiao, X. Fang, H. Lei, Z. Zhang, W. Zhao, GSA: Genome Sequence Archive. *Genom. Proteom. Bioinform.* **15**, 14–18 (2017). doi:10.1016/j.gpb.2017.01.001 Medline

43. BIG Data Center Members, Database Resources of the BIG Data Center in 2018. *Nucleic Acids Res.* **46**, D14–D20 (2018). doi:10.1093/nar/gkx897 Medline

44. J. Dabney, M. Knapp, I. Glocke, M.-T. Gansauge, A. Weihmann, B. Nickel, C. Valdiosera, N. García, S. Pääbo, J.-L. Arsuaga, M. Meyer, Complete mitochondrial genome sequence of a Middle Pleistocene cave bear reconstructed from ultrashort DNA fragments. *Proc. Natl. Acad. Sci. U.S.A.* **110**, 15758–15763 (2013). doi:10.1073/pnas.1314445110 Medline

45. N. Rohland, E. Harney, S. Mallick, S. Nordenfelt, D. Reich, Partial uracil–DNA–glycosylase treatment for screening of ancient DNA. *Phil. Trans. R. Soc. B* **370**, 20130624 (2015). doi:10.1098/rstb.2013.0624 Medline

46. G. Renaud, U. Stenzel, J. Kelso, leeHom: Adaptor trimming and merging for Illumina sequencing reads. *Nucleic Acids Res.* **42**, e141 (2014). doi:10.1093/nar/gku699 Medline

47. R. M. Andrews, I. Kubacka, P. F. Chinnery, R. N. Lightowlers, D. M. Turnbull, N. Howell, Reanalysis and revision of the Cambridge reference sequence for human mitochondrial DNA. *Nat. Genet.* **23**, 147 (1999). doi:10.1038/13779 Medline

48. Q. Fu, C. Posth, M. Hajdinjak, M. Petr, S. Mallick, D. Fernandes, A. Furtwängler, W. Haak, M. Meyer, A. Mittnik, B. Nickel, A. Peltzer, N. Rohland, V. Slon, S. Talamo, I. Lazaridis, M. Lipson, I. Mathieson, S. Schiffels, P. Skoglund, A. P. Derevianko, N. Drozdov, V. Slavinsky, A. Tsybankov, R. G. Cremonesi, F. Mallegni, B. Gély, E. Vacca, M. R. G. Morales, L. G. Straus, C. Neugebauer-Maresch, M. Teschler-Nicola, S. Constantin, O. T. Moldovan, S. Benazzi, M. Peresani, D. Coppola, M. Lari, S. Ricci, A. Ronchitelli, F. Valentin, C. Thevenet, K. Wehrberger, D. Grigorescu, H. Rougier, I. Crevecoeur, D. Flas, P. Semal, M. A. Mannino, C. Cupillard, H. Bocherens, N. J. Conard, K. Harvati, V. Moiseyev, D. G. Drucker, J. Svoboda, M. P. Richards, D. Caramelli, R. Pinhasi, J. Kelso, N. Patterson, J. Krause, S. Pääbo, D. Reich, The genetic history of Ice Age Europe. *Nature* **534**, 200–205 (2016). doi:10.1038/nature17993 Medline

49. T. S. Korneliussen, A. Albrechtsen, R. Nielsen, ANGSD: Analysis of Next Generation Sequencing Data. *BMC Bioinform.* **15**, 356 (2014). doi:10.1186/s12859-014-0356-4 Medline

50. P. Skoglund, B. H. Northoff, M. V. Shunkov, A. P. Derevianko, S. Pääbo, J. Krause, M. Jakobsson, Separating endogenous ancient DNA from modern day contamination in a Siberian Neandertal. *Proc. Natl. Acad. Sci. U.S.A.* **111**, 2229–2234 (2014). doi:10.1073/pnas.1318934111 Medline

51. H. Weissensteiner, D. Pacher, A. Kloss-Brandstätter, L. Forer, G. Specht, H.-J. Bandelt, F. Kronenberg, A. Salas, S. Schönherr, HaploGrep 2: Mitochondrial haplogroup classification in the era of high-throughput sequencing. *Nucleic Acids Res.* **44**, W58–W63 (2016). doi:10.1093/nar/gkw233 Medline

52. A. Ralf, D. Montiel González, K. Zhong, M. Kayser, Yleaf: Software for Human Y-Chromosomal Haplogroup Inference from Next-Generation Sequencing Data. *Mol. Biol. Evol.* **35**, 1291–1294 (2018). doi:10.1093/molbev/msy032 Medline

53. J. M. Monroy Kuhn, M. Jakobsson, T. Günther, Estimating genetic kin relationships in prehistoric populations. *PLOS ONE* **13**, e0195491 (2018). doi:10.1371/journal.pone.0195491 Medline

54. N. Patterson, A. L. Price, D. Reich, Population structure and eigenanalysis. *PLOS Genet.* **2**, e190 (2006). doi:10.1371/journal.pgen.0020190 Medline

55. I. Olalde, M. E. Allentoft, F. Sánchez-Quinto, G. Santpere, C. W. K. Chiang, M. DeGiorgio, J. Prado-Martínez, J. A. Rodríguez, S. Rasmussen, J. Quilez, O. Ramírez, U. M. Marigorta, M. Fernández-Callejo, M. E. Prada, J. M. V. Encinas, R. Nielsen, M. G. Netea, J. Novembre, R. A. Sturm, P. Sabeti, T. Marquès-Bonet, A. Navarro, E. Willerslev, C. Lalueza-Fox, Derived immune and ancestral pigmentation alleles in a 7,000-year-old Mesolithic European. *Nature* **507**, 225–228 (2014). doi:10.1038/nature12960 Medline

56. M. Raghavan, P. Skoglund, K. E. Graf, M. Metspalu, A. Albrechtsen, I. Moltke, S. Rasmussen, T. W. Stafford Jr., L. Orlando, E. Metspalu, M. Karmin, K. Tambets, S. Rootsi, R. Mägi, P. F. Campos, E. Balanovska, O. Balanovsky, E. Khusnutdinova, S. Litvinov, L. P. Osipova, S. A. Fedorova, M. I. Voevoda, M. DeGiorgio, T. Sicheritz-Ponten, S. Brunak, S. Demeshchenko, T. Kivisild, R. Villems, R. Nielsen, M. Jakobsson, E. Willerslev, Upper Palaeolithic Siberian genome reveals dual ancestry of Native Americans. *Nature* **505**, 87–91 (2014). doi:10.1038/nature12736 Medline

57. P. Skoglund, H. Malmström, A. Omrak, M. Raghavan, C. Valdiosera, T. Günther, P. Hall, K. Tambets, J. Parik, K.-G. Sjögren, J. Apel, E. Willerslev, J. Storå, A. Götherström, M. Jakobsson, Genomic diversity and admixture differs for Stone-Age Scandinavian foragers and farmers. *Science* **344**, 747–750 (2014). doi:10.1126/science.1253448 Medline

58. E. R. Jones, G. Gonzalez-Fortes, S. Connell, V. Siska, A. Eriksson, R. Martiniano, R. L. McLaughlin, M. Gallego Llorente, L. M. Cassidy, C. Gamba, T. Meshveliani, O. Bar-Yosef, W. Müller, A. Belfer-Cohen, Z. Matskevich, N. Jakeli, T. F. G. Higham, M. Currat, D. Lordkipanidze, M. Hofreiter, A. Manica, R. Pinhasi, D. G. Bradley, Upper Palaeolithic genomes reveal deep roots of modern Eurasians. *Nat. Commun.* **6**, 8912 (2015). doi:10.1038/ncomms9912 Medline

59. I. Mathieson, I. Lazaridis, N. Rohland, S. Mallick, N. Patterson, S. A. Roodenberg, E. Harney, K. Stewardson, D. Fernandes, M. Novak, K. Sirak, C. Gamba, E. R. Jones, B. Llamas, S. Dryomov, J. Pickrell, J. L. Arsuaga, J. M. B. de Castro, E. Carbonell, F. Gerritsen, A. Khokhlov, P. Kuznetsov, M. Lozano, H. Meller, O. Mochalov, V. Moiseyev, M. A. R. Guerra, J. Roodenberg, J. M. Vergès, J. Krause, A. Cooper, K. W. Alt, D. Brown, D. Anthony, C. Lalueza-Fox, W. Haak, R. Pinhasi, D. Reich, Genome-wide patterns of selection in 230 ancient Eurasians. *Nature* **528**, 499–503 (2015). doi:10.1038/nature16152 Medline

60. I. Lazaridis, D. Nadel, G. Rollefson, D. C. Merrett, N. Rohland, S. Mallick, D. Fernandes, M. Novak, B. Gamarra, K. Sirak, S. Connell, K. Stewardson, E. Harney, Q. Fu, G. Gonzalez-Fortes, E. R. Jones, S. A. Roodenberg, G. Lengyel, F. Bocquentin, B. Gasparian, J. M. Monge, M. Gregg, V. Eshed, A.-S. Mizrahi, C. Meiklejohn, F. Gerritsen, L. Bejenaru, M. Blüher, A. Campbell, G. Cavalleri, D. Comas, P. Froguel, E. Gilbert, S. M. Kerr, P. Kovacs, J. Krause, D. McGettigan, M. Merrigan, D. A. Merriwether, S. O'Reilly, M. B. Richards, O. Semino, M.

Shamoon-Pour, G. Stefanescu, M. Stumvoll, A. Tönjes, A. Torroni, J. F. Wilson, L. Yengo, N. A. Hovhannisyan, N. Patterson, R. Pinhasi, D. Reich, Genomic insights into the origin of farming in the ancient Near East. *Nature* **536**, 419–424 (2016). doi:10.1038/nature19310 Medline

61. M. A. Yang, X. Gao, C. Theunert, H. Tong, A. Aximu-Petri, B. Nickel, M. Slatkin, M. Meyer, S. Pääbo, J. Kelso, Q. Fu, 40,000-Year-Old Individual from Asia Provides Insight into Early Population Structure in Eurasia. *Curr. Biol.* **27**, 3202–3208.e9 (2017). doi:10.1016/j.cub.2017.09.030 Medline

62. I. Mathieson, S. Alpaslan-Roodenberg, C. Posth, A. Szécsényi-Nagy, N. Rohland, S. Mallick, I. Olalde, N. Broomandkhoshbacht, F. Candilio, O. Cheronet, D. Fernandes, M. Ferry, B. Gamarra, G. G. Fortes, W. Haak, E. Harney, E. Jones, D. Keating, B. Krause-Kyora, I. Kucukkalipci, M. Michel, A. Mittnik, K. Nägele, M. Novak, J. Oppenheimer, N. Patterson, S. Pfrengle, K. Sirak, K. Stewardson, S. Vai, S. Alexandrov, K. W. Alt, R. Andreescu, D. Antonović, A. Ash, N. Atanassova, K. Bacvarov, M. B. Gusztáv, H. Bocherens, M. Bolus, A. Boroneanţ, Y. Boyadzhiev, A. Budnik, J. Burmaz, S. Chohadzhiev, N. J. Conard, R. Cottiaux, M. Čuka, C. Cupillard, D. G. Drucker, N. Elenski, M. Francken, B. Galabova, G. Ganetsovski, B. Gély, T. Hajdu, V. Handzhyiska, K. Harvati, T. Higham, S. Iliev, I. Janković, I. Karavanić, D. J. Kennett, D. Komšo, A. Kozak, D. Labuda, M. Lari, C. Lazar, M. Leppek, K. Leshtakov, D. L. Vetro, D. Los, I. Lozanov, M. Malina, F. Martini, K. McSweeney, H. Meller, M. Menđušić, P. Mirea, V. Moiseyev, V. Petrova, T. D. Price, A. Simalcsik, L. Sineo, M. Šlaus, V. Slavchev, P. Stanev, A. Starović, T. Szeniczey, S. Talamo, M. Teschler-Nicola, C. Thevenet, I. Valchev, F. Valentin, S. Vasilyev, F. Veljanovska, S. Venelinova, E. Veselovskaya, B. Viola, C. Virag, J. Zaninović, S. Zäuner, P. W. Stockhammer, G. Catalano, R. Krauß, D. Caramelli, G. Zariņa, B. Gaydarska, M. Lillie, A. G. Nikitin, I. Potekhina, A. Papathanasiou, D. Borić, C. Bonsall, J. Krause, R. Pinhasi, D. Reich, The genomic history of southeastern Europe. *Nature* **555**, 197–203 (2018). doi:10.1038/nature25778 Medline

63. G. A. Gnecchi-Ruscone, E. Khussainova, N. Kahbatkyzy, L. Musralina, M. A. Spyrou, R. A. Bianco, R. Radzeviciute, N. F. G. Martins, C. Freund, O. Iksan, A. Garshin, Z. Zhaniyazov, B. Bekmanov, E. Kitov, Z. Samashev, A. Beisenov, N. Berezina, Y. Berezin, A. Z. Bíró, S. Évinger, A. Bissembaev, G. Akhatov, A. Mamedov, A. Onggaruly, D. Voyakin, A. Chotbayev, Y. Kariyev, A. Buzhilova, L. Djansugurova, C. Jeong, J. Krause, Ancient genomic time transect from the Central Asian Steppe unravels the history of the Scythians. *Sci. Adv.* **7**, eabe4414 (2021). doi:10.1126/sciadv.abe4414 Medline

64. I. Lazaridis, N. Patterson, A. Mittnik, G. Renaud, S. Mallick, K. Kirsanow, P. H. Sudmant, J. G. Schraiber, S. Castellano, M. Lipson, B. Berger, C. Economou, R. Bollongino, Q. Fu, K. I. Bos, S. Nordenfelt, H. Li, C. de Filippo, K. Prüfer, S. Sawyer, C. Posth, W. Haak, F. Hallgren, E. Fornander, N. Rohland, D. Delsate, M. Francken, J.-M. Guinet, J. Wahl, G. Ayodo, H. A. Babiker, G. Bailliet, E. Balanovska, O. Balanovsky, R. Barrantes, G. Bedoya, H. Ben-Ami, J. Bene, F. Berrada, C. M. Bravi, F. Brisighelli, G. B. J. Busby, F. Cali, M. Churnosov, D. E. C. Cole, D. Corach, L. Damba, G. van Driem, S. Dryomov, J.-M. Dugoujon, S. A. Fedorova, I. Gallego Romero, M. Gubina, M. Hammer, B. M. Henn, T. Hervig, U. Hodoglugil, A. R. Jha, S. Karachanak-Yankova, R. Khusainova, E. Khusnutdinova, R. Kittles, T. Kivisild, W. Klitz, V. Kučinskas, A. Kushniarevich, L. Laredj, S. Litvinov, T. Loukidis, R. W. Mahley, B. Melegh, E. Metspalu, J. Molina, J. Mountain, K. Näkkäläjärvi, D. Nesheva, T. Nyambo, L. Osipova, J. Parik, F. Platonov, O. Posukh, V. Romano, F. Rothhammer, I. Rudan, R. Ruizbakiev, H.

Sahakyan, A. Sajantila, A. Salas, E. B. Starikovskaya, A. Tarekegn, D. Toncheva, S. Turdikulova, I. Uktveryte, O. Utevska, R. Vasquez, M. Villena, M. Voevoda, C. A. Winkler, L. Yepiskoposyan, P. Zalloua, T. Zemunik, A. Cooper, C. Capelli, M. G. Thomas, A. Ruiz-Linares, S. A. Tishkoff, L. Singh, K. Thangaraj, R. Villems, D. Comas, R. Sukernik, M. Metspalu, M. Meyer, E. E. Eichler, J. Burger, M. Slatkin, S. Pääbo, J. Kelso, D. Reich, J. Krause, Ancient human genomes suggest three ancestral populations for present-day Europeans. *Nature* **513**, 409–413 (2014). doi:10.1038/nature13673 Medline

65. S. Mallick, H. Li, M. Lipson, I. Mathieson, M. Gymrek, F. Racimo, M. Zhao, N. Chennagiri, S. Nordenfelt, A. Tandon, P. Skoglund, I. Lazaridis, S. Sankararaman, Q. Fu, N. Rohland, G. Renaud, Y. Erlich, T. Willems, C. Gallo, J. P. Spence, Y. S. Song, G. Poletti, F. Balloux, G. van Driem, P. de Knijff, I. G. Romero, A. R. Jha, D. M. Behar, C. M. Bravi, C. Capelli, T. Hervig, A. Moreno-Estrada, O. L. Posukh, E. Balanovska, O. Balanovsky, S. Karachanak-Yankova, H. Sahakyan, D. Toncheva, L. Yepiskoposyan, C. Tyler-Smith, Y. Xue, M. S. Abdullah, A. Ruiz-Linares, C. M. Beall, A. Di Rienzo, C. Jeong, E. B. Starikovskaya, E. Metspalu, J. Parik, R. Villems, B. M. Henn, U. Hodoglugil, R. Mahley, A. Sajantila, G. Stamatoyannopoulos, J. T. S. Wee, R. Khusainova, E. Khusnutdinova, S. Litvinov, G. Ayodo, D. Comas, M. F. Hammer, T. Kivisild, W. Klitz, C. A. Winkler, D. Labuda, M. Bamshad, L. B. Jorde, S. A. Tishkoff, W. S. Watkins, M. Metspalu, S. Dryomov, R. Sukernik, L. Singh, K. Thangaraj, S. Pääbo, J. Kelso, N. Patterson, D. Reich, The Simons Genome Diversity Project: 300 genomes from 142 diverse populations. *Nature* **538**, 201–206 (2016). doi:10.1038/nature18964 Medline

66. S. Purcell, B. Neale, K. Todd-Brown, L. Thomas, M. A. R. Ferreira, D. Bender, J. Maller, P. Sklar, P. I. W. de Bakker, M. J. Daly, P. C. Sham, PLINK: A tool set for whole-genome association and population-based linkage analyses. *Am. J. Hum. Genet.* **81**, 559–575 (2007). doi:10.1086/519795 Medline

67. P. J. Reimer, W. E. N. Austin, E. Bard, A. Bayliss, P. G. Blackwell, C. B. Ramsey, M. Butzin, H. Cheng, R. L. Edwards, M. Friedrich, P. M. Grootes, T. P. Guilderson, I. Hajdas, T. J. Heaton, A. G. Hogg, K. A. Hughen, B. Kromer, S. W. Manning, R. Muscheler, J. G. Palmer, C. Pearson, J. van der Plicht, R. W. Reimer, D. A. Richards, E. M. Scott, J. R. Southon, C. S. M. Turney, L. Wacker, F. Adolphi, U. Büntgen, M. Capano, S. M. Fahrni, A. Fogtmann-Schulz, R. Friedrich, P. Köhler, S. Kudsk, F. Miyake, J. Olsen, F. Reinig, M. Sakamoto, A. Sookdeo, S. Talamo, The IntCal20 Northern Hemisphere Radiocarbon Age Calibration Curve (0–55 cal kBP). *Radiocarbon* **62**, 725–757 (2020). doi:10.1017/RDC.2020.41

68. Institute of Cultural Relics and Archaeology in Xinjiang, Report on archaeological excavation of the NO.1 Cemetery group of Ayituohan in Habahe County [in Chinese]. *Xinjiang Cult. Relics* **2**, 19–39 (2017).

69. S. Li, The Afanasievo Culture from the discovery of the Ayituohan NO.1 Cemetery in Xinjiang [in Chinese]. *Cult. Relics Xinjiang* **1**, 105–121 (2018).

70. J. Yu, Archaeological records of Bolati tombs [in Chinese]. *Pop. Archaeol.* **6**, 75–79 (2013).

71. W. Guo, New archaeological harvest in Chaganguole township in 2015, Qinghe County, Xinjiang [in Chinese]. *West. Reg. Stud.* **1**, 135–137 (2016).

72. Institute of Cultural Relics and Archaeology in Xinjiang, Archaeological excavation of Songshugou site, Hebukesaier County, Yili region, Xinjiang [in Chinese]. *Xinjiang Cult. Relics* **1** (2018).

73. A. Chen, The characteristics and cultural origin of Chemurchek stone people [in Chinese]. *Res. Turpan* **2**, 105–112 (2012).

74. Institute of Cultural Relics and Archaeology in Xinjiang, The excavation briefing of Tuoganbai NO.2 Cemetery in Habahe, Xinjiang [in Chinese]. *Cult. Relics* **12**, 18–28 (2014).

75. Institute of Cultural Relics and Archaeology in Xinjiang, The excavation briefing on Dongtalede Cemetery in Habahe County, Xinjiang [in Chinese]. *Cult. Relics* **3**, 4–14 (2013).

76. Institute of Archaeology, Xinjiang Academy of Social Sciences, The excavation briefing on Kermuqi cemeteries [in Chinese]. *Cult. Relics* **1**, 23–32 (1981).

77. H. Shao, An introduction to Zhagunluke Culture in Xinjiang [in Chinese]. *Res. China's Front. Archaeol.* **7**, 170–183 (2008).

78. S. Ye, The Jade Road in Steppe and the spread of Onyx beads in China, a from 2000 to 1000 BCE. *Inn. Mong. Soc. Sci.* **4**, 137–147 (2018).

79. C. B. Jixieliefu, *The Ancient History of Southern Siberia* [in Chinese] (Xinjiang People's Press, 1981).

80. G. Tian, S. Guo, Xiongnu relics found in Aluchaideng, Inner Mongolia [in Chinese]. *Archaeology* **4**, 333–338 (1980).

81. J. Yu, X. Hu, Y. Yu, Y. Liu, X. He, J. Zhang, N. Alipujiang, W. Tong, A brief report on the excavation of the tomb in Tuwaxincun, Kanasi River, Buerjin County, Xinjiang [in Chinese]. *Cult. Relics* **4**, 4–16 (2014).

82. B. Wang, X. Qi, The type analysis of stone people in Xinjiang. *West. Reg. Stud.* **4**, 67–76 (1995).

83. X. Xiao, B. Zheng, Excavation of Shanpula tomb in Luopu County, Xinjiang [in Chinese]. *West. Reg. Stud.* **1**, 42–46 (2000).

84. X. Chengzhi, L. Chunxiang, C. Yinqiu, C. Dawei, W. Haijing, Z. Hong, Z. Hui, Mitochondrial DNA analysis of ancient Sampula population in Xinjiang. *Prog. Nat. Sci.* **17**, 927–933 (2007). doi:10.1080/10002007088537493

85. X. Wu, Archaeological excavation of Jierzankale Cemetery in Tashikuergan of Xinjiang in 2013 [in Chinese]. *West. Reg. Stud.* **1**, 124–127 (2014).

86. Institute of Archaeology, Chinese Academy of Social Science, Report on the archaeological excavation of Jierzankale Cemetery in Tashikuergan of Xinjiang [in Chinese]. *Acta Archaeol. Sin.* **2**, 229–252 (2012).

87. M. Wang, X. Zhang, X. Wu, Preliminary study on human bones in Jierzankale Cemetery, Tashikuergan, Xinjiang [in Chinese]. *North. Cult. Relics* **4**, 42–52 (2019).

88. Institute of Archaeology, Chinese Academy of Social Science, Report on archaeological excavation of Liushui site in Yutian County [in Chinese]. *Archaeology* **2016**, 19–36 (2016).

89. X. Museum, Report on excavation of Zhagunluke NO.1, Qiemo County, Xinjiang [in Chinese]. *Acta Archaeol. Sin.* **1**, 89–136 (2003).

90. Institute of Cultural Relics and Archaeology in Xinjiang, The excavation briefing of A_XV region in Qiafuqihaishuiku site in Tekesi, Xinjiang [in Chinese]. *Cult. Relics* **2006**, 32–38 (2006).

91. Y. Wang, A new harvest from the archaeological work in Jirentaigoukou, Nileke County, Xinjiang in 2015 [in Chinese]. *West. Reg. Stud.* **1**, 132–134 (2016).

92. Y. Wang, Q. Ruan, The Jirentaigoukou site, Nileke County, Xinjiang [in Chinese]. *Public Archaeol.* **7**, 57–70 (2017).

93. Y. Wang, X. Yuan, Q. Ruan, The archaeological harvest and preliminary understanding of Jirentaigoukou site in Nileke County, Xinjiang from 2015 to 2018 [in Chinese]. *West. Reg. Stud.* **1**, 133–138 (2019).

94. T. Shui, *A Comparative Study on Various Cultures in the Bronze Age of Xinjiang—The Historical Process of the Early Cultural Exchange Between East and the West Eurasian* [in Chinese] (Science Press, 2002).

95. Institute of Cultural Relics and Archaeology in Xinjiang, Excavation of Kuokesuxi NO.2 Cemetery in Tekesi County, Xinjiang [in Chinese]. *Archaeology* **9**, 3–16 (2012).

96. H. Liu, B. Teer, X. Wang, B. Guan, H. Liu, Archaeological harvest and preliminary understanding of Dunna Expressway-Nileke section in Yili, Xinjiang Province [in Chinese]. *West. Reg. Stud.* **3**, 137–139 (2018).

97. Institute of Cultural Relics and Archaeology in Xinjiang, Excavation of ancient tombs along Dunna Expressway-Nileke section in Yili, Xinjiang [in Chinese]. *Archaeology* **12** (2020).

98. Q. Ruan, A. Niyazi, Y. Wang, A brief report on the excavation of Tangbalesayi Cemetery in Nileke County, Yili [in Chinese]. *Cult. Relics* **5**, 13–22 (2012).

99. Q. Ruan, W. Hu, J. Zhang, The report on the excavation of the Wutulan Cemetery in Nileke, Xinjiang [in Chinese]. *Cult. Relics* **12**, 50–63 (2014).

100. Institute of Cultural Relics and Archaeology in Xinjiang, Report on the excavation of Ayousaigoukou site, and Kalaaoyi site, Nileke County, Yili, Xinjiang [in Chinese]. *Xinjiang Cult. Relics* **2** (2012).

101. Institute of Cultural Relics and Archaeology in Xinjiang, A brief report on the excavation of Ayousaigoukou site, Nileke County, Yili. Xinjiang [in Chinese]. *Cult. Relics* **5**, 13–22 (2012).

102. M. Rasmussen, S. L. Anzick, M. R. Waters, P. Skoglund, M. DeGiorgio, T. W. Stafford Jr., S. Rasmussen, I. Moltke, A. Albrechtsen, S. M. Doyle, G. D. Poznik, V. Gudmundsdottir, R. Yadav, A.-S. Malaspinas, S. S. White 5th, M. E. Allentoft, O. E. Cornejo, K. Tambets, A. Eriksson, P. D. Heintzman, M. Karmin, T. S. Korneliussen, D. J. Meltzer, T. L. Pierre, J. Stenderup, L. Saag, V. M. Warmuth, M. C. Lopes, R. S. Malhi, S. Brunak, T. Sicheritz-Ponten, I. Barnes, M. Collins, L. Orlando, F. Balloux, A. Manica, R. Gupta, M. Metspalu, C. D. Bustamante, M. Jakobsson, R. Nielsen, E. Willerslev, The genome of a Late Pleistocene human from a Clovis burial site in western Montana. *Nature* **506**, 225–229 (2014). doi:10.1038/nature13025 Medline

103. M. Meyer, M. Kircher, M.-T. Gansauge, H. Li, F. Racimo, S. Mallick, J. G. Schraiber, F. Jay, K. Prüfer, C. de Filippo, P. H. Sudmant, C. Alkan, Q. Fu, R. Do, N. Rohland, A. Tandon, M. Siebauer, R. E. Green, K. Bryc, A. W. Briggs, U. Stenzel, J. Dabney, J. Shendure, J. Kitzman, M. F. Hammer, M. V. Shunkov, A. P. Derevianko, N. Patterson, A. M. Andrés, E. E. Eichler, M. Slatkin, D. Reich, J. Kelso, S. Pääbo, A high-coverage genome sequence from an archaic Denisovan individual. *Science* **338**, 222–226 (2012). doi:10.1126/science.1224344 Medline

104. K. Prüfer, F. Racimo, N. Patterson, F. Jay, S. Sankararaman, S. Sawyer, A. Heinze, G. Renaud, P. H. Sudmant, C. de Filippo, H. Li, S. Mallick, M. Dannemann, Q. Fu, M. Kircher, M. Kuhlwilm, M. Lachmann, M. Meyer, M. Ongyerth, M. Siebauer, C. Theunert, A. Tandon, P. Moorjani, J. Pickrell, J. C. Mullikin, S. H. Vohr, R. E. Green, I. Hellmann, P. L. F. Johnson, H. Blanche, H. Cann, J. O. Kitzman, J. Shendure, E. E. Eichler, E. S. Lein, T. E. Bakken, L. V. Golovanova, V. B. Doronichev, M. V. Shunkov, A. P. Derevianko, B. Viola, M. Slatkin, D. Reich, J. Kelso, S. Pääbo, The complete genome sequence of a Neanderthal from the Altai Mountains. *Nature* **505**, 43–49 (2014). doi:10.1038/nature12886 Medline

105. P. Skoglund, S. Mallick, M. C. Bortolini, N. Chennagiri, T. Hünemeier, M. L. Petzl-Erler, F. M. Salzano, N. Patterson, D. Reich, Genetic evidence for two founding populations of the Americas. *Nature* **525**, 104–108 (2015). doi:10.1038/nature14895 Medline

106. M. E. Allentoft, M. Sikora, K.-G. Sjögren, S. Rasmussen, M. Rasmussen, J. Stenderup, P. B. Damgaard, H. Schroeder, T. Ahlström, L. Vinner, A.-S. Malaspinas, A. Margaryan, T. Higham, D. Chivall, N. Lynnerup, L. Harvig, J. Baron, P. Della Casa, P. Dąbrowski, P. R. Duffy, A. V. Ebel, A. Epimakhov, K. Frei, M. Furmanek, T. Gralak, A. Gromov, S. Gronkiewicz, G. Grupe, T. Hajdu, R. Jarysz, V. Khartanovich, A. Khokhlov, V. Kiss, J. Kolář, A. Kriiska, I. Lasak, C. Longhi, G. McGlynn, A. Merkevicius, I. Merkyte, M. Metspalu, R. Mkrtchyan, V. Moiseyev, L. Paja, G. Pálfi, D. Pokutta, Ł. Pospieszny, T. D. Price, L. Saag, M. Sablin, N. Shishlina, V. Smrčka, V. I. Soenov, V. Szeverényi, G. Tóth, S. V. Trifanova, L. Varul, M. Vicze, L. Yepiskoposyan, V. Zhitenev, L. Orlando, T. Sicheritz-Pontén, S. Brunak, R. Nielsen, K. Kristiansen, E. Willerslev, Population genomics of Bronze Age Eurasia. *Nature* **522**, 167–172 (2015). doi:10.1038/nature14507 Medline

107. C. Posth, N. Nakatsuka, I. Lazaridis, P. Skoglund, S. Mallick, T. C. Lamnidis, N. Rohland, K. Nägele, N. Adamski, E. Bertolini, N. Broomandkhoshbacht, A. Cooper, B. J. Culleton, T. Ferraz, M. Ferry, A. Furtwängler, W. Haak, K. Harkins, T. K. Harper, T. Hünemeier, A. M. Lawson, B. Llamas, M. Michel, E. Nelson, J. Oppenheimer, N. Patterson, S. Schiffels, J. Sedig, K. Stewardson, S. Talamo, C. C. Wang, J.-J. Hublin, M. Hubbe, K. Harvati, A. Nuevo Delaunay, J. Beier, M. Francken, P. Kaulicke, H. Reyes-Centeno, K. Rademaker, W. R. Trask, M. Robinson, S. M. Gutierrez, K. M. Prufer, D. C. Salazar-García, E. N. Chim, L. Müller Plumm Gomes, M. L. Alves, A. Liryo, M. Inglez, R. E. Oliveira, D. V. Bernardo, A. Barioni, V. Wesolowski, N. A. Scheifler, M. A. Rivera, C. R. Plens, P. G. Messineo, L. Figuti, D. Corach, C. Scabuzzo, S. Eggers, P. DeBlasis, M. Reindel, C. Méndez, G. Politis, E. Tomasto-Cagigao, D. J. Kennett, A. Strauss, L. Fehren-Schmitz, J. Krause, D. Reich, Reconstructing the Deep Population History of Central and South America. *Cell* **175**, 1185–1197.e22 (2018). doi:10.1016/j.cell.2018.10.027 Medline

108. V. Shinde, V. M. Narasimhan, N. Rohland, S. Mallick, M. Mah, M. Lipson, N. Nakatsuka, N. Adamski, N. Broomandkhoshbacht, M. Ferry, A. M. Lawson, M. Michel, J. Oppenheimer, K. Stewardson, N. Jadhav, Y. J. Kim, M. Chatterjee, A. Munshi, A. Panyam, P. Waghmare, Y. Yadav, H. Patel, A. Kaushik, K. Thangaraj, M. Meyer, N. Patterson, N. Rai, D. Reich, An Ancient Harappan Genome Lacks Ancestry from Steppe Pastoralists or Iranian Farmers. *Cell* **179**, 729–735.e10 (2019). doi:10.1016/j.cell.2019.08.048 Medline

109. M. Sikora, V. V. Pitulko, V. C. Sousa, M. E. Allentoft, L. Vinner, S. Rasmussen, A. Margaryan, P. de Barros Damgaard, C. de la Fuente, G. Renaud, M. A. Yang, Q. Fu, I. Dupanloup, K. Giampoudakis, D. Nogués-Bravo, C. Rahbek, G. Kroonen, M. Peyrot, H. McColl, S. V.

Vasilyev, E. Veselovskaya, M. Gerasimova, E. Y. Pavlova, V. G. Chasnyk, P. A. Nikolskiy, A. V. Gromov, V. I. Khartanovich, V. Moiseyev, P. S. Grebenyuk, A. Y. Fedorchenko, A. I. Lebedintsev, S. B. Slobodin, B. A. Malyarchuk, R. Martiniano, M. Meldgaard, L. Arppe, J. U. Palo, T. Sundell, K. Mannermaa, M. Putkonen, V. Alexandersen, C. Primeau, N. Baimukhanov, R. S. Malhi, K.-G. Sjögren, K. Kristiansen, A. Wessman, A. Sajantila, M. M. Lahr, R. Durbin, R. Nielsen, D. J. Meltzer, L. Excoffier, E. Willerslev, The population history of northeastern Siberia since the Pleistocene. *Nature* **570**, 182–188 (2019). doi:10.1038/s41586-019-1279-z Medline

110. Q. Fu, H. Li, P. Moorjani, F. Jay, S. M. Slepchenko, A. A. Bondarev, P. L. F. Johnson, A. Aximu-Petri, K. Prüfer, C. de Filippo, M. Meyer, N. Zwyns, D. C. Salazar-García, Y. V. Kuzmin, S. G. Keates, P. A. Kosintsev, D. I. Razhev, M. P. Richards, N. V. Peristov, M. Lachmann, K. Douka, T. F. G. Higham, M. Slatkin, J.-J. Hublin, D. Reich, J. Kelso, T. B. Viola, S. Pääbo, Genome sequence of a 45,000-year-old modern human from western Siberia. *Nature* **514**, 445–449 (2014). doi:10.1038/nature13810 Medline

111. C. C. Wang, H.-Y. Yeh, A. N. Popov, H.-Q. Zhang, H. Matsumura, K. Sirak, O. Cheronet, A. Kovalev, N. Rohland, A. M. Kim, S. Mallick, R. Bernardos, D. Tumen, J. Zhao, Y.-C. Liu, J.-Y. Liu, M. Mah, K. Wang, Z. Zhang, N. Adamski, N. Broomandkhoshbacht, K. Callan, F. Candilio, K. S. D. Carlson, B. J. Culleton, L. Eccles, S. Freilich, D. Keating, A. M. Lawson, K. Mandl, M. Michel, J. Oppenheimer, K. T. Özdoğan, K. Stewardson, S. Wen, S. Yan, F. Zalzala, R. Chuang, C.-J. Huang, H. Looh, C.-C. Shiung, Y. G. Nikitin, A. V. Tabarev, A. A. Tishkin, S. Lin, Z.-Y. Sun, X.-M. Wu, T.-L. Yang, X. Hu, L. Chen, H. Du, J. Bayarsaikhan, E. Mijiddorj, D. Erdenebaatar, T.-O. Iderkhangai, E. Myagmar, H. Kanzawa-Kiriyama, M. Nishino, K.-I. Shinoda, O. A. Shubina, J. Guo, W. Cai, Q. Deng, L. Kang, D. Li, D. Li, R. Lin, R. Nini, R. Shrestha, L. X. Wang, L. Wei, G. Xie, H. Yao, M. Zhang, G. He, X. Yang, R. Hu, M. Robbeets, S. Schiffels, D. J. Kennett, L. Jin, H. Li, J. Krause, R. Pinhasi, D. Reich, Genomic insights into the formation of human populations in East Asia. *Nature* **591**, 413–419 (2021). doi:10.1038/s41586-021-03336-2 Medline

112. M. A. Yang, X. Fan, B. Sun, C. Chen, J. Lang, Y.-C. Ko, C.-H. Tsang, H. Chiu, T. Wang, Q. Bao, X. Wu, M. Hajdinjak, A. M.-S. Ko, M. Ding, P. Cao, R. Yang, F. Liu, B. Nickel, Q. Dai, X. Feng, L. Zhang, C. Sun, C. Ning, W. Zeng, Y. Zhao, M. Zhang, X. Gao, Y. Cui, D. Reich, M. Stoneking, Q. Fu, Ancient DNA indicates human population shifts and admixture in northern and southern China. *Science* **369**, 282–288 (2020). doi:10.1126/science.aba0909 Medline

113. C. Ning, T. Li, K. Wang, F. Zhang, T. Li, X. Wu, S. Gao, Q. Zhang, H. Zhang, M. J. Hudson, G. Dong, S. Wu, Y. Fang, C. Liu, C. Feng, W. Li, T. Han, R. Li, J. Wei, Y. Zhu, Y. Zhou, C.-C. Wang, S. Fan, Z. Xiong, Z. Sun, M. Ye, L. Sun, X. Wu, F. Liang, Y. Cao, X. Wei, H. Zhu, H. Zhou, J. Krause, M. Robbeets, C. Jeong, Y. Cui, Ancient genomes from northern China suggest links between subsistence changes and human migration. *Nat. Commun.* **11**, 2700 (2020). doi:10.1038/s41467-020-16557-2 Medline